DETAILED STUDY OF THE 1 SEPTEMBER 2001 DEBRIS FLOW ON THE NATURAL HILLSIDE ABOVE LEI PUI STREET

GEO REPORT No. 154

Maunsell Geotechnical Services Ltd.

GEOTECHNICAL ENGINEERING OFFICE

CIVIL ENGINEERING AND DEVELOPMENT DEPARTMENT

THE GOVERNMENT OF THE HONG KONG

SPECIAL ADMINISTRATIVE REGION

DETAILED STUDY OF THE 1 SEPTEMBER 2001 DEBRIS FLOW ON THE NATURAL HILLSIDE ABOVE LEI PUI STREET

GEO REPORT No. 154

Maunsell Geotechnical Services Ltd.

**This report was originally produced in October 2002
as GEO Landslide Study Report No. LSR 8/2002**

Table of Contents

Table of Contents

Table of Contents

Table of Contents

First published, December 2004

Prepared by:

Geotechnical Engineering Office,
Civil Engineering and Development Department,
Civil Engineering and Development Building,
101 Princess Margaret Road,
Homantin, Kowloon,
Hong Kong.

PREFACE

In keeping with our policy of releasing information which may be of general interest to the geotechnical profession and the public, we make available selected internal reports in a series of publications termed the GEO Report series. The GEO Reports can be downloaded from the website of the Civil Engineering and Development Department (http://www.cedd.gov.hk) on the Internet. Printed copies are also available for some GEO Reports. For printed copies, a charge is made to cover the cost of printing.

The Geotechnical Engineering Office also produces documents specifically for publication. These include guidance documents and results of comprehensive reviews. These publications and the printed GEO Reports may be obtained from the Government's Information Services Department. Information on how to purchase these documents is given on the last page of this report.

R.K.S. Chan
Head, Geotechnical Engineering Office
December 2004

Table of Contents
Table of Contents
Table of Contents
Table of Contents

FOREWORD

This report presents the findings of an investigation into the landslide (GEO Incident No. 2001/09/0057), which occurred on 1 September 2001 above Lei Pui Street, Shek Lei Estate, Kwai Chung. The debris flow was triggered by a landslide involving about 250 m^3 of rock and soil on the steep natural hillside above a 25 m high cliff. The landslide debris and entrained material with an estimated maximum volume of 780 m^3 was deposited mainly within the lower part of the hillside and an active construction site, situated about 10 m above Lei Pui Street. About 50 m^3 of outwash material was deposited on Lei Pui Street and the Shek Lei Estate. The landslide demolished two squatter structures which had been vacated about two hours before the event and Lei Pui Street was closed for 3 days. No casualties were reported.

The key objectives of the detailed study were to document the facts about the landslide, present relevant background information, establish the probable causes of the failure and present the key findings. The scope of the study comprised site reconnaissance, desk study, detailed mapping, ground investigation and laboratory testing, together with theoretical analyses.

The report was prepared as part of the 2001/2002 Landslide Investigation Consultancy for the Geotechnical Engineering Office, Civil Engineering Department, under Agreement No. CE 72/2000. This is one of a series of reports produced during the consultancy by Maunsell Geotechnical Services Ltd.

L. J. Endicott

Dr. L.J. Endicott
Project Director
Maunsell Geotechnical Services Ltd.

Agreement No. CE 72/2000
Landslide Investigation Consultancy for Landslides Reported within Kowloon and the New Territories between April 2001 and the End of 2002

Table of Contents
Table of Contents
Table of Contents
Table of Contents

CONTENTS

Page No.

Page No.

1. INTRODUCTION

At about 10:50 p.m. on 1 September 2001, while the Black Rainstorm and Landslip Warnings were hoisted, a landslide (GEO Incident No. 2001/09/0057) occurred on the natural hillside above Lei Pui Street, Shek Lei Estate, Kwai Chung (Figure 1 and Plate 1). The landslide debris spilled over a 25 m high cliff and impacted upon a flatter portion of the hillside composed of colluvium overlying saprolite, which was entrained with the material from the landslide source to develop into a debris flow along the drainage line below. The volume of the landslide in the source area was about 250 m^3. A maximum active volume (see Section 4.1) of about 780 m^3 (including entrained material) was mobilised along the length of the debris trail. The debris flow demolished two squatter structures (Figure 2) located on the north flank of the drainage line. The four occupants of the squatter structures had vacated their dwellings about two hours before the debris flow event because of concerns about their personal safety due to the possibility of rain-induced landslides. Most of the debris came to rest within an active construction site above Lei Pui Street and about 50 m^3 of outwash material entered Lei Pui Street, Shek Pai Street and some open areas in Shek Lei Estate (Figure 2). Lei Pui Street was closed for 3 days. No casualties were reported as a result of the landslide incident.

Following the incident, Maunsell Geotechnical Services Ltd. (MGSL), GEO's landslide investigation consultants, carried out a detailed study of the incident under Agreement No. CE 72/2000.

This report presents the findings of the detailed study, which comprised the following key tasks:

(a) review of relevant documents relating to the development of the site and the sequence of events leading up to the landslide,

(b) interviews with witnesses to the debris flow event,

(c) topographic surveys and detailed mapping of the landslide source area and debris trail,

(d) aerial photograph interpretation, geomorphological and engineering geological mapping,

(e) ground investigation and laboratory testing,

(f) theoretical stability assessment of the source area,

(g) analysis of the rainfall records,

(h) debris flow modelling, and

(i) diagnosis of the probable causes of the landslide and the subsequent debris flow.

Table of Contents
Table of Contents
Table of Contents
Table of Contents

2. THE SITE

2.1 Site Description

The landslide occurred at an elevation of about 220 mPD on the steep (approximately 41°) northwest-facing vegetated hillside, about 135 m above Lei Pui Street (Figure 2 and Plate 1). Below this area, the natural hillside locally comprises steep (between 52° and 58°) rock cliffs overlooking less steep terrain with rounded spurs and valleys, where several ephemeral drainage lines converge into a streamcourse within the former squatter area of Kam Shan Village. The streamcourse continues through an active construction site (formerly a quarry) above a sharp bend in Lei Pui Street, uphill from a junction with Shek Pai Street (Figure 2 and Plate 2).

A few squatter structures are located on the lower hillside to the southeast of the streamcourse. Two squatter structures (with squatter control survey Nos. RTW/7E/156 and RTW/7E/158 registered by the Housing Department (HD) under their 1982 Squatter Structure Survey, hereinafter referred to as squatter structures Nos. RTW/7E/156 and RTW/7E/158 in this report) were completely demolished by the September 2001 landslide. These structures were situated within unallocated Government land on a platform on the north bank (Plate 3) of the ephemeral drainage line near its confluence with the streamcourse (Figures 2 and 3, and Plate 4).

Lei Pui Street, which is a two-lane, two-way carriageway, is the only access to the CNEC Christian College and Pope Paul VI College and the residential housing blocks located in the upper levels of Shek Lei Estate to the south of Shek Wah House (Figure 2). The gradient of the section of Lei Pui Street between the sharp bend below the active construction site and the junction with Shek Pai Street, is about 1 in 10. Shek Pai Street, which has a gradient of about 1 in 20, runs along the eastern edge of the lower levels of Shek Lei Estate.

The hillside above the landslide source area is inclined at about 45° and is generally densely vegetated with shrubs and small trees, with the exception of areas of steeper granite rock outcrop. From about 80 m above the source area, the vegetation thins out to scrub and tall grass adjacent to the crest of the ridgeline. The cliff immediately below the landslide source area is part of a sparsely vegetated granite rock outcrop, with overhanging blocks and sloping ledges (Figure 3 and Plate 5). The lower hillside, below the rock outcrop, slopes more gently towards Lei Pui Street at an average angle of about 30°. On this part of the hillside, the vegetation changes to dense woodland except for locally cultivated areas and former squatter platforms.

On either side of the streamcourse are several registered cut slopes, including slopes Nos. 7SW-C/C1255, 7SW-C/C1056, 7SW-C/1252, 7SW-C/1253 and 7SW-C/1053 and disturbed terrain features including slopes Nos. 7SW-C/DT81 and 7SW-C/DT201, which are associated with the cultivated areas (Figure 2).

The remains of a 3.5 m span concrete footbridge that provided access to the hillside on either side of the streamcourse are located about 10 m below the confluence of the drainage line and the streamcourse, some 200 m below the landslide source (Drawing No. 1 and Plates 6 and 7).

The gradient of the streamcourse between the footbridge (Drawing No. 1) and the top

Table of Contents
Table of Contents
Table of Contents
Table of Contents

of the approximately 15 m high rock slope (No. 7SW-C/C182) around the active construction site (Figure 3) is approximately 1 in 7 (i.e. about 8°). At the time of the incident, slope No. 7SW-C/C182 and the approximately 12 m high rock slope (No. 7SW-C/C180), which overlooks Lei Pui Street, were being upgraded as part of the Landslip Preventive Measures (LPM) Programme under Contract No. CE 18/99. The upgrading works included construction of a 25 m long rectangular concrete drainage channel (Plates 8, 9 and 10), approximately 2 m wide by 1.2 m deep with 250 mm thick side walls and wing walls behind the crest of slope No. 7SW-C/C182 and a drainage channel with similar dimensions across the floor of the active construction site. In addition, the works included underpinning of an existing retaining wall (Plate 11) and construction of a 2 m wide stepped cascade (Plates 12 and 13) cut into the face of the rock slope to direct the stream flow from the upper drainage channel into another concrete channel which runs across the floor of the active construction site. The channel is on the northwest side of an existing Water Supplies Department (WSD) compound with a pump house and associated facilities (Drawing No. 1 and Plates 6, 13, 14 and 15). A temporary fence had previously been erected along Lei Pui Street below the active LPM works site (Plate 16).

2.2 Regional Geology

The 1:100 000 scale geological map published by the Hong Kong Geological Survey (HKGS), indicates that the study area is underlain by porphyritic fine-grained granite and equigranular medium-grained granite of the Needle Hill granite pluton (Sewell et al, 2000). The equigranular coarse and fine to medium-grained granite of the Sha Tin granite pluton has a northeast to southwest contact which passes through the Lower Shing Mun Reservoir about 500 m to the east of the study area.

The 1:20 000 scale geological map sheet No. 7, published by the HKGS, indicates that a contact between the fine-grained granite and medium-grained granite is situated at an elevation of about 300 mPD (i.e. about 80 m above the source of the landslide) near the ridgeline, trending in a north-easterly direction (Figure 4). Feldsparphyric rhyolite dykes, which trend northeast to southwest, are shown to intrude both types of granite near the ridgeline.

According to the HKGS 1:20 000 scale geological map, no geological faults are shown to intersect the landslide source, although north-south trending photogeological lineaments are shown within and adjacent to the study area catchment. The northeast to southwest trending Lead Mine Pass Fault is shown approximately 1 km to the northwest of the September 2001 landslide main catchment and has a similar orientation to the main ridge and some of the dykes. The map shows three lobes of colluvium (Qdt-mixed debris flow and talus deposits) on the hillside, with the central lobe being located on the path of the landslide debris trail (Figure 4).

3. HISTORY OF THE SITE

3.1 Site Development

The history of development at the site has been determined from an examination of old survey maps, together with an interpretation of aerial photographs and a review of relevant

Table of Contents
Table of Contents
Table of Contents
Table of Contents

documentary information (Figure 5). Detailed observations from the aerial photograph interpretation (API) are given in Appendix A.

In 1949, the site in the immediate vicinity of the landslide was undeveloped. Some time before 1963, a cultivation terrace (designated as ‘AG1 1963’ in Figure 5) was formed adjacent to the drainage line (Figure 5) at the location where squatter structures Nos. RTW/7E/156 and RTW/7E/158 (registered by HD) were destroyed by the 1 September 2001 debris flow. The construction of Shek Lei Estate commenced in the mid-1960s and Shek Pai Street and Blocks 6 and 9 of Shek Lei Estate were completed by 1967. The slope at the back of the former quarry, which is now registered as slope No. 7SW-C/C182 (Figure 2) at the foot of the streamcourse is seen to be active in 1967. Site development continued with the construction of Lei Pui Street up to the entrance of the CNEC Christian College and Pope Paul VI College and formation of the platform for Shek Wah House by 1973. The transmitter station on the ridgeline above the landslide site had been constructed by 1973.

Squatter structures Nos. RTW/7E/156 and RTW/7E/158 can first be seen on the 1973 aerial photographs. The number of squatter structures and cultivated terraces increased appreciably up to 1974 with slopes Nos. 7SW-C/C1255 and 7SW-C/C1056 (Figures 2 and 5) in place by 1973. Squatter structures were erected in the former quarry site by 1974, which appears to have been abandoned some time before. The number of squatter structures on the subject hillside increased after 1981, when slope No. 7SW-C/C1060 was formed, presumably to allow the squatter development on the platform below (Figures 2 and 5). A new squatter platform with a low retaining wall (less than 1 m high) adjacent to the ephemeral drainage line, along which the September 2001 landslide debris flowed, was observed in the 1981 aerial photographs at an approximate elevation of 145 mPD (Figure 5).

The number of squatter structures adjacent to slope No. 7SW-C/C1056 and within the quarry area increased between 1982 and 1984 (Figure 5). The WSD pump house and associated toilet were constructed within the former quarry area in 1987, as part of the Squatter Area Improvement works undertaken by the HD (Figure 5). The platform of the present-day Shek Wah House (Figure 2) appears to have been used for recreational purposes between 1982 and 1987 before being cleared for the construction of Shek Wah House, which was completed between 1991 and 1993.

The WSD Kowloon Reservoir collector tunnel and the WSD Tai Po - Butterfly Valley Aqueduct (constructed between 1997 and 2000), pass beneath the hillside at levels of approximately 155 mPD and 50 mPD respectively (Figure 5).

3.2 Squatter Clearance

In connection with the Government’s Non-Development Clearance (NDC) Programme to clear vulnerable squatters on slope safety grounds, the GEO carried out inspections of the Shek Lei Hill area in 1984 and 1992.

Following recommendations made for clearance in January 1985, the clearance and demolition of squatter structures commenced in 1985 and continued until 1988 (Figure 6). No recommendations were made for clearance of squatter structures Nos. RTW/7E/156 and RTW/7E/158 under the NDC Programme in 1985 (Figure A5). After 1992, the number of

Table of Contents
Table of Contents
Table of Contents
Table of Contents

squatter structures in the Shek Lei Hill area decreased further with the implementation of the 1992 NDC Re-inspection Programme. The GEO recommendations for clearance on slope safety grounds were forwarded to HD in November 1992, which included squatter structures Nos. RTW/7E/156 and RTW/7E/158. The extent of squatter structures on the hillside in early 1993 is shown in Plates 17 and 18. At this time there were a total of approximately 40 squatter dwellings within the pathway of the debris flow.

Following minor landslide incidents (GEO Incidents Nos. MW93/5/2 and MW93/5/17) within Shek Lei Hill (Kam Shan) Village (within the former quarry) in May 1993, GEO recommended that all structures within the quarry should be immediately and permanently cleared. In June 1993, NDC was recommended to commence in July 1993 and to be completed by January 1994. Following GEO's recommendations, all except about 10% of the squatter structures within the village area were to be cleared (Figure A6). The remaining squatter structures were agreed to be cleared on "other grounds" in a NDC Liaison Meeting held in August 1993 (see Section A.3.1 of Appendix A).

By 24 March 1995, most of the squatter structures had been cleared and the land was handed over to District Lands Office (DLO) on 24 March 1995 (Appendix A). However, the registered owner of squatter structures Nos. RTW/7E/156 and RTW/7E/158 refused screening and insisted on staying.

During site inspections carried out by the LPM consultant, Scott Wilson (Hong Kong) Limited (SW), in December 1999 squatter structures were observed within the abandoned quarry. On 30 November 2000, eleven squatter structures were cleared from the site adjacent to slope No. 7SW-C/C182 (Appendix A). The site was formally handed over to SW for upgrading works under the LPM Programme on 11 December 2000.

3.3 Past Instability

3.3.1 General

This section describes the past instability that has been identified or inferred in previous regional and local studies and GEO Incident Reports. The previous studies, which include the assessment of potential instability under the Geotechnical Area Studies Programme (GASP) for development planning purposes, are essentially interpretative while the GEO Incident Reports are essentially factual records of site inspections. A detailed interpretative account of the previous instability and geomorphology of the area based on site-specific API and field mapping carried out for this study is given in Section 5.5.

3.3.2 Natural Terrain Landslide Inventory (NTLI)

In 1995, GEO compiled the Natural Terrain Landslide Inventory (NTLI), from the interpretation of high-level (20,000 feet) aerial photographs dating from 1945 to 1994 (Evans et al, 1997; King, 1997). Based on the high-level 1964 aerial photographs, seven landslides were located within the catchment which drains into the active construction site above Lei Pui Street (Figure 7). All the landslides are recorded as being less than 20 m wide at the widest point. One landslide (07SWC2004) was located close to the upper part of the 1 September 2001 landslide debris trail, approximately 130 m downhill of the crown of

Table of Contents
Table of Contents
Table of Contents
Table of Contents

the landslide scar. The closest NTLI landslide to the September 2001 landslide was identified approximately 5 m from the south flank of the debris trail just below the rock cliff at about Chainage 60 (NTLI Reference No. 07SWC0038).

3.3.3 Large Landslide Database

The GEO's large landslide database contains no records of large landslides within the study area.

3.3.4 Geotechnical Area Studies Programme (GASP)

In GASP Report No. II, which included a regional appraisal of the Central New Territories (GCO, 1987) for outline strategic planning purposes, the Geotechnical Land Use Map (GLUM) identifies the hillside near the source of the 1 September 2001 landslide as being Class IV terrain (i.e. terrain with extremely high geotechnical limitations). The lower hillside areas in the study area are classified as Class III terrain (i.e. with high geotechnical limitations), and occasional areas of Class II terrain (i.e. moderate limitations) on the flatter, lower-lying slopes. The Generalised Limitations and Engineering Appraisal Map (GLEAM) classifies the middle and upper hillside of the study area as a "zone of constraints for development".

The Physical Constraints Map (PCM) indicates that the study area lies within "zones of general instability" associated with both colluvial and in-situ terrain. The Engineering Geology Map indicates that the hillside is a zone of instability underlain by granite with a colluvial lobe located below the granite slabs, also identified as a zone of instability. A north-south trending photogeological lineament, which terminates within the colluvial lobe, is also shown on this map.

3.3.5 GEO Incident Reports

According to GEO's Landslide Incident records, a total of 9 incidents have been reported within the study area at the locations shown in Figure 7. All the incidents were located in the lower hillside of the study area, adjacent to squatter structures. The incidents were minor, with volumes between 0.5 m^3 and 4 m^3. Eight of the incidents involved small sized unregisterable man-made slopes, with one occurring on natural hillside.

3.4 Previous Studies

In December 2000, SW prepared a Stage 3 Study Report No. S3R 118/2000 entitled "Feature No. 7SW-C/C182 Kam Shan Village Shek Lei, Kwai Chung", covering the proposed upgrading works to the slope. The report contains an API study, which covers parts of the catchment on the hillside above.

The inferred relict and recent landslides identified by SW (Figure 7) are broadly consistent with MGSL's interpretation carried out for this study (Section 5.5). A large relict

Table of Contents Table of Contents Table of Contents Table of Contents

landslide (about 150 m across) was identified by SW within the granite outcrop of the upper catchment above the 2001 landslide source area. This same feature was identified by MGSL during mapping and detailed API as a persistent structurally controlled break in slope, along which several relict landslides and rockslides have been identified (Section 5.5).

SW's API plan shows several lobes of colluvium below the granite outcrop, on the middle and lower hillside. The extent of this colluvium generally agrees with the findings of MGSL, although the exact boundaries have been refined with the benefit of the detailed API and field mapping work (Section 5.5).

4. DESCRIPTION OF THE LANDSLIDE

4.1 General

A detailed 1:250 scale map together with cross-sections of the landslide and the debris trail is shown on Drawing No. 1, which also shows the chainage reference (starting from the crown of the landslide source) that was established along the centreline of the landslide and debris trail for the purposes of field mapping. A longitudinal section of the landslide scar is shown in Figure 3, which includes the mass-balance along the debris trail. A detailed description of the landslide and debris trail is presented in the following sections.

4.2 Source (Chainage 0 to Chainage 25)

The crown of the source area is located at approximately 233 mPD, on a natural hillside inclined at approximately 41°, within an area of granite bedrock with thin, colluvial cover (Drawing No. 1, Section 1-1). An oblique aerial photograph taken in 1993 shows the landslide source and the surrounding portion of the upper hillside were heavily vegetated with shrubs and small trees (Plate 17).

The pre-failure ground surface profile (Figures 8, 9 and 10) has been re-constructed from field estimates of depleted thickness and the pre-failure topography shown on the existing 1:1000 survey sheet No. 7SW22B. The landslide source was up to 26 m long (i.e. along the north flank and 15 m wide at the base (Figure 8 and Plate 5) and the maximum depth of the landslide scar (measured normal to the ground surface) is about 1.5 m adjacent to the north flank. The volume of detached material is estimated to be approximately 250 m^3.

The surface of rupture is formed by undulating sheeting joints that dip from about 45° in the north portion of the source area to about 31° in the south portion. Along the north flank of the main scarp, the deepest exposed profile comprises approximately 0.5 m of colluvium, overlying 1.0 m of moderately to slightly decomposed granite (see Section 5). Along the upper portion of the south flank of the scar, adjacent to existing granite outcrop, the depth of detached material reduces to zero.

4.3 Upper Debris Trail (Chainage 25 to Chainage 128)

The steep 25 m high rock cliff (ranging from about 52° to 58°), just below the landslide source, contains overhanging facets and sloping ledges developed along major

Table of Contents
Table of Contents
Table of Contents
Table of Contents

toppling and sheeting joints that strike across the hillside (Figure 3 and Plate 5). The rock face shows signs of severe abrasion, with the stems of small shrubs and trees stripped bare of branches and bark. From the abrasion marks above small ledges on the face of the cliff, it is estimated that approximately 5 m^3 of soil was eroded from the cliff.

At the toe of the rock cliff, the gradient of the slope decreases to approximately 40°, where colluvial deposits overlie completely decomposed and highly decomposed granite (Plate 19). The upper edge of the colluvium is less than 0.3 m thick and this material overlies a similar thickness of completely decomposed granite (CDG). The colluvium is clast supported (talus) with approximately equal proportions of angular cobbles and boulders of slightly to moderately decomposed granite and up to 25% silty sand and gravel. The lack of decomposition of the cobble and boulder clasts and their 'loose' nature (being easily excavated by a hand pick), indicates that the colluvium is relatively recent.

The largest volume of landslide debris originated from the north side of the landslide source. Directly below the north side of the scar, between Chainages 40 and 70 at the base of the cliff, up to 1.0 m thickness of colluvium and CDG were eroded, while the depth of depletion below the south side of the landslide source varies from 300 mm to zero (Plate 5). The contrast in depths of erosion across the base of the cliff probably reflected the different impact forces from the wedge-shaped mass of landslide debris, which cascaded down from the landslide source above (Plate 5). The volume of material eroded between Chainage 40 and Chainage 70 was approximately 125 m^3.

Between Chainages 70 and 115, the gradient along the drainage line decreases to about 1 in 1.7 (about 30°), and the thickness of eroded colluvial deposits increases. Along this section of the trail the erosion channel bifurcates into two channels, a main channel on the north side and a minor channel on the south side (Plates 20 and 21). Bedrock is exposed in the main channel with up to 2.2 m thickness of loose, bouldery colluvial deposits being freshly exposed along the north side of the channel in a sub-vertical bank. Recent colluvium was exposed in the base of the south channel. Two minor ephemeral drainage lines at the same locations as these erosion channels are visible on the 1963 aerial photographs. The approximate shapes of the pre-existing drainage lines were taken into account, when calculating the volumes of erosion caused by the September 2001 debris flow.

A lobe of recent colluvium between the two channels extended between Chainages 77 and 102. Debris was transported over the lobe with minor surface erosion and flattening of vegetation taking place and subsequent deposition of a thin layer of fine debris. Along the flanks of the trail, zones of transportation between 1 m and 4 m wide were observed together with localised deposits of coarse, remoulded debris and loose boulders along the periphery (Plates 20 and 21). At about Chainage 85, an ephemeral drainage line converges with the north erosion channel. At this location, several large boulders up to 1.5 m across accumulated from the September 2001 event. Large boulders of similar dimensions and a colluvial "levee" from previous events were also present. One newly displaced boulder, about 2.5 m across, was located at Chainage 85. This boulder was too large to have been part of the relatively thin granite slabs from the landslide source, and it probably originated from a previous landslide. The volume of material eroded between Chainages 70 and 102 was approximately 260 m^3.

At about Chainage 102 the two erosion channels converge and the trail narrows to

Table of Contents
Table of Contents
Table of Contents
Table of Contents

approximately 10 m in width. Just further down the debris trail, at about Chainage 117, the width of the trail was about 8 m, and a 0.4 m thick layer of 'older' colluvium (as indicated by highly to completely decomposed cobble and boulder clasts and a medium dense to dense silty sand matrix) was observed below much thicker recent colluvium at the base of the south flank of the erosion channel and in the bed of the drainage line (Section 2-2, Drawing No. 1). Between Chainages 102 and 128, approximately 70 m^3 of erosion of mainly recent colluvium occurred with minor accumulations of coarse debris with a volume of approximately 5 m^3.

4.4 Lower Debris Trail (Chainage 128 to Chainage 325)

Between Chainages 125 and 148, the trail flattens and widens out to approximately 25 m where a platform for a former squatter structure was located (Plate 21). A 1 m high rubble retaining wall formed the south side of this feature, constricting the ephemeral drainage line to about 2 m in width (Section 3-3, Drawing No. 1). Owing to the angle of entry of the debris flow onto the former squatter platform, the debris flow was directed across the platform and was deflected by the small cut slope along the north side of the platform to flow over granite slabs below. At Chainage 137, a superelevation of 3° was estimated from the marks along the sides of the debris trail. A thin layer (< 100 mm) of fine remoulded debris was deposited on the platform by the debris flow.

Below the former squatter platform, the debris flow cascaded over steep (about 35° to 45°) granite rock slabs, and locally removed a thin layer (< 200 mm) of topsoil and colluvium, which was mixed with much household refuse (Plate 21). The north side of the debris flow destroyed squatter structures Nos. RTW/7E/156 and RTW/7E/158, which were located on a small platform near the base of the rock slabs and the remains were pushed about 10 m further downhill to Chainage 185, where the flattened remains including household items were piled up against a lamp post (Drawing No. 1 and Plates 3, 4, 21 and 22). The structures consisted of wood and light corrugated steel sheet with an adjoining canopy. Fine, remoulded debris with occasional boulders accumulated on the squatter platform to a depth of about 300 mm. On 3 September 2001, this material was found to be still fully saturated and extremely soft.

The former concrete stairway leading to squatter structures Nos. RTW/7E/156 and RTW/7E/158 and the steel hand-railings of a concrete stairway along the south flank of the debris trail at about Chainage 185, were demolished by the impact of the debris (Plate 23).

At the base of the steep rock outcrop at Chainage 190, the trail intersects the main streamcourse which drains a large sub-catchment to the south (84,000 m^2), and changes direction by about 85° towards the northwest (Drawing No. 1). The debris flow impacted upon the west bank of the main streamcourse, leaving debris marks on the bank up to a height of about 3 m. About 12 m^3 of fresh, bouldery debris, reworked by subsequent stream flow was observed to have been deposited on a flat-lying, former squatter platform in the main streamcourse up to 15 m upstream of the confluence with the debris trail (Drawing No. 1 and Plate 23). No debris marks higher than about 1.3 m were observed on the banks of the main streamcourse opposite the 3 m high debris marks on the west bank.

Between Chainages 200 and 243, the debris trail was approximately 10 m in width. The deck of a 3.5 m span footbridge with concrete abutments located at Chainage 200 was demolished by the debris trail (Plates 6, 7 and 22) although the deck of the footbridge was never

Table of Contents
Table of Contents
Table of Contents
Table of Contents

subsequently located. At Chainage 200, some concrete steps were detached by the impact of debris on the west bank of the streamcourse and were transported approximately 5 m downstream to Chainage 205 (Plate 7) and just beyond at Chainage 207 a large boulder about 1.8 m by 1.4 m had been deposited (Drawing No. 1 and Plate 7). Approximately 25 m^3 of fine and coarse remoulded and re-worked debris was deposited in patches along the streamcourse between Chainages 200 and 243 at the end of the inlet to the upper drainage channel.

At Chainage 243, the debris travelling along the north bank of the channel demolished the north wing wall at the inlet of the upper drainage channel (Plates 9 and 12). The debris swept alongside the north bank of the drainage channel and the former squatter area, demolishing hand-railings, flattening a lamp post (Plates 9 and 12) and demolishing and transporting sections of temporary hoardings (Plate 8), at the boundary of the LPM site.

About 80 m^3 of coarse, remoulded debris containing boulders up to about 1 m across was deposited on the north side of the upper drainage channel (Plate 10). The trial pits excavated in this location (see Section 5) encountered coarse, matrix-supported debris up to 0.6 m in depth, containing construction materials and twisted steel reinforcement bars. The flattened hoardings, transported at the front of the debris, came to rest against the north wing wall behind the crest of slope No. 7SW-C/C182 (Plate 10). The hoardings and deposited material formed a “levee”, which deflected subsequent material across the drainage channel to impact upon and overturn the south wing wall (Plate 12). At about Chainage 270, the south wall of the drainage channel was severely scoured by debris (Plate 24).

The extent and nature of the debris flow material, which reached the active construction site, are shown in Plates 13 to 15. The lower concrete drainage channel constructed across the floor of the active construction site was completely infilled and buried by debris. The debris came to rest against the hoardings on the east and north sides of the WSD compound around the pump house and against the fences in front of the footbridge and steel gantry, resulting in minor buckling of the supports, with the most severe damage concentrated at the corner of the pump house compound. The hoardings are similar in construction to those alongside the upper reinforced concrete channel with the addition of light, steel-angle diagonal bracings (Plate 11). The perimeter fence of the pump house compound was just within the line of hoardings and was supported by 200 mm square reinforced concrete posts at 3 m centres.

The debris front material deposited immediately behind the fences and footbridge comprised (in terms of volume) approximately 60% to 70% boulders and cobbles, about 15% tree fragments and construction debris, and about 15% to 25% sandy gravel with organic material (Plate 15). The trial pits excavated within the quarry site revealed coarse, remoulded debris up to 600 mm deep with about 65% cobbles and boulders. Similar material was found to have infilled the concrete drainage channel, across the floor of the active construction site. Finer sands and silts with less than 25% cobbles and boulders were deposited around the periphery of the debris front within the quarry, partly engulfing a compressor and excavator up to 300 mm in depth (Drawing No. 1 and Plate 13). The total debris accumulation in the active construction site was about 530 m^3.

Below cut slope No. 7SW-C/C182, minor deposition of fine and occasional coarse material was observed, with about 3 m^3 of coarse debris being trapped behind the temporary fence at the toe of the slope along Lei Pui Street (Plate 16). One panel of the chain-link

Table of Contents
Table of Contents
Table of Contents
Table of Contents

mesh was partly torn from the steel-angle supports, which were slightly deformed by the impact of the debris.

4.5 Outwash Entering Lei Pui Street

About 50 m^3 of outwash consisting of silty sand and gravel (with only occasional cobbles and boulders up to 300 mm across found within 100 m of the active construction site) entered Lei Pui Street and continued along Shek Pai Street and into open areas of Shek Lei Estate (Figure 2 and Plate 2).

5. GEOMORPHOLOGY, GEOLOGY AND HYDROGEOLOGY OF THE LANDSLIDE SITE

5.1 General

The subsurface conditions at the landslide site were determined by reviewing existing records, aerial photograph interpretation, geological mapping and ground investigation.

5.2 Previous Ground Investigation

Previous ground investigations (Figure 11) carried out within the study area consist of boreholes, trial pits, slope stripping near the active construction site above slope No. 7SW-C/C180 and three trial pits at the location of the transmitter station on the ridgeline about 100 m southeast of the landslide site. These investigations generally confirmed the regional geology shown in Figure 4.

5.3 Current Ground Investigation

The detailed ground investigations (GI) carried out for this study were completed in two phases (Figure 12).

5.3.1 Phase 1 Ground Investigation

The first phase GI was carried out by Gammon Construction Ltd., the Landslide Investigation Consultancy ground investigation term contractor, and included four trial pits Nos. TP1 to TP4, which were excavated to depths of between 0.9 m and 2.0 m along the debris trail, and five trial pits Nos. TPA to TPE, which were excavated to depths of between 0.9 m and 2.25 m in the active construction site, to investigate the nature and characteristics of the landslide debris. Replacement trial pits Nos. TP1A and TPE2 were excavated because of obstructions encountered in trial pits Nos. TP1 and TPE respectively.

5.3.2 Phase 2 Ground Investigation

The second phase GI was undertaken by the CED's ground investigation term contractor, GCE (HK) Ltd., to investigate the landslide source area and the hillside at the base

Table of Contents
Table of Contents
Table of Contents
Table of Contents

of the rock cliff adjacent to the flanks of the debris trail. This investigation comprised a 15.2 m inclined drillhole, i.e. No. DH1 at 45° to the horizontal, five vertical drillholes Nos. DH2 to DH6, which extended to depths of between about 14.7 m and 15.4 m, six trial pits Nos. TP5 to TP10, which were excavated to depths of between 1.6 m and 3.2 m, and four slope strips Nos. SS1 to SS4.

Impression packer tests and acoustic televiewer surveys were carried out in drillholes DH1 to DH6 to establish the nature and orientation of joints within the rock at the landslide source (Figures 9 and 10). Gamma density probe surveys were carried out in drillholes DH3, DH4, DH5 and DH6.

5.4 Laboratory Testing

During the Phase 1 GI, bulk samples were taken from various horizons within the trial pits for laboratory classification and index testing. Particle Size Distribution (PSD) tests were carried out on samples of the landslide debris material and the results indicate that the matrix is composed of predominantly sand and gravel (64% to 95%). Silt and clay contents were found to range from 5% to 15% and from 0% to 22% respectively.

During the Phase 2 GI, large disturbed samples were recovered from various horizons in the trial pits for laboratory classification and index testing. Rock core samples were recovered from the drillholes and shear box tests were carried out on both natural rock joints and saw-cut rock joints (Figure 13). The results of both soil and rock testing are summarised in Table 2. PSD test results of the colluvium indicate that the composition of the colluvium comprises predominantly sands and gravels, with sand and gravel contents ranging from 47% to 80%. The silt and clay contents range from about 10% to 20% and 7% to 36% respectively. Shear box tests carried out on natural rock joint surfaces gave basic friction angles of between 37° and 42°.

5.5 Geomorphology and Past Failures

The geomorphological assessment was carried out using information obtained from desk studies and field studies. The desk study included detailed API and review of available documentation and literature. The API was primarily based on low-level photographs dating from 1949 to 2000, supplemented by field mapping using contoured ortho-rectified photographs from 1963 and 2000 to enable accurate location of features. From the API, 18 relict landslides and 8 recent landslides were identified within the catchment of the 1 September 2001 landslide by MGSL. All these relict and recent landslides were likely to be less than 50 m^3 based on interpretation by MGSL. The field studies included detailed geological and geomorphological mapping.

The plan area of the hillside directly above the source of the 1 September 2001 landslide is about 3,500 m^2. Sub-catchment A, which contains the landslide source, has a plan area of approximately 26,000 m^2 (Figure 14) and the larger sub-catchment that drains into the debris trail at about Chainage 190 has a plan area of approximately 84,000 m^2. Between Chainage 190 and cut slope No. 7SW-C/180 above Lei Pui Street, the total catchment area increases from about 110,000 m^2 to 133,000 m^2.

Table of Contents
Table of Contents
Table of Contents
Table of Contents

The main geomorphological findings of the detailed API and field mapping are shown in Figure 15. The study area has been divided into five terrain units, each with distinct geomorphological characteristics. These distinct characteristics may be a reflection of different landform ages. Terrain Units 1 to 3 comprise the upper hillside, middle rock outcrops and lower hillside respectively. The source of the 1 September 2001 landslide is located within Terrain Unit 2.

Terrain Unit 1 lies immediately to the west of the main ridgeline and comprises rounded, west-facing slopes dipping at between 30° and 40° and containing about 13 inferred relict landslides and one recent landslide (L1-97). Rock outcrops are sparse, and the nature of the topography suggests that rockhead is relatively deep. The significant depth of decomposition may possibly be due to the underlying rock being coarser-grained and therefore more susceptible to weathering. This terrain unit is primarily a zone of active depletion which has released a large amount of landslide debris over geological time scale.

Terrain Unit 2 lies immediately below Terrain Unit 1 and consists primarily of fine-grained granite rock outcrops inclined at between about 40° and 50°, which have developed along prominent sheeting joints that are intermittently broken by a series of sub-linear cliffs and ledges running almost directly across the strike of the slabs.

The geomorphology and stability of the hillside in Terrain Unit 2 is heavily influenced by the underlying rock structure. Figure B1 in Appendix B shows a stereoplot and kinematic stability assessment of the joint sets mapped within the site. The main findings of this assessment are that the Set 1 sheeting joints are adversely orientated for stability with regard to planar sliding and that the Set 2 joints are adversely orientated for stability with regard to toppling failure and may form release surfaces and potential tension cracks, which allow plane sliding. The sub-vertical Set 3 and Set 4 joints also strike at a high angle to the strike of the Set 1 and Set 2 joints and may form lateral release surfaces, allowing slabs of rock to detach from the rock outcrops. These main structural controls on the stability of the hillside are illustrated in Plate 25. The API has shown that the main structural patterns evident near the source area are consistent throughout the full extent of the hillside in which the rock structure is visible.

The Set 2 joints have been identified as being a contributing factor to the 1 September 2001 landslide in that they form overhanging release surfaces cutting directly across the strike of the sheeting joints (see Figure B1, Appendix B and Plate 25). Site observations indicate that these joints are frequently open near the ground surface indicating that movements have taken place. Based on examination of low-level aerial photographs, many of the rock cliffs contain large-scale blocks that are separated by tension cracks orientated in a similar direction to the Set 2 joints. Mapping of the rock face above the 1 September 2001 landslide source also confirms the dilated nature of the steeper portions of the rock cliffs (Plate 26). From the above observations, it is inferred that many of the cliffs mark the scarps of structurally controlled instability that have failed by a combination of toppling and sliding, and that many of the remaining scarps can be regarded as being potentially unstable. The API carried out for the SW study (see Section 3.2) also identified an extensive joint-controlled relict landslide, which extends across the series of cliffs in the upper portion of Terrain Unit 2 (Figure 7) and broadly corresponds to the main belt of structurally controlled relict instability identified in Figure 15.

Table of Contents
Table of Contents
Table of Contents
Table of Contents

As a consequence of the relict landslides in Terrain Unit 1 and the unstable nature of the cliffs in Terrain Unit 2, the flatter-lying ledges within Terrain Unit 2 are partially covered with colluvium (Figure 15). The most extensive and thickest areas of colluvium include the area above the 1 September 2001 landslide source (Plate 5). Large colluvial boulders (up to 2.5 m by 1.5 m) were found lying close to the edge of a ledge above the landslide source area that are being undermined by erosion of the underlying loose, sandy colluvium (located in the lower lobe of colluvium indicated in Plate 5). Clast-supported colluvium (talus) can also be found resting on an overhung sheeting joint directly beneath the landslide source (Figure 8). Erosion by the landslide has exposed a section through the colluvium, which reveals loose, clast-supported, angular cobbles, boulders and gravel in a subordinate matrix of silty sand (talus).

To the north of the source area of the 1 September 2001 landslide, three much smaller landslides have been identified from API, as occurring in about 1967, 1981 and 1992. These have probably occurred in a thin layer of colluvium and have estimated volumes less than 20 m^3. The 1967 landslide L1-67, which is at a similar level to, and within 5 m of the north flank of the 1 September 2001 landslide source, has probably been caused by erosion along the ephemeral drainage line. It is inferred that Terrain Unit 2 is primarily a zone of active depletion and transportation, which retains only a small proportion of any landslide debris, due to the overall steepness and regularity of the rock slabs.

Terrain Unit 3 lies below the lower edge of the rock outcrop of Terrain Unit 2. The rounded nature of the terrain indicates that rockhead is relatively deep (except where occasionally exposed in the ephemeral drainage lines). A substantial proportion of this terrain unit is covered by colluvium, which is greater than 1 m thick as indicated in Figure 15. The terrain directly below the 1 September 2001 landslide is drained by a number of ephemeral drainage lines which, from aerial photographs, appear to have been recently (in geological time scale) incised into a sheet of colluvial material, containing remnants of colluvial levees. This may indicate that many landslides have originated from Sub-catchment A over relatively recent geological time. The colluvium near the foot of the granite slabs below the landslide source is generally thin, and contains slightly to moderately decomposed clasts, with little saprolite development between the colluvium and bedrock. This indicates that the colluvium is relatively recent and that a process of frequent erosion by debris avalanches, similar to the 1 September 2001 landslide, has probably occurred near the foot of the cliff on a geological timescale. Terrain Unit 3 is primarily a zone of deposition of debris from landslides in Terrain Units 1 and 2 above. Transportation of material occurs along drainage lines and streamcourses in the form of debris flows and hyper-concentrated stream flow. Considering the activity and extent of the zones of depletion in Terrain Units 1 and 2, the banks of many of the ephemeral drainage lines between the rounded spurs at the base of the rock slabs could contain colluvium greater than 2 m thick.

Terrain Unit 4 is composed of rounded, north to northeast facing slopes with few rock outcrops and is totally different in character to the main, west-facing hillside of Terrain Unit 2. The lack of structural control may be due to the absence of sheeting joints, and could also be due to the hillside being orientated at a very oblique angle to the strike of the main rock structure (the strike of the main sheeting joint and back-release/toppling joint sets), which trends north-northeast to south-southwest. All the six landslides that have been identified (RL14-63 to RL18-63 and L1-63), appear to be closely associated with instability near the over-steepened heads of ephemeral drainage lines.

Table of Contents
Table of Contents
Table of Contents
Table of Contents

Terrain Unit 5 is composed of rounded, south-facing slopes with few rock outcrops. In the present study, three landslides have been identified (L1-49, L1-94 & L2-97), which appear to be associated with undercutting by an ephemeral stream along the east edge of the terrain unit.

Figure 7 shows the locations of landslides that have been inferred from previous studies. The seven NTLI landslides identified from high-level photographs below Terrain Unit 2 do not correspond to the locations of landslides identified from the API of low-level photographs carried out for this study and for the SW Stage 3 LPM Study of Slope No. 7SW-C/C182 (see Section 3.2). It would appear that the highly reflective and possibly eroded nature of some of the drainage lines along the upper edge of Terrain Unit No. 3 might have been mistaken as landslides on the NTLI high-level photographs.

5.6 Geology of the Landslide Site

The landslide source lies within a natural hillside underlain by extensive, steeply dipping, fine-grained, slightly to moderately decomposed granite slabs that exhibit a well-defined geological structure (Plate 25). A geological plan and sections through the landslide source are shown in Figures 8, 9 and 10 and a stereoplot showing the orientation of the main joint sets is shown in Figure B1, Appendix B.

The Set 1 stress relief/sheeting joints are rough and undulating with the dip typically ranging from 31° to 50° (average about 41°) and a dip direction ranging from 270° to 298°. The joints are often moderately to highly decomposed within 5 mm to 80 mm of the joint surfaces and commonly contain highly to completely decomposed rock and structureless sand infill of up to 100 mm thick, and occasional sandy silt infill of up to 40 mm thick. The maximum persistence of the joints is at least 18 m. The spacing of the joints varies between 0.2 m and 1.0 m with an average of about 0.3 m within the flanks of the source. These joints are very unfavourably orientated in terms of instability with regard to planar sliding failure.

The Set 2 joints are rough and planar with the dip typically ranging from 60° to 70° and a dip direction ranging from 100° to 110°. The joints are often moderately decomposed within 5 mm to 20 mm of the surfaces and are occasionally infilled with structureless silty sand up to 30 mm thick. The maximum persistence of the joints is at least 20 m. The spacing of the joints varies between 0.2 m and 6.0 m with an average of about 1.0 m within the flanks of the landslide source. These joints tend to form toppling/back release surfaces for planar failure on Set 1 joints.

The Set 3 joints are rough and planar to irregular and are sub-vertical with a strike of about 005° to 010°. The joints are often moderately decomposed within 5 mm to 20 mm of the surfaces. The maximum persistence of the joints is about 5 m with an average of about 1.5 m within the landslide source. The spacing of the joints varies between 0.2 m and 2.0 m (average about 0.3 m within the flanks of the source). These joints provide side-release surfaces for planar failure on the Set 1 joints. Owing to their lack of continuity and general irregularity, the side-release surfaces tend to be stepped and are formed in combination with Set 2 joints.

The Set 4 joints typically dip from about 45° to 55°, and have a dip direction ranging

Table of Contents
Table of Contents
Table of Contents
Table of Contents

from about 40° to 50°. The spacing of these joints varies between 20 m and 50 m and form a persistent 'major' joint set. The joints include some areas that appear sheared, with striated quartz infill and up to 20 mm thickness of mylonite noted near the base of the surface of rupture, although no evidence was observed to indicate any movement (offset).

The overall angle of the source area is approximately 41° and is sub-parallel to the stress-relief/sheeting joints, which generally define the granite outcrops across the hillside and form the floor of the landslide source. The fine-grained granite shows little variation in texture and grain size, but the darker mafic (magnesium and iron-rich) minerals have been locally leached by near-surface weathering, particularly near the lower portion of the south flank, which locally tends to give a very light-grey "aplitic" appearance to the rock. However, the drillholes indicate that the rock below the surface of rupture is generally light pinkish grey mottled brown, fine-grained, strong to moderately strong, slightly to moderately decomposed granite with closely to widely-spaced joints.

A general view of the floor of the lower surface of rupture is shown in Plate 27. The source floor is defined by stress-relief joints that dip between 31° and 44° in a west to west-northwest direction and the exposed joint surfaces are rough and undulating. Several light to dark grey-brown patches of silty sand joint infill were observed adhering to the floor of the landslide source at local, steeply-inclined joints striking across the floor. Joint infill contains abundant rootlets and is probably the result of washing in of fines into dilations caused by progressive, downhill movement of the rock slabs over many years. Some of the sub-vertical Set 2 joints, which penetrate the source floor, are dilated by up to 30 mm (Plate 28).

The granite slabs exposed in the flanks of the scar are moderately to slightly decomposed and have a maximum thickness of about 1 m along the north flank and about 0.3 m along the south flank. The slabs are separated from each other by up to 100 mm of highly to completely decomposed granite and structureless silty sand that contains soil pipes up to about 50 mm across (Plates 29 and 30).

Colluvium up to 0.6 m thick is exposed along the north flank (Plate 29) and the crown of the landslide scar, but the south flank has only an intermittent colluvial cover of less than 250 mm in thickness. The colluvium is clast-supported (talus) with abundant tree roots and is composed of sub-angular boulders and cobbles in a 15% to 20% loose, gravelly silty sand matrix, with a maximum boulder size of 400 mm.

About 1.5 m below the edge of the landslide source is a prominent sheeting joint which extends below the full width of the scar (Plate 31 and Figures 8 to 10). Below the north portion of the scar, recent colluvium has accumulated on the joint surface, below a major Set 2 toppling joint. The Set 2 joint continues through the rock mass in the south portion of the scar, and crosses a major Set 4 shear which is infilled with striated quartz. The Set 4 shear runs for at least 50 m across the exposed cliff face and surface of rupture (Figure 8 and Plate 25). The fault breccia encountered in the inclined drillhole No. DH1, adjacent to a 20 mm thick shear plane inclined at 60° to the drillhole axis, may represent the Set 4 shear as indicated on Section B-B in Figure 10.

The uppermost 3 m of the rock mass below the surface of rupture contains a number of inferred sheeting joints, up to 200 mm wide (inferred from zones of poor or no recovery

Table of Contents
Table of Contents
Table of Contents
Table of Contents

where completely decomposed granite or sediment infilling may exist) and microfractured zones, e.g. in drillholes Nos. DH1, DH2 and DH3 (Figures 9 and 10). Low-density zones recorded during the gamma density probe surveys generally correlated well with highly fractured zones or 'no recovery' zones recorded during the drilling.

About 50% of the surface of rupture is composed of moderately to slightly decomposed granite. However, approximately 35% of the surface of rupture is highly to completely decomposed or coated with silty sand infill material up to 50 mm thick. About 15% of the surface of rupture is within colluvium, mainly in the uppermost parts of the landslide scar (Figure 8).

Some evidence of shearing through interlocking blocks was noted in both flanks of the surface of rupture (Figure 8 and Plates 32 and 33). In particular, some corners of moderately decomposed blocks and also some surfaces up to 200 mm in length show no surface staining and have powdery surfaces that appear to have been created by recent shearing (Plate 32). Many of the remaining rock blocks in the flanks are partly dislodged and form a very rough profile to the sides of the landslide scar (Plate 33).

The roughness of the surface of rupture was surveyed in detail by measuring the local inclination using 210 mm and 420 mm diameter plates on a 0.2 m by 0.2 m grid in two areas of the surface of rupture (Figure 8). An account of the measurements and derivation of the roughness angle (i) is contained in Appendix B. A representative small-scale roughness angle of between 9° and 11° for the overall surface of rupture was obtained from an analysis of the plate measurements.

Estimates of the Joint Roughness Coefficient (JRC) obtained by comparing the profiles of the exposed sheeting joints with published profiles to which a range of dimensionless JRC values are ascribed (Barton, 1990), gave values of JRC, which ranged from 8 to 12. Field estimates of the large-scale wavelength and amplitude are approximately 4 m to 5 m and 150 mm to 200 mm respectively. These estimates give extreme values for (i) of between 3.5° and 6°.

Below the source area at the foot of the cliff, the trial pit and slope strips identified that the hillside adjacent to the upper debris trail comprises colluvium/debris flow deposits of at least 0.5 m thick, overlying residual soil and/or completely decomposed granite (CDG). Close to the flanks of the landslide scar the thickness of colluvium in trial pits Nos. 6 and 7 is up to 2 m. The colluvium is generally formed of both matrix and clast-supported angular cobbles and boulders of moderately to slightly decomposed granite in a loose to medium dense gravelly, silty sand matrix, suggesting that the material is relatively young and is a mixture of both debris flow and talus deposits. Occasional faint layering with more frequent boulders at the base or top of the deposits was observed, indicating possibly more than one phase of deposition. The three lobes of mixed debris flow and talus deposits shown on the HKGS 1:20 000 scale geological map (Figure 4), were generally confirmed by the field work where lobes or accumulations of debris flow deposits within drainage lines were observed in juxtaposition with talus deposits. Both types of deposits were laterally extensive and relatively recent (as indicated by the angularity and degree of decomposition of clasts), which suggest a fairly active depositional environment below the granite outcrop within the study area.

A distinctive, rounded, lobe-shaped spur lies on the south flank of the upper debris trail.

Table of Contents
Table of Contents
Table of Contents
Table of Contents

The trial pits and soil strips indicate that this feature consists mainly of insitu material (residual soil and completely decomposed granite with only about 1.1 m thickness of colluvium in trial pit No. 9). CDG was also encountered locally within 200 mm of the ground surface in slope strip No. SS1. The thickness of saprolite is at least 1 m, increasing up to at least 2.5 m near the crest of the spur. Moderately decomposed granite was only encountered in trial pit No. 8, near a drainage line at a depth of 1.5 m.

5.7 Groundwater Conditions

The catchment directly above the landslide source has an area of about 3500 m^2 (Figure 14), and the convex (in plan) nature of the terrain does not lend itself to concentration of surface run-off into the landslide source area. When inspected from the foot of the cliff below the source on 4 September 2001, no seepage could be detected from the source area. However, abundant seepage could be observed from within the rock slabs adjacent to and above the landslide in the weeks following the rainstorm of 1 September 2001. After direct access to the source area had been established, erosion pipes up to 50 mm across and seepage (after heavy rain) were observed from the surface of rupture and the underlying sheeting joints (Plates 34 and 35).

The steeply dipping planar rock slabs would promote intense runoff during times of heavy rainfall, but the near-surface rock mass has extensive dilated joints that strike across the hillside that could easily become filled with water and build up cleft water pressures during heavy rain.

The early morning standing water levels recorded in the drillholes in the vicinity of the source area were generally within 2.5 m to 4 m below ground surface, which corresponds to the depth range of significantly dilated and decomposed sheeting joint surfaces. This could indicate that drilling fluid generally escaped via the sheeting joints overnight, or it could indicate a standing water level within the rock mass, possibly prevented from being drained by relatively impermeable, major joint sets and shears that strike across the hillside (i.e. Sets 2 and 4).

6. ANALYSIS OF RAINFALL RECORDS

The GEO automatic raingauge nearest to the site, No. N06, is located at CNEC Christian College, Lei Pui Street, approximately 500 m to the west (Figure 1). The daily rainfall recorded from 31 July to 3 September 2001, together with the hourly rainfall from 30 August to 2 September 2001, is shown in Figure 16. Amber and Red Rainstorm Warnings were hoisted at 5:30 p.m. and 10:05 p.m. respectively on 1 September 2001. The Black Rainstorm Warning and Landslip Warning were hoisted at 10:45 p.m. on 1 September 2001, and were cancelled at 03:15 a.m. and 10:00 a.m. on 2 September 2001 respectively.

The rain was heavy in the evening of 1 September 2001 between 9:30 p.m. and 11:00 p.m. The 24-hour and 12-hour rainfall before the landslide was 202.5 mm and 181.5 mm respectively. The maximum 1-hour rolling rainfall was recorded as 97 mm between 9:50 p.m. and 10:50 p.m. on 1 September 2001. Analysis of the return periods of

Table of Contents
Table of Contents
Table of Contents
Table of Contents

the rainfall intensities for the 1 September 2001 rainstorm for different durations based on historical rainfall data at the Hong Kong Observatory (Lam & Leung, 1994), shows that the 2-hour rainfall was the most severe, with a corresponding return period of about 14 years. Similar results were also obtained using the statistical parameters derived by Evans & Yu (2001) based on the analysis of the data recorded by GEO raingauge No. N06.

The maximum rolling rainfall for the rainstorm on 1 September 2001 has been compared with the previous available data on severe rainstorms recorded by raingauge No. N06 since it became operational in June 1983 (Figure 17). The maximum rolling rainfall for the 1 September 2001 rainstorm prior to 10:50 p.m. is comparable to that of the previous most severe rainstorms recorded at raingauge No. N06 for durations of between 2 hours and 3 hours. After 8:30 p.m. on 1 September 2001, the highest 15 minute rainfall intensities were 30 mm between 10:15 p.m. and 10:30 p.m. and 28 mm between 10:30 p.m. and 10:45 p.m. (Figure 18).

7. PROBABLE SEQUENCE OF EVENTS

The probable sequence of events has been reconstructed from accounts given by witnesses, records of the Police and detailed field mapping by MGSL.

The occupants of squatter structures Nos. RTW/7E/156 and RTW/7E/158 reported as having been alerted by the unusual barking of their dogs at about 8:30 p.m. on 1 September 2001 during heavy rainfall. They subsequently noticed that muddy water was running in the ephemeral drainage line, although the time interval between being alerted by the dogs and noticing the muddy stream was not certain. The four occupants of squatter structures RTW/7E/156 and RTW/7E/158, which were subsequently destroyed by the 1 September 2001 debris flow, decided to vacate their squatter structures shortly afterwards and ran down the steps in front of the squatter structures and made their way across the concrete bridge and steps (between Chainages 200 and 205), which were subsequently also demolished by the debris flow.

Based on the Police reports, it is most likely that the main debris flow occurred at about 10:50 p.m. The incident was first reported to the Police Emergency Unit at 10:55 p.m. The witnesses interviewed include minibus drivers, villagers and the residents of Shek Wah House of Shek Lei Estate. A minibus driver on Route No. 86 reported that his vehicle, while proceeding along Lei Pui Street from the junction at Shek Pai Street and Lei Pui Street, encountered debris on the road and a torrent of water flowing down the road. He reported that the gushing water made him lose control of the vehicle causing a minor accident. The driver also observed a large quantity of soil, water, vegetation, rubbish, kitchen utensils and a cooking gas cylinder being swept down Lei Pui Street towards his minibus. Reports from the Police indicate that they arrived at the scene at 10:58 p.m. in response to the initial emergency telephone call. On arrival, the Police found that both lanes of Lei Pui Street were blocked by landslide debris. Interviewed residents of Shek Wah House reported having heard a loud noise (interpreted to be a dull-sounding, loud noise of short duration) and one reported the smell of fresh vegetation and soil, although none of the witnesses could estimate reliably the timing of these events.

Based on the reported barking of dogs, the muddy water flowing down the drainage

Table of Contents Table of Contents Table of Contents Table of Contents

line and the evacuation of the residents of squatter structures Nos. RTW/7E/156 and RTW/7E/158, it is possible that a part of the source area failed prior to the main debris flow event. The most intense rainfall was recorded between 10:15 p.m. and 10:45 p.m. (Section 7), very shortly before the debris flow which most probably occurred at about 10:50 p.m. (Figure 18).

8. THEORETICAL ANALYSIS OF SLOPE STABILITY AND DEBRIS MOBILITY

8.1 Slope Stability Analysis

8.1.1 General

Theoretical stability analyses of the source area have been carried out to assist in the diagnosis of the mechanisms and causes of the failure. The main objective of the analyses was to investigate the likely range of operational shear strength parameters along the failure surface, corresponding to various possible groundwater levels at the time of failure.

The analyses were based on data obtained from the post-failure ground investigation, laboratory testing, site observations and measurements. A cross-section of the source area, range of groundwater levels and joint roughness angles adopted in the analyses are shown in Figure 19. For the purposes of the analysis, a 1 m thick by 12 m wide by 20 m long rock slab dipping at 41° was assumed. A range of heights of water table was assumed to simulate the possible range of groundwater conditions at the time of failure. The influence of possible cleft water pressure within the rock joints immediately behind the scarp of the failure was also examined.

The results of the analyses are presented in Figure 20 for a range of effective friction angles (ϕ') and apparent cohesion c'_a.

8.1.2 Conditions at Failure

Field observations revealed the primary failure mechanism to be translational sliding along pre-existing, persistent, undulating sheeting joints, with an average inclination of about 41° which are sub-parallel to the ground surface. Mainly moderately, and moderately to highly decomposed granite, with patches of highly and completely decomposed granite and remnant silty sand infill material, were exposed on the surface of rupture. The sheeting joint dilation and infilling exposed in the source area indicate a history of incremental movement.

In the stability analysis, the shear strength of the persistent, wavy sheeting joints is considered to be essentially frictional with an effective friction angle comprising a basic angle of friction (ϕ_b) and an additional joint roughness angle component (i) provided by small and large scale asperities. The work required to dilate joints over asperities is reflected in increased shear strength. Scale effects and joint-wall rock are also considered in the analysis (Barton, 1990).

Derivation of the range of 'i' values from field measurements using the Richards & Cowland approach is shown in Appendix B. This approach assumes that rock-to-rock contact exists over the entire failure surface although the strength of the joint-wall rock and

Table of Contents Table of Contents Table of Contents Table of Contents

the strength and thickness of any joint infilling is not considered. The basic friction angle (ϕ_b), derived from shear box tests on saw-cut samples of granite from the post-landslide ground investigation, was found to vary from 32° to 42°. Other studies in Hong Kong have found typical friction angles of 34° and 38°, for slightly and moderately decomposed granite respectively on saw-cut joints tested in the laboratory (Hencher & Richards, 1982).

Derivation of the range of effective friction angle using Barton's approach is also shown in Appendix B. This approach considers the influence of joint wall compressive strength and scale effects, which directly allow for the increased probability of zones of weaker material occurring over larger joint surfaces. In the application of Barton's approach, the basic friction angle ϕ_b is assumed to be 36°, which was derived from shear box tests on saw-cut samples of granite from the post-landslide ground investigation.

During heavy rain, the near-surface discontinuities within the source area are likely to have been substantially or totally filled with water, and cleft water pressure within the steeply dipping discontinuities is likely to have developed. A range of apparent shear strength in terms of angle of effective friction and apparent cohesion has been calculated for a theoretical factor of safety of 1.0 for different possible water levels below the pre-failure ground surface.

The results of the analyses shown in Figure 20 indicate that for a high groundwater condition, failure could occur with either a high angle of friction (ϕ_b + i) or a high apparent cohesion (c'_a). Alternatively, failure could occur with a combination of relatively modest friction and apparent cohesion values under high groundwater conditions.

8.1.3 Influence of Sheeting Joint Continuity and Interlocking Blocks

The continuity of sheeting joints potentially affects the shear strength by providing shear resistance along the basal surface of rupture. Several breaks in slope or flattened ledges were observed and measured in the field, which may have contributed to some shear resistance. However, no rock 'bridges' were observed in the floor of the source. Interlocking blocks within the flanks of the source area are also a possible source of apparent cohesion, which could provide additional resistance to failure. Minor localised areas were observed to have the presence of sheared intact rock along the edges of protruding blocks (Figure 8 and Plates 32 and 33). Although these locations are small in area, they may still have provided significant shear resistance, as the failed slab is very slender and the shearing forces are relatively low.

8.1.4 Influence of Field Roughness and Waviness

Weathering and infill along a joint surface can significantly reduce the effective shear strength. A Joint Compressive Strength (JCS) value of 2 MPa has been used in the Barton shear strength calculations, as the basal surface of rupture contains significant areas of highly to completely decomposed granite along the sheeting joints. The shear strength is also likely to be reduced significantly when large parts of the rock joint surfaces are not in rock-to-rock contact.

Considering the typical site conditions, the likely operational range of effective angles

Table of Contents
Table of Contents
Table of Contents
Table of Contents

of friction will be between 39° and 53° as indicated in Figure 20. This range has mainly been derived by adding the range of 'I' values derived from the 420 mm plate measurements to the possible range of basic angle of friction which lies between 32° and 42°. The values from the 420 mm plate measurements were used instead of the values obtained from the 210 mm plate because the aperture of the sheeting joints is generally wide and infill extensive. Consideration of the lowest angle of friction (39°) derived from the calculations in Appendix B using Barton's method with correction for scale effects has also been given in setting the lower bound angle of friction at 39°. Assuming fully saturated conditions and an operating range of apparent friction angle of between 39° and 53°, failure could occur within a range of apparent cohesion between 3 kPa and 10 kPa.

8.2 Debris Mobility Analysis

A series of debris mobility calculations (Appendix C) has been carried out to gain an insight into the likely sequence of events and mobility of the debris flow. It should be noted that any computer model of a debris flow will inevitably be a major simplification of the process, owing to the highly complex nature of this type of event. The key assumptions of the debris flow runout model used are given in Appendix C. The parameters used are presented below. Several analyses were carried out, with the debris parameters, volume of entrainment and deposition directly affecting the thrust on the debris front being adjusted to obtain best-fit velocities and average debris heights as compared with the field measurements.

The initial mass after commencement of failure was modelled as a 0.75 m thick by 15 m wide sheet of saturated solids inclined at 41° with a saturated unit weight of 24 kN/m^3. An equivalent total stress bulk friction angle (ϕ_{bulk}) of 18.6°, zero turbulence and a velocity of 0.01 m/s were assumed to represent the initial conditions. The parameters of the debris were gradually changed to simulate the breaking-up and mixing of the mass as it cascaded down the cliff. Beyond Chainage 50, it was assumed that the mass comprised a mixture of failed colluvium, boulders and entrained material with a saturated unit weight of 19.7 kN/m^3 and a total stress bulk friction angle of 11.3°. A Voellmy turbulence coefficient of 500 m/s^2 was also assumed.

The back-analysed velocity profile indicates an impact velocity of about 14 m/s at the base of the cliff, and velocities of between 8 m/s and 11 m/s along the upper trail to Chainage 125. The velocity sharply reduces to about 5 m/s on the flat-lying abandoned squatter platform between Chainages 125 and 145, before accelerating to about 14 m/s over the steep, rocky slope between Chainages 145 and 173. The demolished squatter structures Nos. RTW/7E/156 and RTW/7E/158 were located at Chainage 168, where the calculated velocity is about 10 m/s. A volume of about 50 m^3 of immediate entrainment of colluvium and saprolite at the base of the cliff gives a good match between the calculated and measured average height profiles up to Chainage 190 at the junction with sub-catchment B.

In order to match the field estimates of velocity and debris height below Chainage 190, approximately 80 m^3 of active debris has to be lost from the debris front and the total stress bulk friction angle probably reduced to about 8°. It was observed that about 12 m^3 of fresh debris consisting of boulders up to 1 m in length was found to be scattered up the streamcourse of sub-catchment B for about 15 m. It is considered that a much larger amount of bouldery debris front material would have been initially deposited at this location. Using

Table of Contents
Table of Contents
Table of Contents
Table of Contents

the United States Department of Agriculture Soil Conservation Service (SCS) Unit Hydrograph Method (Chow et al, 1988) and adopting the rainfall intensity profile as recorded by the nearest automatic raingauge No. N06 on 1 September 2001, a range of run-off coefficients between 0.7 and 0.96 (having regard to the vegetation cover and the likely degree of ground saturation) were derived which represent runoff within sub-catchment B. These correspond to calculated discharge rates of between 2 m^3/s and 3 m^3/s in terms of surface runoff. The removal of bouldery material and the mixing with flood-water from sub-catchment B is considered likely to have increased the mobility of the initial debris front.

Beyond the confluence with sub-catchment B, the velocity gradually reduces to about 4 m/s by the lower end of the upper drainage channel at Chainage 270. After cascading over the quarry face at Chainage 280, the debris began to spread out and deposit on the floor of the active construction site at about Chainage 320, where the debris front had very little active thrust and was rapidly decelerating. The calculated velocity at Chainage 305 (i.e. corner of the pump-house) is approximately 4 m/s.

The total length of time between failure at the source and deposition of the debris front at Chainage 320 was calculated in the model to be 47 seconds. In view of the good match with the field data and measurements (Figure C1), the model is considered to represent a reasonable approximation of the mobility of the debris front.

9. DIAGNOSIS OF THE LANDSLIDE

9.1 Mode and Sequence of Failure at the Source

The main failure at the source probably occurred at about 10:50 p.m. on 1 September 2001 and involved a rockfall with some overlying colluvium. The failure took place by translational sliding along adversely dipping sheeting joints in the source area between Chainages 0 and 24, at an elevation of between 210 mPD and 233 mPD. The morphology of the source area indicates that the initial failure may have taken place in the lower half of the source area (where there is a greater depth of depletion) with subsequent, probably rapid, detachment of material in the upper half of the source area (shallower depth of depletion) occurring due to loss of toe support.

The first indications of an imminent failure were about two hours earlier when the occupants of squatter structures Nos. RTW/7E/156 and RTW/7E/158 were alerted by the barking of their dogs and appearance of muddy water flowing along the drainage line. As a consequence, they chose to vacate their dwellings despite heavy rainfall at the time. It is possible that the dogs heard the sound of an initial landsliding (which could comprise some local detachments), a harbinger of the main event. No direct evidence of such an early failure could be found on site, owing to the widespread disturbance of the ground caused by the main debris flow.

9.2 Initiation Mechanisms and Probable Causes of Failure

The landslide involved failure on two adversely orientated sets of rock joints, namely a series of sheeting joints (Set 1) and sub-vertical joints (Set 2), which are sub-parallel to the strike of the Set 1 joints and form overhanging release surfaces for sliding. It is likely that

Table of Contents
Table of Contents
Table of Contents
Table of Contents

infiltration, particularly during the period of heavy rain between 8:30 p.m. and about 10:50 p.m., led to the build up of cleft water pressures in the sub-vertical rock joints and groundwater pressure at the basal joint planes causing a number of blocks to become unstable.

The theoretical slope stability analyses have shown that sliding failure of the rock mass could occur with an unfavourable combination of factors, including friction angle, undulations and waviness of the sheeting joints and properties of the infill (where present), steepness of the sliding surface and build up of water pressure within the joints. It is also possible that an individual block along the edges of the landslide scar could remain in place by interlocking with adjacent blocks and slabs although deterioration of the joint condition due to small intermittent downhill movements over time (possibly due to heavy rainstorms in the past) could have led to progressive loosening and gradual reduction in shearing resistance. Therefore apparent equilibrium may be maintained for many years until the joints weaken or key blocks move beyond a certain threshold, which then allows failure during a comparatively unexceptional rainstorm.

The occurrence of dilated, infilled joints is evidence of general deterioration, relaxation and previous small-scale movements of the near-surface rock mass. Initially, such deterioration could be accounted for by stress relief within the near-surface rock mass and/or the effects of past heavy rainstorms, causing progressive opening up of joints, with subsequently increased infiltration of water, weathering and sediment infilling over time.

9.3 Transport Mechanisms and Mobility of the Landslide Debris

The debris resulting from the landslide at the source area is considered to comprise rock boulders and possibly some colluvium. The landslide debris is likely to have cascaded over the steep cliff immediately below the source area and developed into a debris flow. The estimated total active volume of the landslide was about 780 m^3.

At the base of the cliff, especially below the north side of the source area where the thickness of detached rock is greatest, the impact of the debris would have resulted in displacement and entrainment of the colluvium (up to 1 m thick) and saprolite present at this location (Plate 5). As the thin regolith was probably fully saturated during the heavy rain, fluidisation upon impact by the landslide debris involving undrained loading of the saturated regolith, would probably have also contributed to the development of the debris flow.

During the initial fall, it is also possible that a number of boulders bounced on the rocky, lower portion of the cliff and became airborne. Some of the clastic debris and large boulders, which had been deposited on the flanks of the upper debris trail may have been transported by this means. From close examination of the erosion channels and flattened vegetation below the cliff in the upper part of the debris trail, the bulk of the debris appears to have acted as a debris flow.

Approximately 450 m^3 of colluvium and saprolite was eroded by the debris flow in the upper part of the trail between Chainages 50 and 125. Most of this material was probably entrained directly by the debris flow, but a small proportion may have been eroded by overland flow, after the debris flow had removed the protective layer of vegetation. The debris marks along the sides of the trail were observed to be relatively low, indicating that the

Table of Contents
Table of Contents
Table of Contents
Table of Contents

debris probably travelled as an elongated mass, possibly in more than one phase.

Between Chainages 125 and 145, the debris trail flattens and widens out to about 25 m, at the location of a former squatter platform (Drawing No. 1). At Chainage 137, the superelevation estimated from the positions of the marks on the sides of the debris trail indicates that the flow velocity was about 5 m/s and the fact that the debris on the squatter platform was fine-grained suggests that it was probably deposited after the passage of the main debris front.

Below the former squatter platform, the debris flow cascaded over steep (about 35° to 45°) rock slabs, and demolished squatter structures Nos. RTW/7E/156 and RTW/7E/158, which were located on a small platform near the base of the rock slabs at Chainage 168. The force of the debris was sufficient to flatten and transport the flimsy structures by about 10 m down the drainage line, depositing the remains on the north flank of the debris trail against a lamp post, which was partly overturned. At the location of the squatter structures, a velocity of about 10 m/s has been estimated from the debris mobility analysis.

At the confluence of the drainage line and the ephemeral streamcourse (Chainage 190), the debris flowed towards the northwest, changing direction by about 85°. Above the confluence, sub-catchments A and B have plan areas of approximately 26,000 m^2 and 83,700 m^2 respectively and hence a considerable amount of additional surface water could have been injected into the debris flow at this point. At the time of the incident, the discharge from sub-catchment B is estimated to have been about 2 m^3/s to 3 m^3/s.

About 12 m^3 of debris, consisting of boulders up to 1 m long, was found to have been deposited along the streamcourse of sub-catchment B over a length of some 15 m near the confluence. The sharp change in direction of the debris flow at this location probably caused a much larger volume of bouldery debris from the debris front to be deposited, forming a dam across the streamcourse which drains sub-catchment B. The dam could have deflected any new debris arriving from the uphill area and at the same time floodwater (from sub-catchment B) could have backed up behind the dam. Based on field mapping observations of flow marks and debris location, it is postulated that the dam probably breached, after the build-up of a sufficient head of water over an estimated period of 2 minutes to 5 minutes. The sudden surge of floodwater following the dam break would have been enough to rejuvenate the debris flow and remobilise most of the bouldery material forming the dam.

The removal of bouldery material from the debris front and mixing with floodwater from sub-catchment B probably enhanced the mobility of the initial debris front below Chainage 190, enabling it to travel along the flatter section of the streamcourse which has an overall gradient of about 1 in 7 (i.e. about 8°) between Chainages 190 and 270.

Analysis of the impact and extent of damage to the reinforced concrete wing wall at Chainage 243 indicates that the velocity of the initial debris front was probably of the order of about 8 m/s at this location. The flat profile and energy loss by frictional contact with the underlying construction materials and the energy absorbed by the hoardings, which were crushed and transported between Chainages 243 and 270, would have caused the debris flow to slow down. In parallel with this, approximately 80 m^3 of remoulded debris was deposited along the north side of the concrete drainage channel. The hoardings at Chainage 270

Table of Contents
Table of Contents
Table of Contents
Table of Contents

probably prevented the north wing wall at the outlet of the drainage channel from being demolished by absorbing some energy through deflection and deformation. Analysis of the curved trajectories of scour marks (caused by the transported boulders within the concrete channel) on the south wall at the end of the drainage channel behind the crest of slope No. 7SW-C/C182, indicates an average debris velocity of about 4 m/s.

On entering the active construction site, the debris cascaded onto the floor of the site and, by spreading out, would have lost a considerable amount of velocity and momentum. Much of the debris came to rest against the hoardings and fence around the compound on the northeast of the pump house and the fences in front of the footbridge and steel gantry, where the thickness was approximately 1 m. The relatively minor damage to these hoardings and fences indicates that the debris front was probably moving slowly at this location.

Analysis of the debris flow indicates that the initial debris front probably travelled from the source area to the lower edge of the active construction site in less than about 50 seconds. As most of the coarse debris was deposited within the active LPM construction site above Lei Pui Street, it is considered that the debris flow essentially terminated within the disused quarry. The travel angle of the channelised debris flow (disregarding the outwash material) is about 23°. The comparatively light construction of the temporary fences and hoardings that successfully retained the coarse debris indicates that the velocity and momentum of the debris flow had substantially reduced after impacting the floor of the active construction site.

10. CONCLUSIONS

The 1 September 2001 debris flow, which occurred on the hillside above Lei Pui Street, Shek Lei Estate, Kwai Chung, was probably triggered by infiltration through shallow colluvium (talus) and the subsequent development of cleft water pressures within joints in the underlying granite rock mass during severe rainfall preceding the failure. The estimated total active volume of the channelised debris flow was about 780 m^3. Most of the debris was deposited within an active construction site just above Lei Pui Street and about 50 m^3 of outwash material entered Lei Pui Street, Shek Pai Street and some open areas in Shek Lei Estate, as a result of which Lei Pui Street was closed for 3 days. No casualties were reported.

The rainstorm, with a return period of about 14 years, was slightly less severe, in terms of short to medium-duration rainfall, than the May 1993 and May 1997 rainstorms, which are the two most severe rainstorms recorded in the area since June 1983, when the nearest automatic raingauge was installed. The rainstorm preceding the landslide was not exceptionally heavy. This suggests that progressive deterioration of the marginally stable hillside at this location probably played a significant role in the 1 September 2001 debris flow.

The hillside has a history of both soil and rock failures. In particular, structurally controlled rock slides are vulnerable to rain-induced failures owing to the unfavourable orientation of the sheeting joints and a steeply dipping major joint set that strikes across the hillside to form potential release surfaces and tension cracks. The sheeting joints daylight in the steep cliff below the landslide source and theoretical stability analysis has demonstrated the potential for rock mass translational failure by sliding along the steeply dipping joints (with an average dip of about 41°) as a result of infiltration and the associated increase in basal joint and cleft water pressures.

Table of Contents
Table of Contents
Table of Contents
Table of Contents

The shearing resistance necessary to maintain equilibrium during previous periods of heavy rain was probably provided by the roughness and lack of large-scale persistence of the sheeting joints in addition to the arching and interlocking of the blocks of rock, both parallel and normal to the hillside. However, progressive weathering, dilation, infilling of joints and rotation of the 'key blocks' probably reached the critical point, where the reduction in effective shear strength was sufficient to trigger the failure of rock slabs in the source area of the landslide during the heavy rainstorm on 1 September 2001.

The scale of the initial landslide at the source, with a volume of about 250 m^3, was relatively modest but the landslide debris descended over a steep rock cliff immediately in front of the source area, thereby gaining further energy to continue down the hillside. Upon impacting the colluvium at the toe of the cliff, fluidisation of the material possibly occurred due to undrained loading effects and the generation of excess pore water pressures of the probably wet material. The wet landslide debris incorporating a fluidised mass flowed along a drainage line, mixing with more surface water and further increasing the debris mobility. In this upper section of the landslide debris trail (between Chainage 45 and Chainage 135), a further 455 m^3 of material was entrained from the predominantly colluvium and saprolite substrate.

At about Chainage 168, the debris flow cascaded over steep rock slabs and demolished squatter structures Nos. RTW/7E/156 and RTW/7E/158, which were located on a small platform. The confluence of the debris flow with the streamcourse draining sub-catchment B at Chainage 190 probably increased the mobility of the debris by the injection of additional floodwater from sub-catchment B following the breaching of a temporary debris dam at this location. The temporary debris dam had probably built up because the debris mass had to change direction by about 85° at this point.

As most of the coarse debris was deposited within the active construction site above Lei Pui Street, it is considered that the debris flow essentially terminated within the quarry. The travel angle of the debris flow (disregarding the outwash material) is about 23°. Outwash from the landslide debris flowed around the WSD compound and spilled over the crest of slope No. 7SW-C/C180, partly damaging the temporary fence at the toe of the slope along Lei Pui Street.

The occupants of squatter structures Nos. RTW/7E/156 and RTW/7E/158 evacuated from their dwellings about two hours before the debris flow event took place. Had they remained in their dwellings they would almost certainly have been injured and possibly would have perished. Furthermore, potential casualties could have been extremely serious were it not for the NDC Programme of squatter clearance, which was carried out on the lower hillside and the disused quarry in 1985 and 1995 respectively, together with the clearance carried out within the LPM construction site in 2000 for the temporary possession of land for the upgrading works on cut slope No. 7SW-C/C180.

11. REFERENCES

Addison, R. (1986). Geology of Sha Tin, Geotechnical Control Office, Hong Kong, 85 p. (Hong Kong Geological Survey Memoir No. 1).

Table of Contents

Table of Contents

Table of Contents

Table of Contents

Ayotte, D., Evans, N. & Hungr, O. (1999). Runout analysis of debris flows and avalanches in Hong Kong. Proceedings of the Symposium on Slope Stability and Landslides, organised by the Vancouver Geotechnical Society, Vancouver, B.C., Canada, May 1999, pp 39-46.

Bagnold, R.A. (1954). Experiments on a gravity-free dispersion of large solid spheres in a Newtonian fluid under shear. Proceedings of the Royal Society of London, Series A 225, pp 49-63.

Barton, N. (1990). Scale effects or sampling bias. Scale Effects in Rock Masses, Balkema, Rotterdam, edited by Pino da Cunha, pp 31-55.

Barton, N.R. & Bandis, S.C. (1990). Review of predictive capabilities of JRC-JCS model in engineering practice. Proceedings of the International Symposium on Rock Joints, Balkema, Rotterdam, edited by N. Barton and O. Stephansson, pp 603-610.

Chen, P.Y.M. (1994). Methods of Tests for Soils in Hong Kong for Civil Engineering Purposes (Phase 1 Tests). Geotechnical Engineering Office, Hong Kong, 91 p. (GEO Report No. 36).

Chow, V.T., Maidment, D.R. & Mays, L.W. (1988). Applied Hydrology - McGraw Hill International Editions, Civil Engineering series, pp 201-234.

Evans, N.C., Huang, S.W. & King, J.P. (1997). The Natural Terrain Landslide Study Phases I and II. Special Project Report No. SPR 5/97, Geotechnical Engineering Office, Hong Kong, 199 p. plus 2 drawings.

Evans, N.C. & Yu, Y.F. (2001). Regional Variation in Extreme Rainfall Values. Geotechnical Engineering Office, Hong Kong, 81 p. (GEO Report No. 115).

Geotechnical Control Office (1986). Solid and Superficial Geology of Sha Tin, Hong Kong Geological Survey, Map Series HGM20, Sheet 11, 1:20 000 scale. Geotechnical Control Office, Hong Kong, 1 map.

Geotechnical Control Office (1987). Geotechnical Area Studies Programme - Central New Territories. Geotechnical Control Office, Hong Kong, GASP Report No. II, 165 p., plus 4 maps.

Geotechnical Control Office (1998). Guide to Rock and Soil Descriptions (Geoguide 3). Geotechnical Control Office, Hong Kong, 189 p.

Hencher, S.R. & Richards, L.R. (1982). The basic frictional resistance of sheeting joints in Hong Kong granite. Hong Kong Engineer, vol. 11, No. 2, pp 21-25.

Hencher, S.R. & Richards, L.R. (1989). Laboratory direct shear testing of rock discontinuities. Ground Engineering, vol. 22, No. 2, pp 24-31.

Hoek, E., Kaiser, P.K. & Bawden, W.F. (1995). Support of Underground Excavations in Hard Rock. A.A. Balkema, Rotterdam, 215 p.

Table of Contents
Table of Contents
Table of Contents
Table of Contents

Hungr, O., Morgan, G.C. & Kellerhals, R. (1984). Quantitative analysis of debris torrent hazards for design of remedial measures. Canadian Geotechnical Journal, vol. 21, pp 663-677.

Hungr, O. (1995). A model for the runout analysis of rapid flow slides, debris flows, and avalanches. Canadian Geotechnical Journal, vol. 32, pp 610-623.

Hungr, O., Sun, H.W. & Ho, K.K.S. (1999). Mobility of selected landslides in Hong Kong - pilot back-analysis using a numerical model. Proceedings of the HKIE Geotechnical Division Seminar on Geotechnical Risk Management, May 1999, Hong Kong Institution of Engineers, pp 169-175.

King, J.P. (1996). The Tsing Shan Debris Flow. Special Project Report No. SPR 6/96, Geotechnical Engineering Office, Hong Kong, 3 volumes, 427 p., 129 p. & 166 p.

King, J.P. (1997). Natural Terrain Landslide Study - The Natural Terrain Landslide Inventory. Technical Note TN 10/97, Geotechnical Engineering Office, Hong Kong, 116 p.

King, J.P. (1999). Natural Terrain Landslide Study - The Natural Terrain Landslide Inventory. Geotechnical Engineering Office, Hong Kong, 127 p. (GEO Report No. 74).

Lam, C.C. & Leung, Y.K. (1994). Extreme Rainfall Statistics and Design Rainstorm Profiles at Selected Locations in Hong Kong. Royal Observatory, Hong Kong, Technical Note No. 86, 89 p.

Lo, D.O.K. (2000). Review of Natural Terrain Landslide Debris-resisting Barrier Design. Geotechnical Engineering Office, Hong Kong, 91 p. (GEO Report No. 104).

Maunsell Geotechnical Services Ltd. (2000). Detailed Design of Check Dam at Sham Tseng San Tsuen, Debris Flow Barrier (Check Dam) Design, Vol. I & II. Report prepared for Geotechnical Engineering Office, Hong Kong, 116 p. plus Appendices A-H.

Ng, K.C., Parry, S., King, J.P., Franks, C.A.M., & Shaw, R. (2002). Guidelines For Natural Terrain Hazard Studies. Special Project Report No. SPR 1/2002, Geotechnical Engineering Office, Hong Kong.

Richards, L.R. & Cowlands, J.W. (1982). The effect of surface roughness on the field shear strength of sheeting joints in Hong Kong granite. Hong Kong Engineer, vol. 11, No. 10, pp 39-43.

Sewell, R.J., Campbell, S.D.G., Fletcher, C.J.N., Lai, K.W. & Kirk, P.A. (2000). The Pre-Quaternary Geology of Hong Kong, Hong Kong Geological Survey Memoir, Geotechnical Engineering Office, Hong Kong, 181 p plus 1 map.

Strange, P.J. & Shaw, R. (1986). Geology of Hong Kong Island and Kowloon, Geotechnical Control Office, Hong Kong, 134 p. (Hong Kong Geological Survey Memoir No. 2).

Table of Contents
Table of Contents
Table of Contents
Table of Contents

Takahashi, T. & Yoshida, H. (1979). Study on the Deposition of Debris Flows, Part I - Deposition due to Abrupt Change in Bed Slope. Annuals, Disaster Prevention Research Institute, Kyoto University, vol. 22, paper B-2.

Wong, H.N. & Ho, K.K.S. (1996). Travel distance of landslide debris. Proceedings of the Seventh International Symposium on Landslides, Trondheim, Norway, vol. 1, pp 417-422.

Table of Contents

Table of Contents

Table of Contents

Table of Contents

LIST OF TABLES

Table of Contents
Table of Contents
Table of Contents

Table 1 - Maximum Rolling Rainfall at GEO Raingauge No. N06 for Selected Durations Preceding the Landslide of 1 September 2001 and the Estimated Return Periods

Duration	Maximum Rolling Rainfall (mm)	End of Period	Estimated Return Period (Years) (See Note 2)
5 Minutes	12.0	22:45 hours on 1 September 2001	< 2
15 Minutes	30.0	22:30 hours on 1 September 2001	3
1 Hour	97.0	22:50 hours on 1 September 2001	8
2 Hours	154.5	22:50 hours on 1 September 2001	14
4 Hours	163.0	22:50 hours on 1 September 2001	5
12 Hours	181.5	22:50 hours on 1 September 2001	2
24 Hours	202.5	22:50 hours on 1 September 2001	< 2
48 Hours	208.5	22:50 hours on 1 September 2001	< 2
4 Days	371.5	22:50 hours on 1 September 2001	3
7 Days	405.5	22:50 hours on 1 September 2001	3
15 Days	406.0	22:50 hours on 1 September 2001	< 2
31 Days	506.5	22:50 hours on 1 September 2001	< 2

Notes:
(1) Maximum rolling rainfall was calculated from 5-minute rainfall data.
(2) Return periods were derived from Table 3 of Lam & Leung (1994) and using data from Evans & Yu (2000). The return periods obtained by the two methods do not show a significant difference.
(3) The use of 5-minute data for return period of rainfall durations between 2 hours and 31 days results in better data resolution, but may slightly over-estimate the return periods using Lam & Leung (1994)'s data, which are based on hourly rainfall for these durations.
(4) The time of landslide was around 10:30 to 11:00 pm of 1 Septembber 2001, according to the eyewitnesses and the Hong Kong Police Force's record. For the purpose of rainfall analysis, the time of landslide was assumed to be 10:50 p.m.
(5) The nearest GEO raingauge to the landslide site is raingauge No. N06 situated at about 0.5 km to the west of the site.

Table of Contents
Table of Contents
Table of Contents
Table of Contents

Table 2 - Summary of Laboratory Test Results

A. Classification and Index Test

Sample Location	Sample Depth below Ground Level (m)	Material Type	Sample Type	Particle Size Distribution: Gravel (%)	Particle Size Distribution: Sand (%)	Particle Size Distribution: Silt (%)	Particle Size Distribution: Clay (%)	Liquid Limit (%)	Plastic Limit (%)
TP 5	0.5	Coll / Debris Flow Deposit	Bulk	7	40	17	36	75	31
	1.0	Residual Soil	Bulk	10	41	18	31	76	31
	2.5	CDG	Bulk	10	43	20	27	71	31
TP 6	1.0	Coll / Debris Flow Deposit	Bulk	40	40	10	10	46	21
	2.0	Coll / Debris Flow Deposit	Bulk	37	44	11	8	49	22
TP 7	0.5	Coll / Debris Flow Deposit	Bulk	30	48	11	11	50	23
	1.5	Coll / Debris Flow Deposit	Bulk	21	53	12	14	58	26
	2.5	CDG	Bulk	17	58	10	15	55	25
TP 8	0.5	Coll / Debris Flow Deposit	Bulk	31	50	12	7	36	21
TP 9	0.5	Coll / Debris Flow Deposit	Bulk	20	48	15	17	60	27
	1.5	Residual Soil	Bulk	15	46	15	24	71	31
	2.5	CDG	Bulk	13	65	12	10	56	34
TP 10	0.5	Residual Soil	Bulk	20	48	14	18	52	26
	1.0	Residual Soil	Bulk	9	52	20	19	56	28

B. Shear Box Test

Sample Location	Sample Depth below Ground Level (m)	Joint Type	Peak Shear Strength (uncorrected)	Basic Shear Strength (corrected)
DH 2 (1)	4.30	Natural	55	38
DH 2 (6)	4.78	Natural	52	42
DH 2 (14)	9.61	Natural	46	37
DH 2 (3)	5.76	Saw-cut	36	34
DH 2 (5)	5.76	Saw-cut	36	32
DH 6 (10)	14.75	Saw-cut	43	42

Legend:

Coll Colluvium CDG Completely Decomposed Granite

Notes: (1) Laboratory Tests carried out by Public Works Central Laboratory (August 2002).
(2) See Figure 12 for Location of Drillholes and Trial Pits.

Table of Contents
Table of Contents
Table of Contents
Table of Contents

LIST OF FIGURES

Table of Contents
Table of Contents
Table of Contents

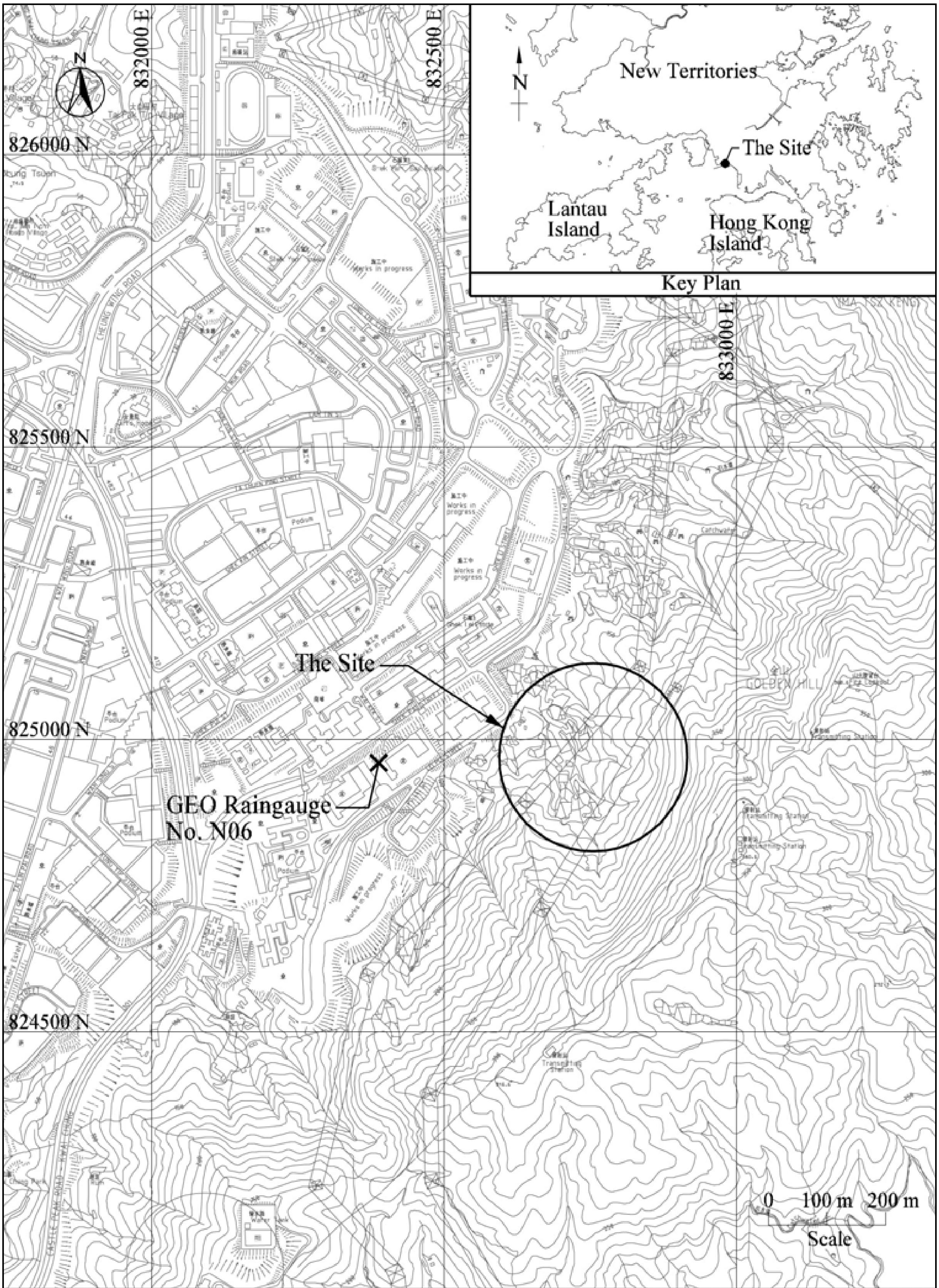

Note : Base plan is extracted from 1 : 1000 survey sheets Nos. 11NW2A, 2B, 2C and 2D dated 2001.

Figure 1 - Location Plan

Table of Contents
Table of Contents
Table of Contents
Table of Contents

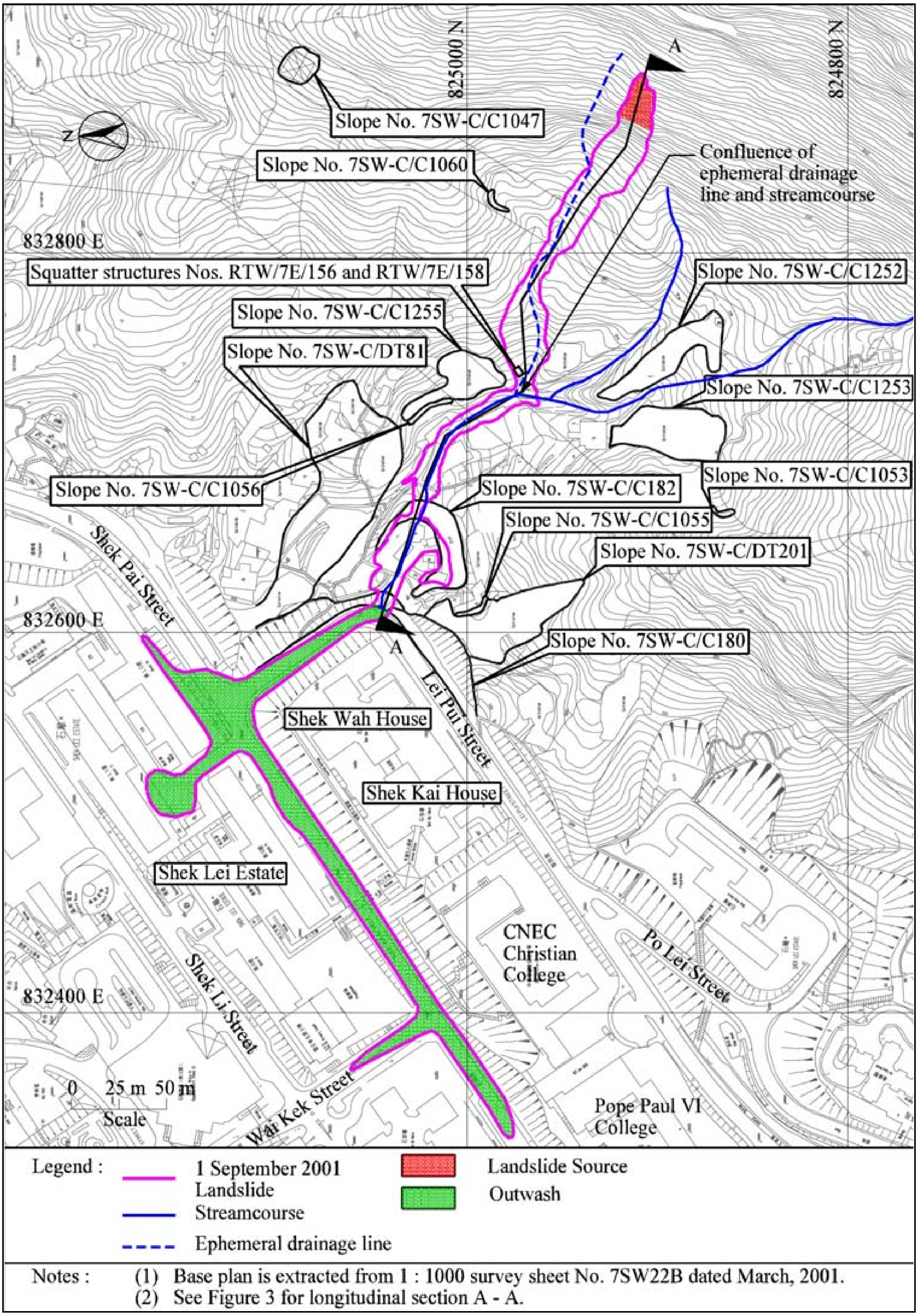

Figure 2 - Site Plan

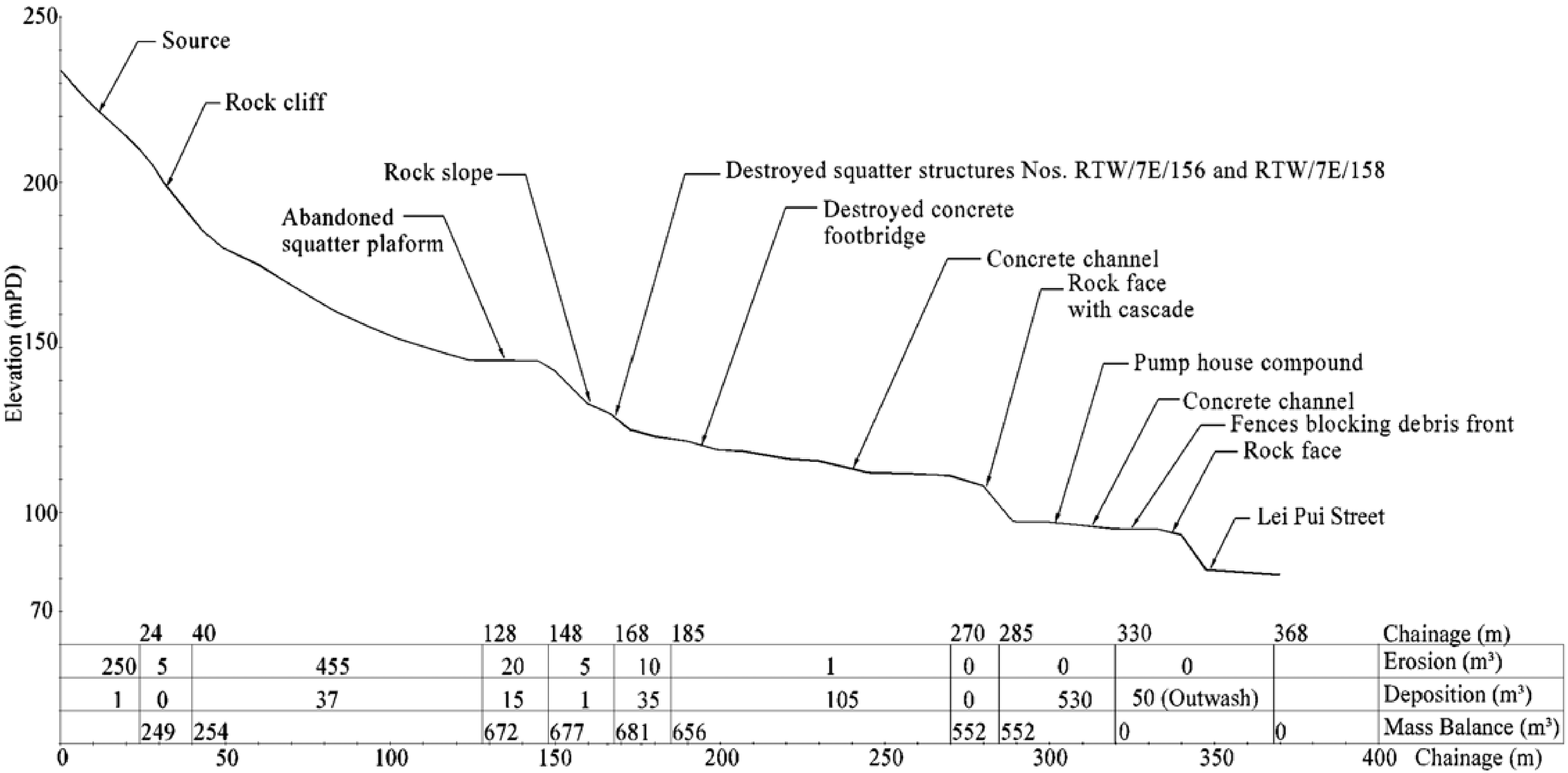

Chainage (m)	0	24	40	128	148	168	185	270	285	330	368
Erosion (m³)	250	5	455	20	5	10	1	0	0	0	
Deposition (m³)	1	0	37	15	1	35	105	0	530	50 (Outwash)	
Mass Balance (m³)		249	254	672	677	681	656	552	552	0	0

Note : See Figure 2 for location of Section.

Figure 3 - Longitudinal Section (A - A) of the Source and Debris Trail

Table of Contents Table of Contents Table of Contents Table of Contents

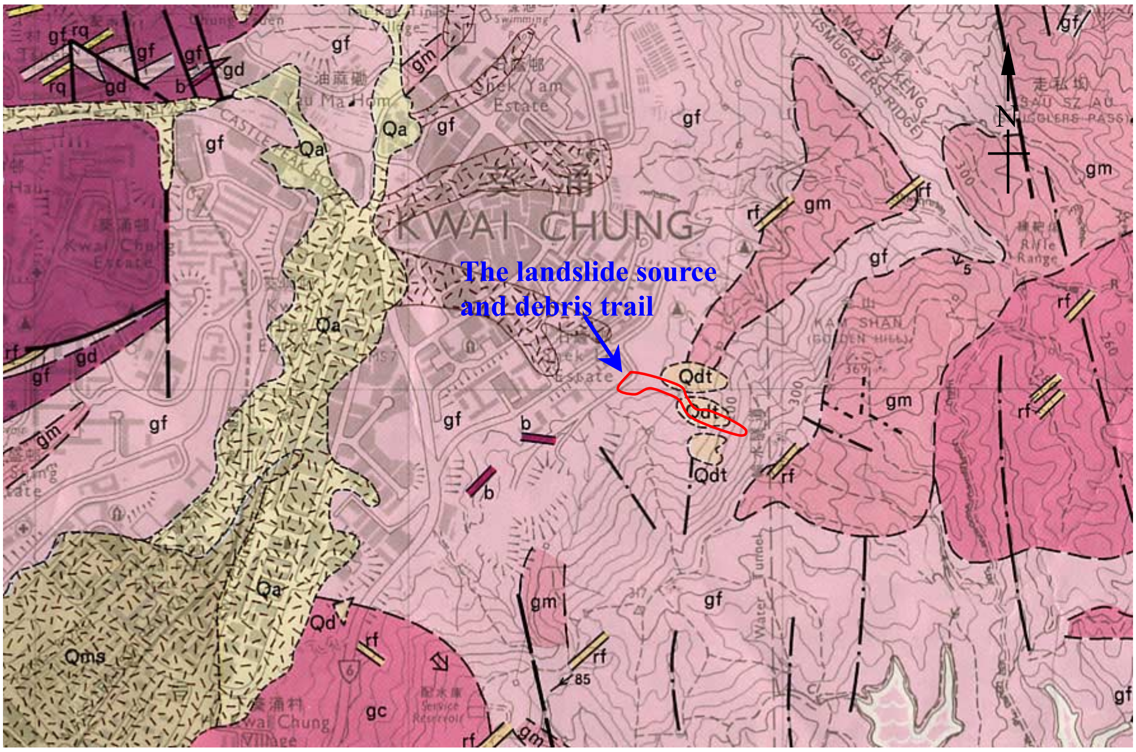

LEGEND:

0 m — 1000 m
Scale

SUPERFICIAL DEPOSITS

Qa	Pleistocene and Holocene Clay/silt, sand and gravel (Alluvium)
Qdt	Holocene and Pleistocene Mixed Qd and Qt (Mixed debris flow and talus deposits) Qd - Unsorted sand, gravel, cobbles and boulders; clay/silt matrix Qt - Gravel, cobbles and boulders; sparse finer-grained matrix

SOLID GEOLOGY

b	Basalt
rq	Quartzphyric rhyolite
rf	Feldsparphyric rhyolite
gf	Fine-grained granite
gm	Medium-grained granite
gc	Coarse-grained granite
gd	Granodiorite

GEOLOGICAL LINES

- Geological boundary, superficial deposits
- Geological boundary, solid rock (* Broken lines denote uncertainty)
- Fault (crossmark indicates downthrow side)
- Mineral vein
- Photogeological lineament

STRUCTURAL SYMBOLS

- 22 Intrusive contact

MISCELLANEOUS SYMBOLS

- Mine adit, abandoned

Note: Extracted from Hong Kong Geological Survey, Map Series HGM20, Sheet No. 7, 1:20 000 scale (GCO, 1986)

Figure 4 - Regional Geology

Table of Contents
Table of Contents
Table of Contents
Table of Contents

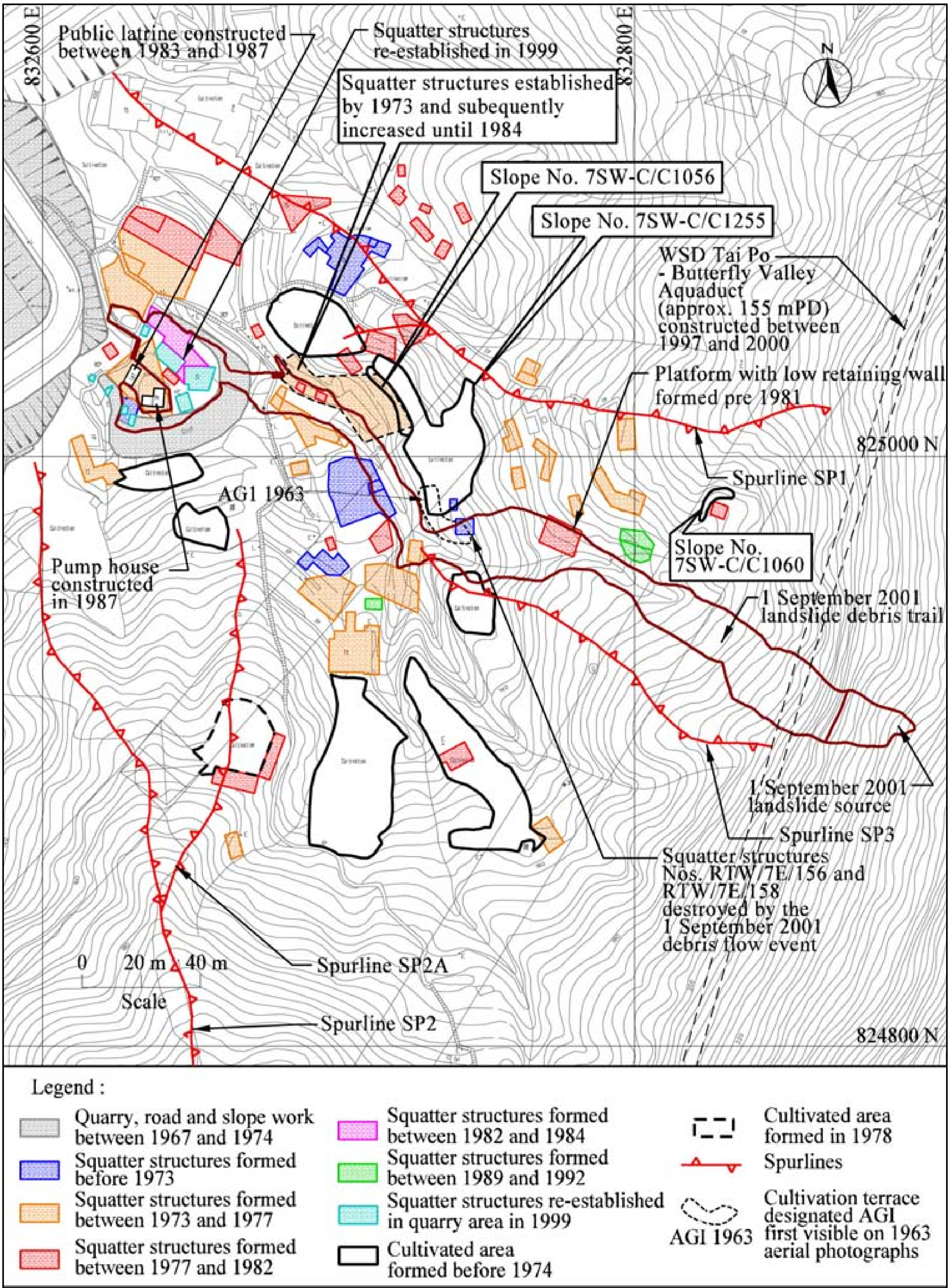

Notes : (1) Base plan is extracted from 1 : 1000 survey sheet No. 7SW22B dated March, 2001.
(2) No significant establishment of squatter structures between 1984 and 1989.

Figure 5 - Site Development History

Table of Contents
Table of Contents
Table of Contents
Table of Contents

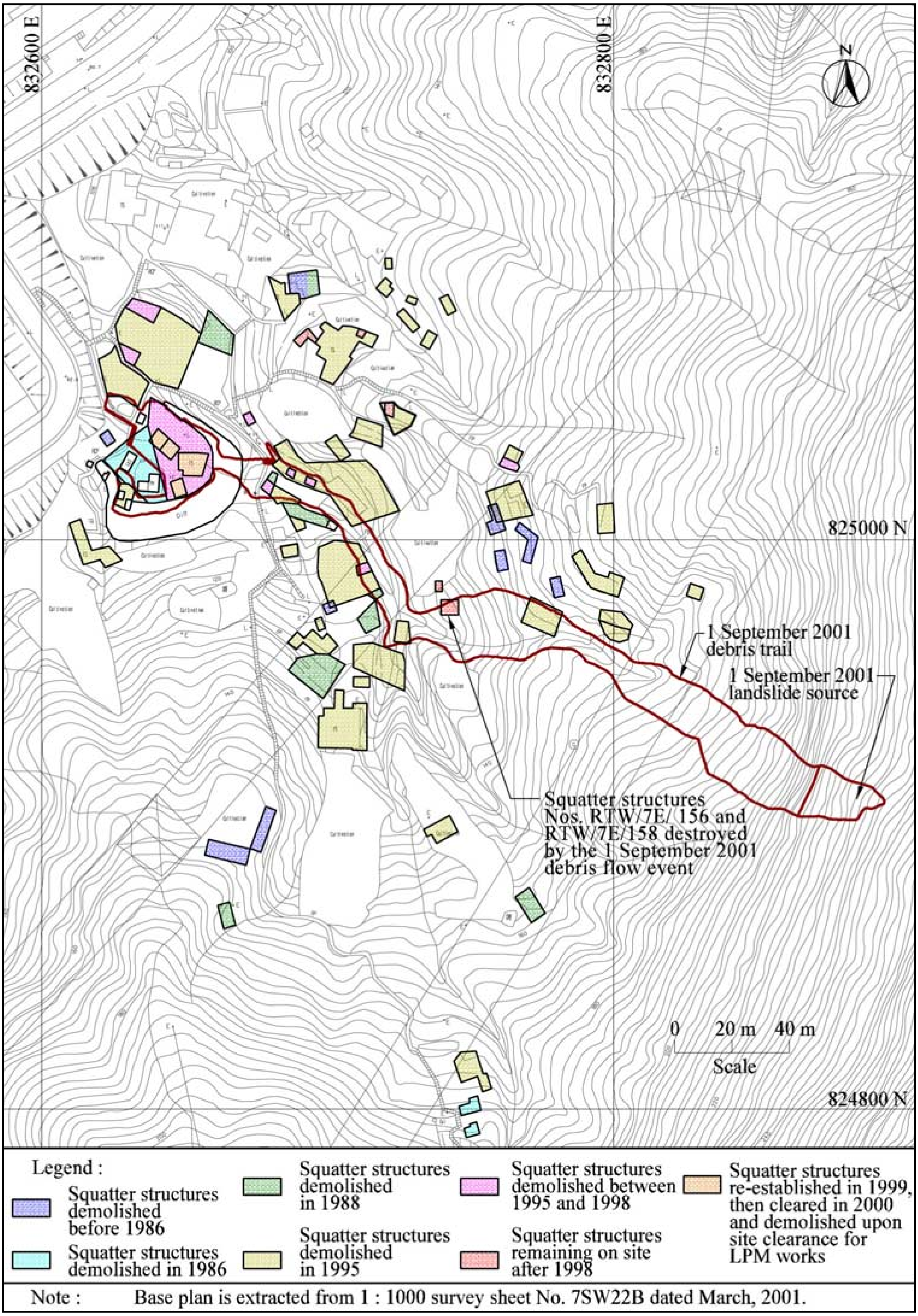

Figure 6 - Demolition History of Squatter Structures

Table of Contents
Table of Contents
Table of Contents
Table of Contents

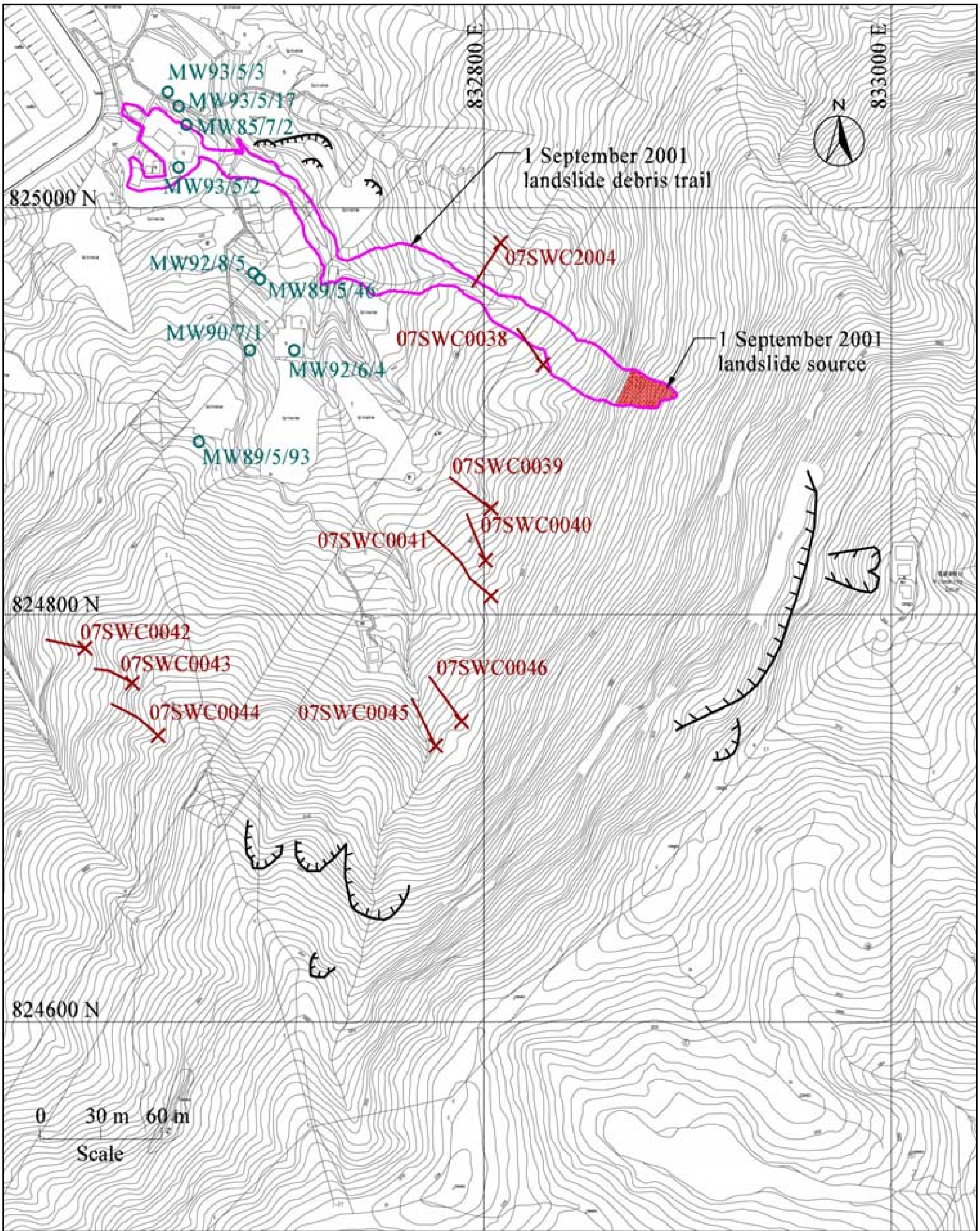

Legend :

07SWC0043 NTLI No. 7SWC0043

MW89/5/93 GEO Incident No. MW89/5/93

Possible relict landslide scars identified from the Stage 3 Study Report S3R 118/2000

Note : Base plan is extracted from 1 : 1000 survey sheets Nos. 7SW22B, 7SW22D, 7SW23A and 7SW23D dated 2001.

Figure 7 - Previous Recorded Landslides

Table of Contents Table of Contents Table of Contents Table of Contents

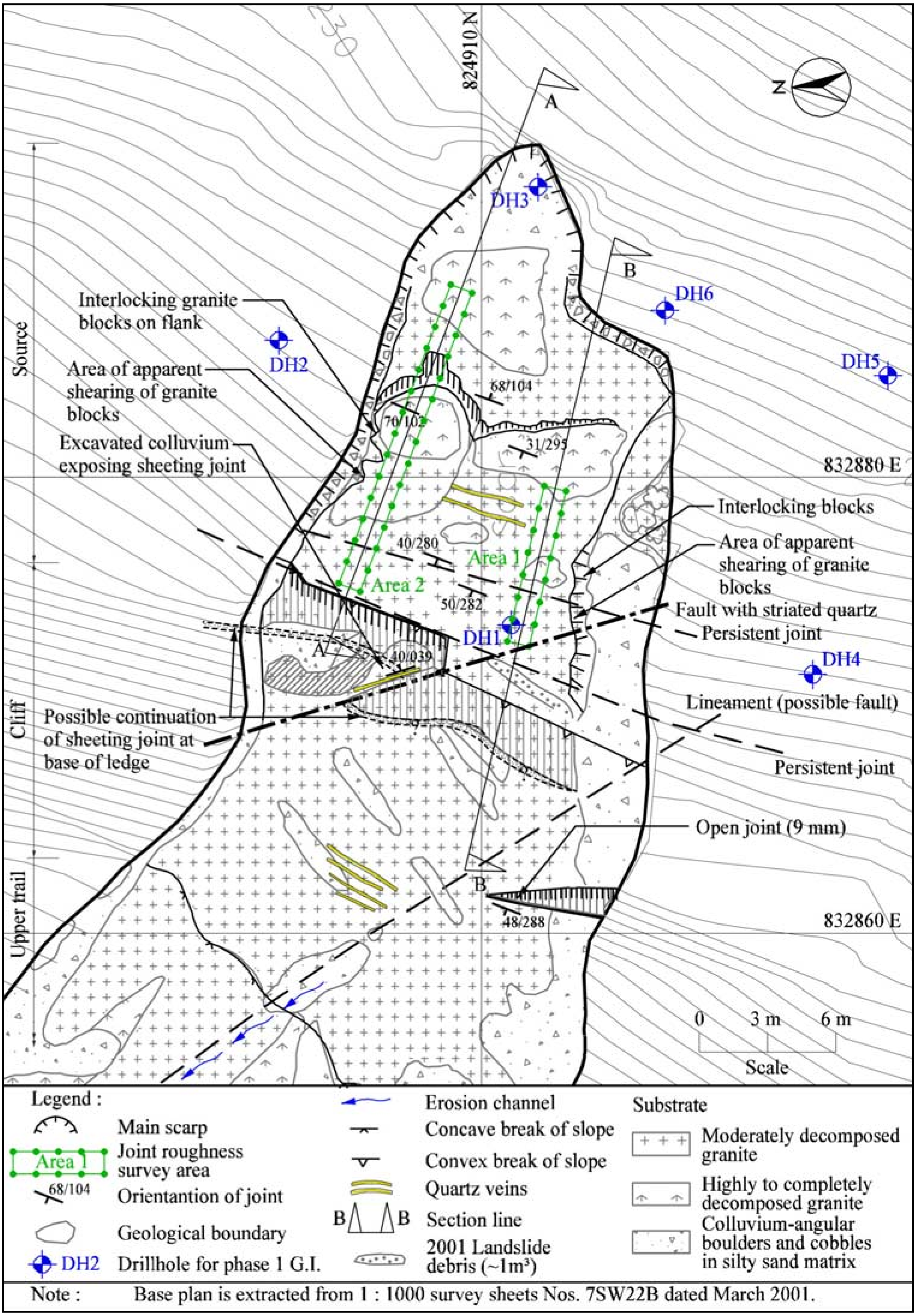

Figure 8 - Plan of Source Area Geology

Table of Contents
Table of Contents
Table of Contents
Table of Contents

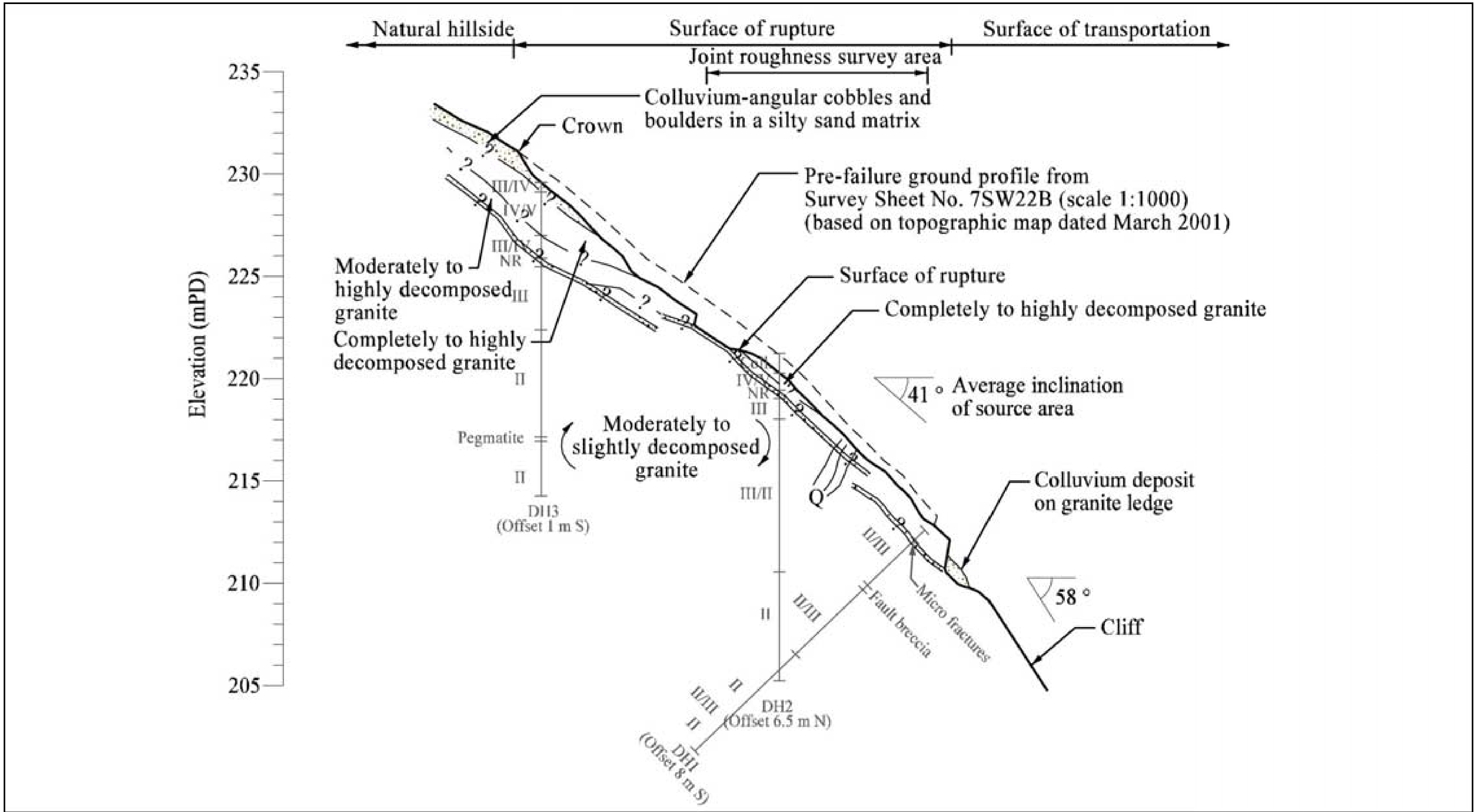

Legend : Colluvium —?—Inferred geological boundary ═?═ Inferred sheeting joint Q Quartz veins DH1 Drillhole log from phase 2 G.I.

Notes : (1) See Figure 8 for location of section.
(2) Section geometry based on topographic survey drawing and site measurement.

Figure 9 - Section A-A Showing Geology of the Source Area

Table of Contents
Table of Contents
Table of Contents
Table of Contents

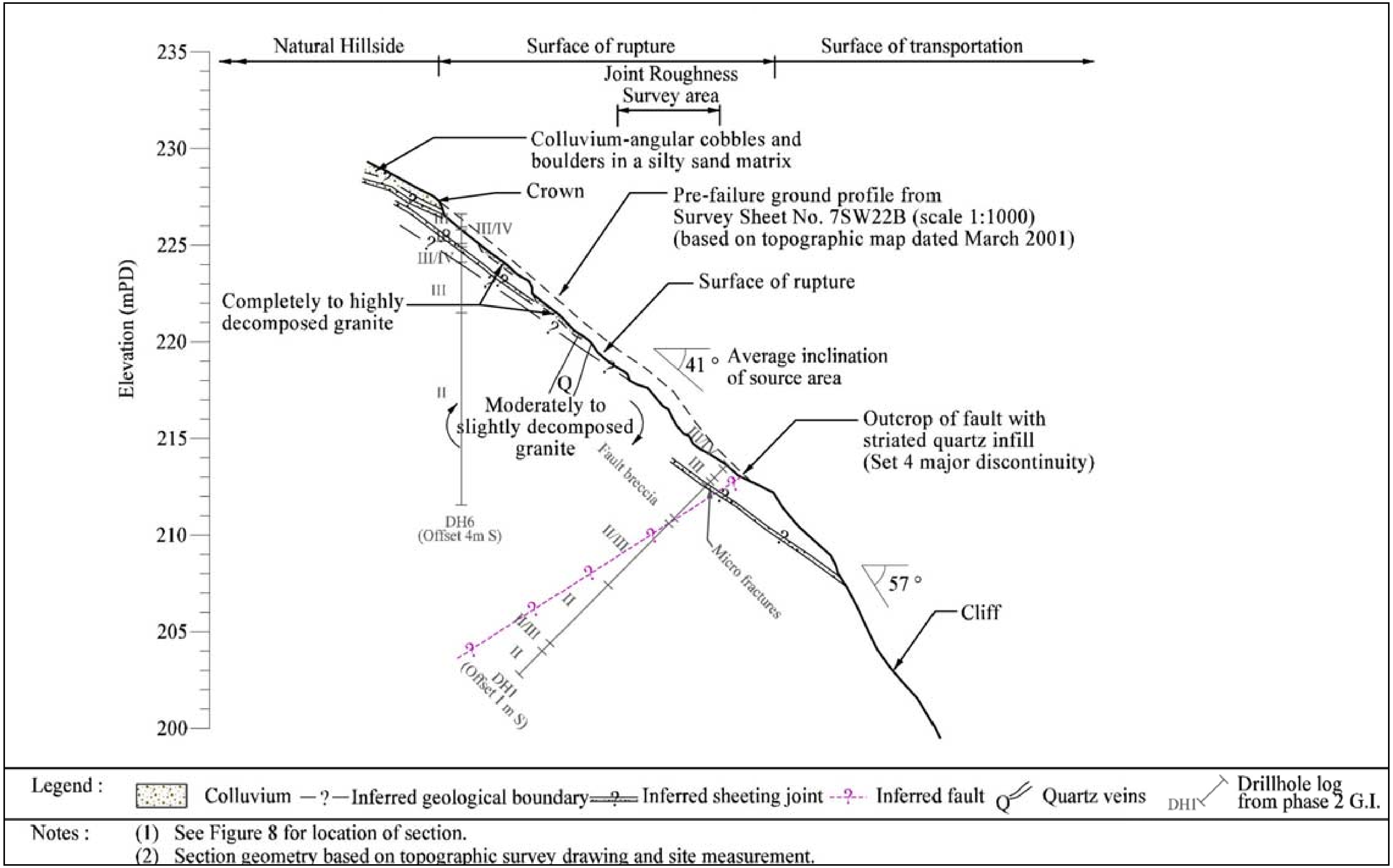

Figure 10 - Section B-B Showing Geology of the Source Area

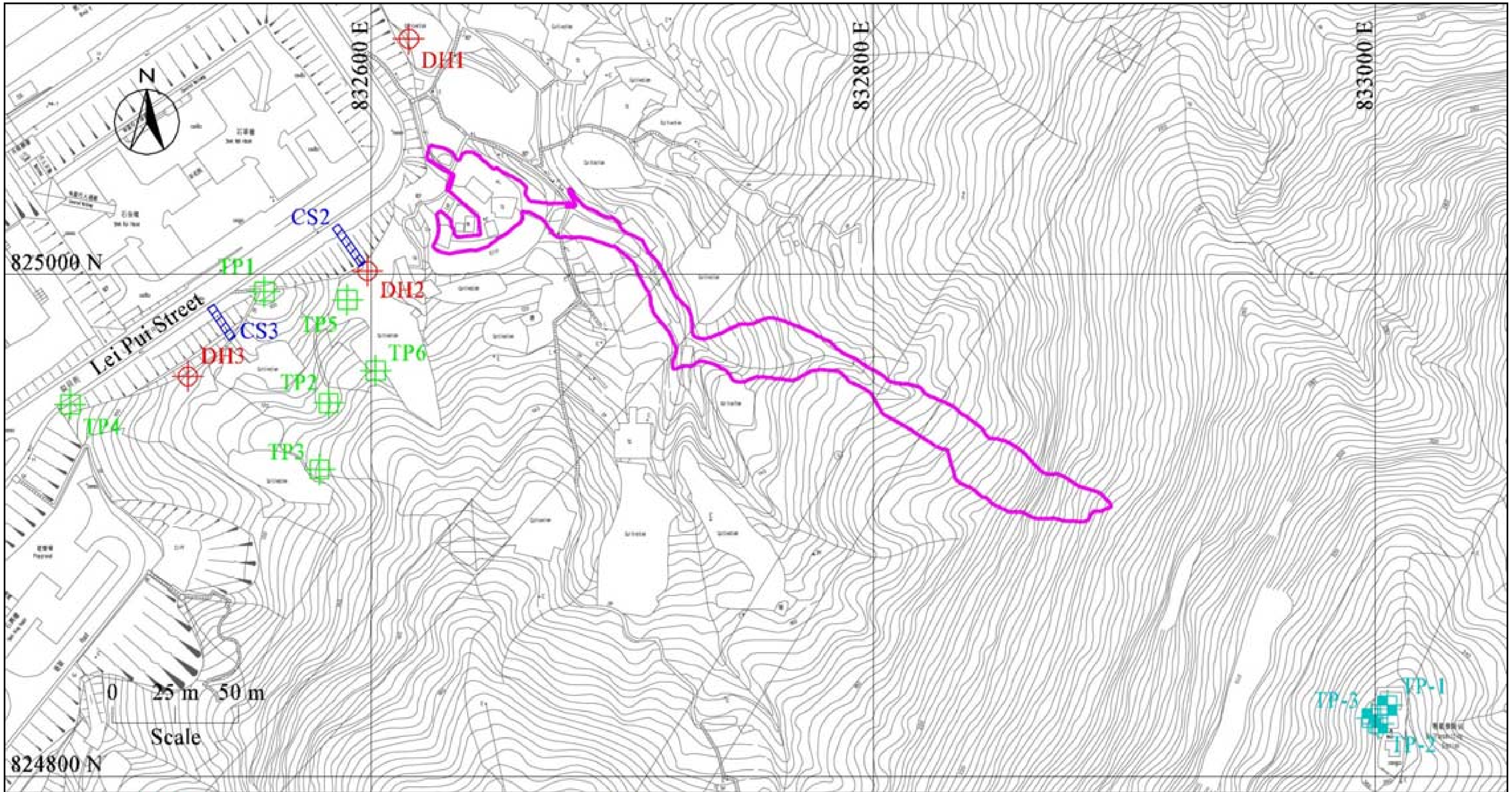

Legend :

- DH1 Drillhole carried out by Lam Geotechnics Limited in March 2000
- TP1 Trial pit carried out by Lam Geotechnics Limited in March 2000
- CS2 Slope stripping carried out by Lam Geotechnics Limited in March 2000
- TP-1 Trial pit carried out by Compact Construction Engineering Co. Ltd. in April 1988
- 1 September 2001 Landslide

Note : Base plan is extracted from 1 : 1000 survey sheets Nos. 7SW22B and 7SW23A, dated March 2001.

Figure 11 - Plan of Pre-2001 Ground Investigation

Table of Contents
Table of Contents
Table of Contents
Table of Contents

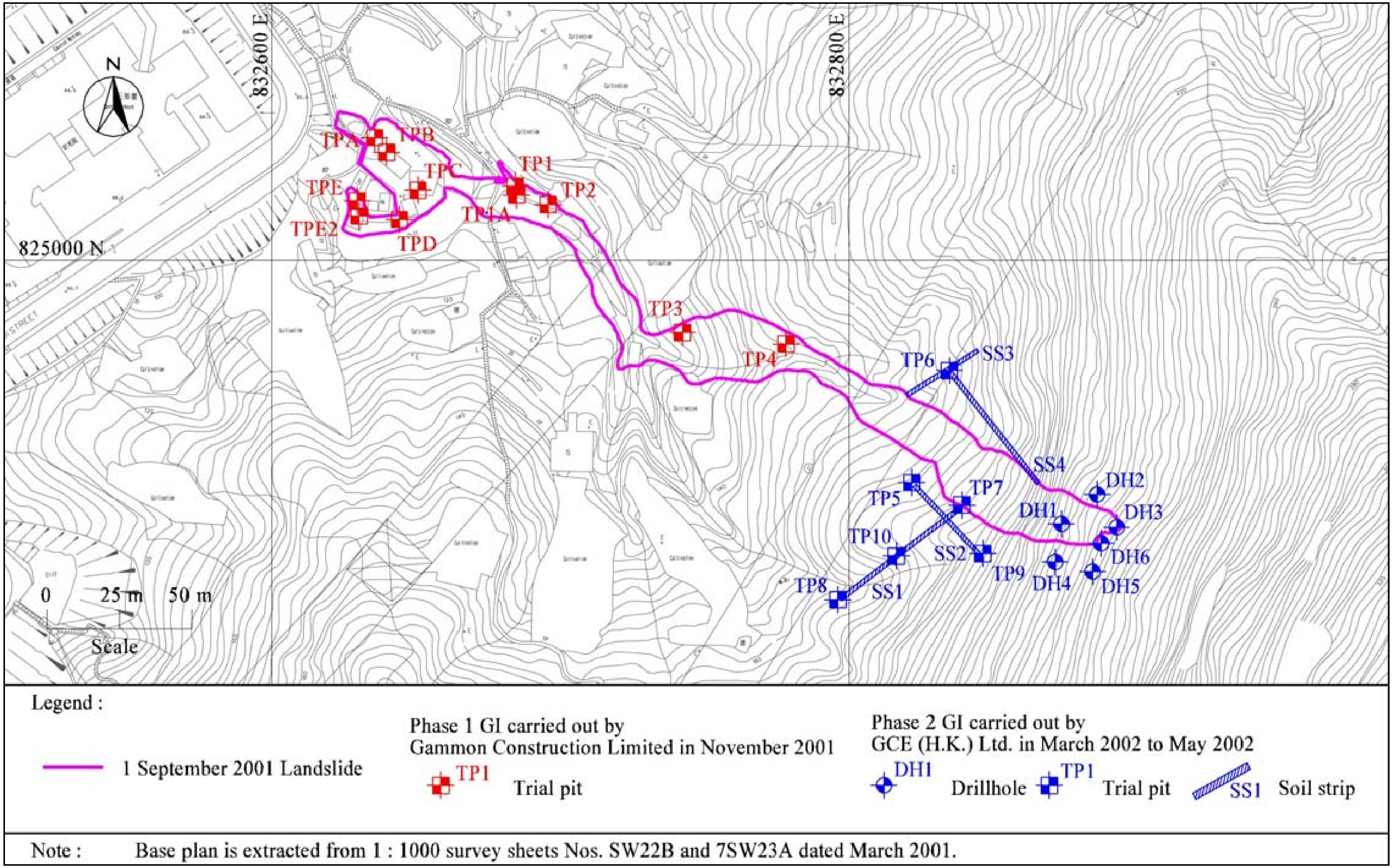

Figure 12 - Plan of the Phase 1 and Phase 2 Ground Investigations Undertaken after the 1 September 2001 Landslide

Table of Contents
Table of Contents
Table of Contents
Table of Contents

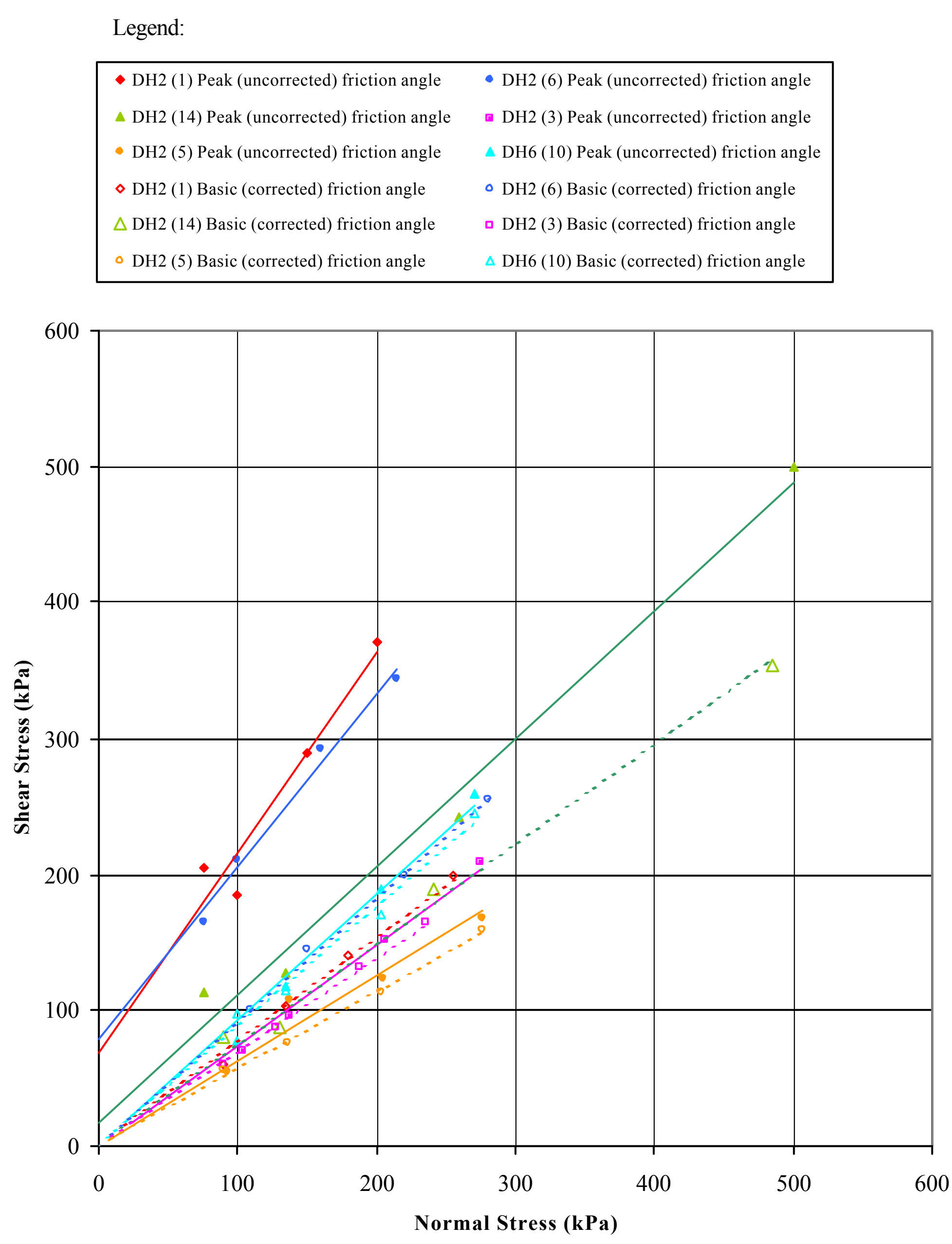

Notes: (1) Direct Shear Tests carried out by Public Works Central Laboratory (September 2002).
(2) See Table 2 for sample details.
(3) See Figure 12 for Location of Drillholes.

Figure 13 - Summary of Direct Shear Test Results on Rock Joints

Table of Contents
Table of Contents
Table of Contents
Table of Contents

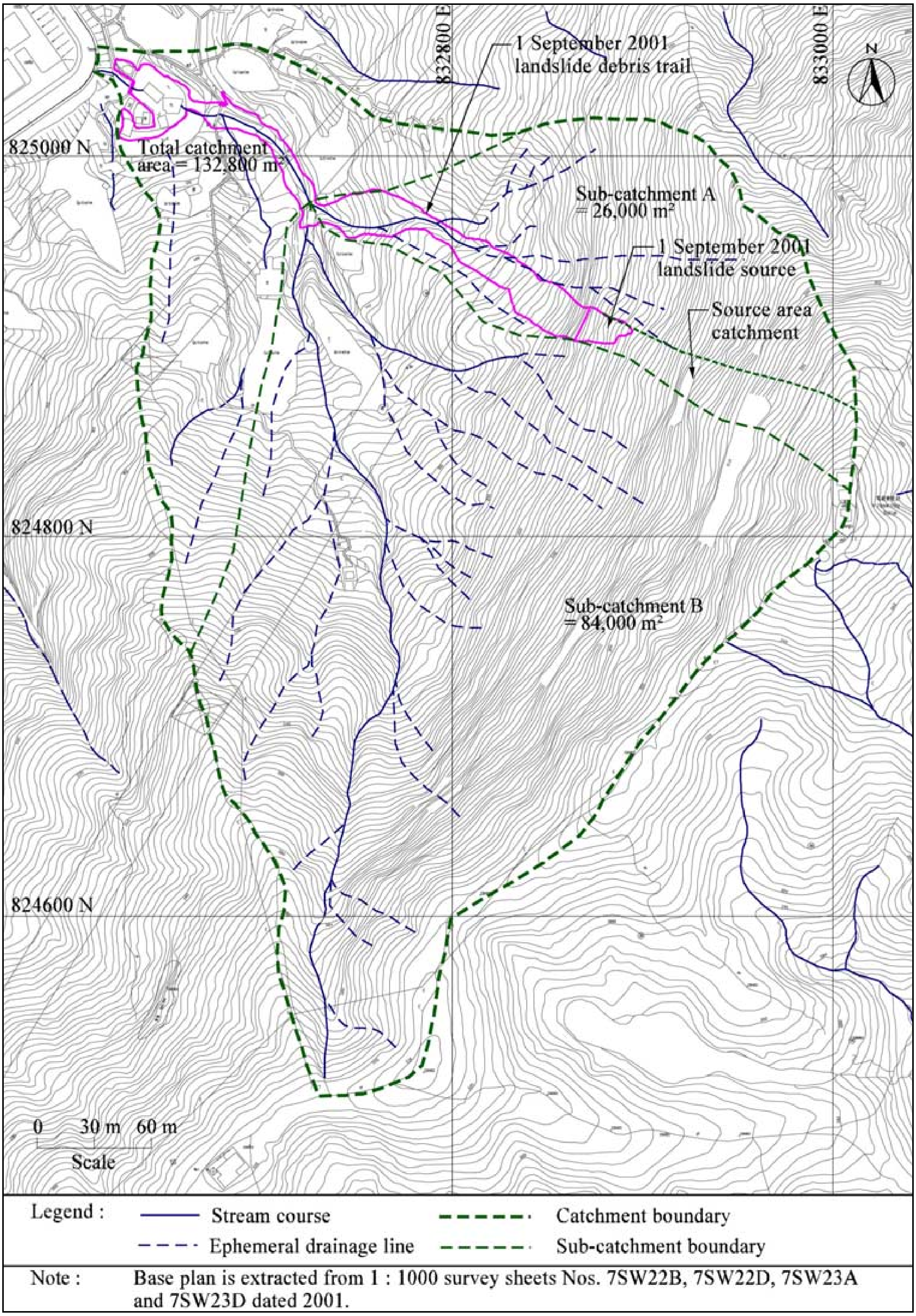

Figure 14 - Plan of Study Area Catchment

Table of Contents
Table of Contents
Table of Contents
Table of Contents

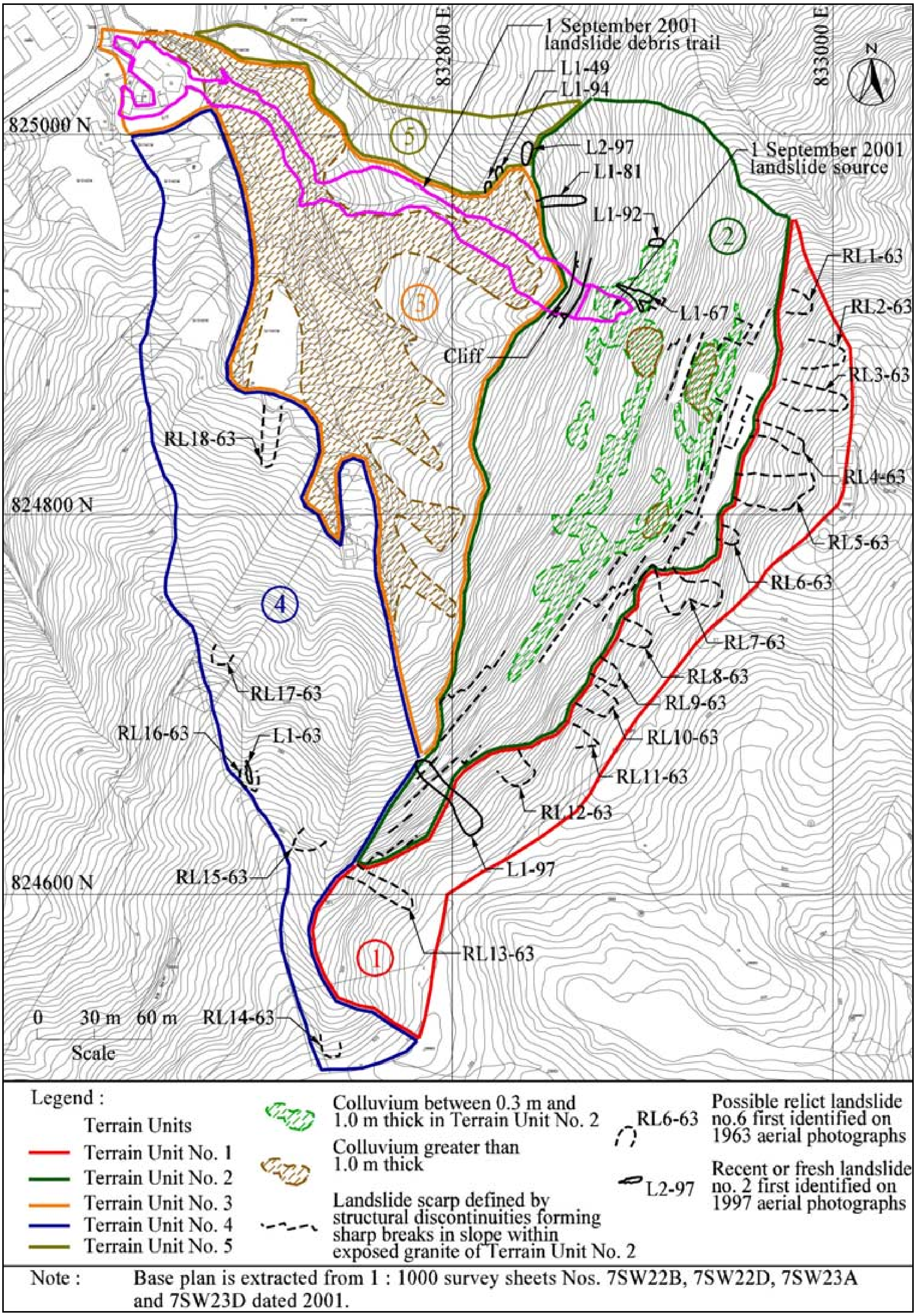

Figure 15 - Landslides and Geomorphology Inferred from API and Field Mapping

Table of Contents

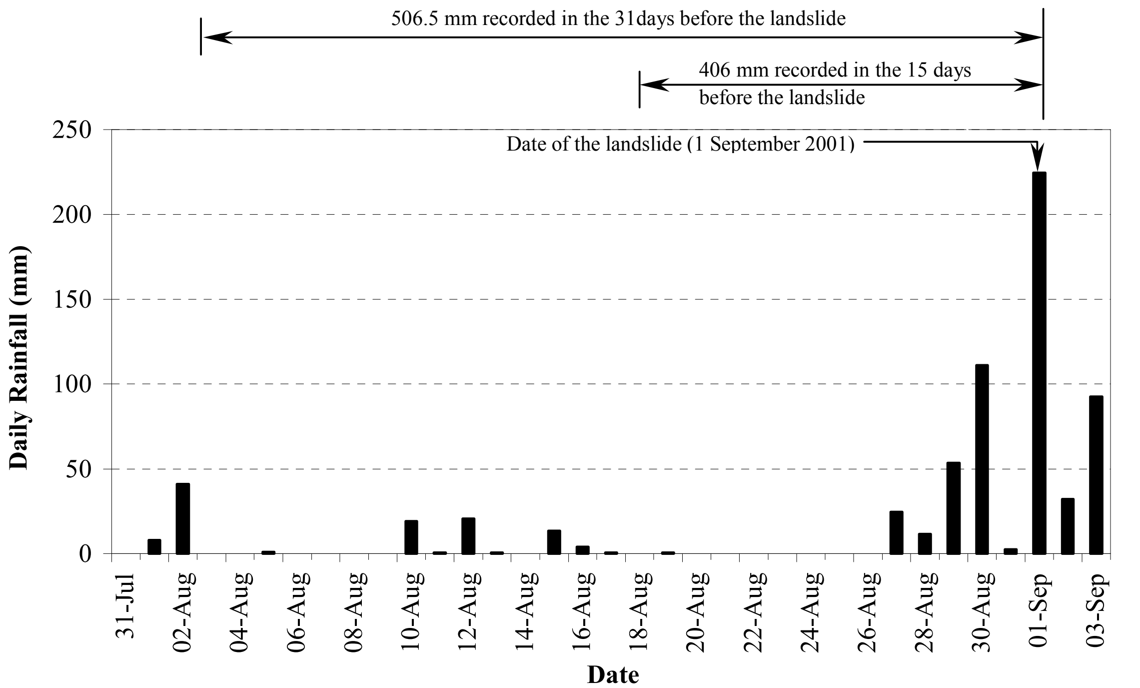

(a) Daily Rainfall Recorded at GEO Raingauge No. N06 from 30 July to 3 September 2001

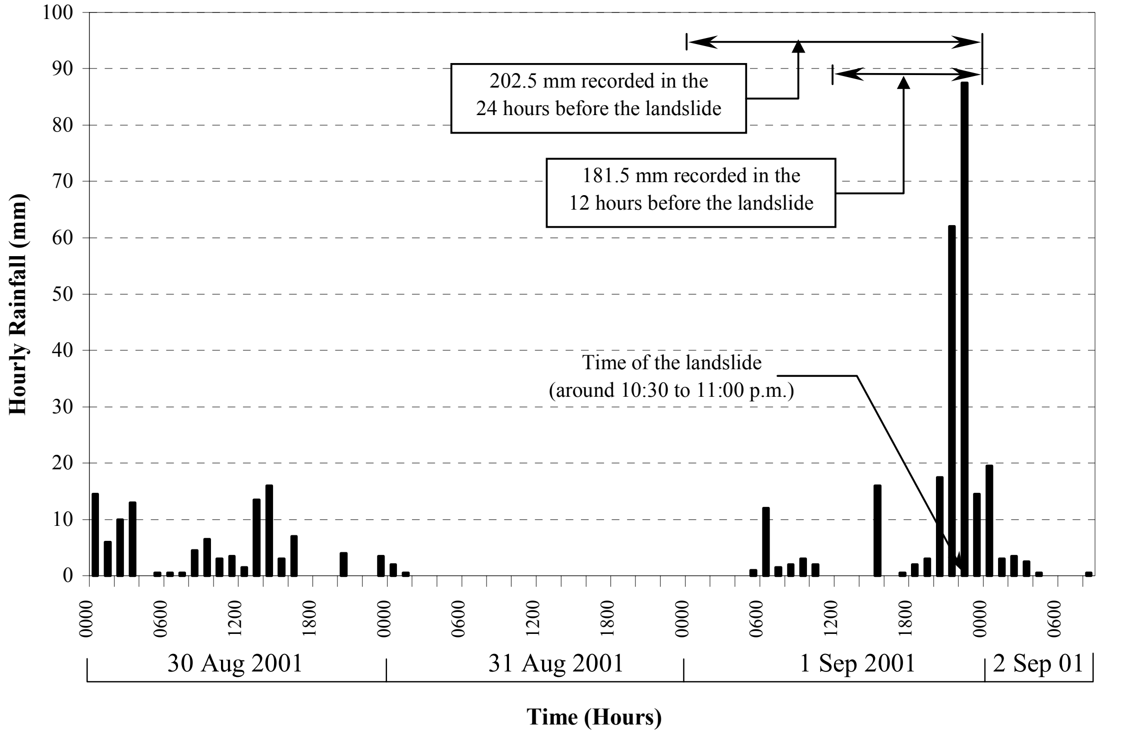

(b) Hourly Rainfall Recorded at GEO Raingauge No. N06 from 30 August to 2 September 2001

Figure 16 - Daily and Hourly Rainfall Recorded at GEO Raingauge No. N06

Table of Contents
Table of Contents
Table of Contents
Table of Contents

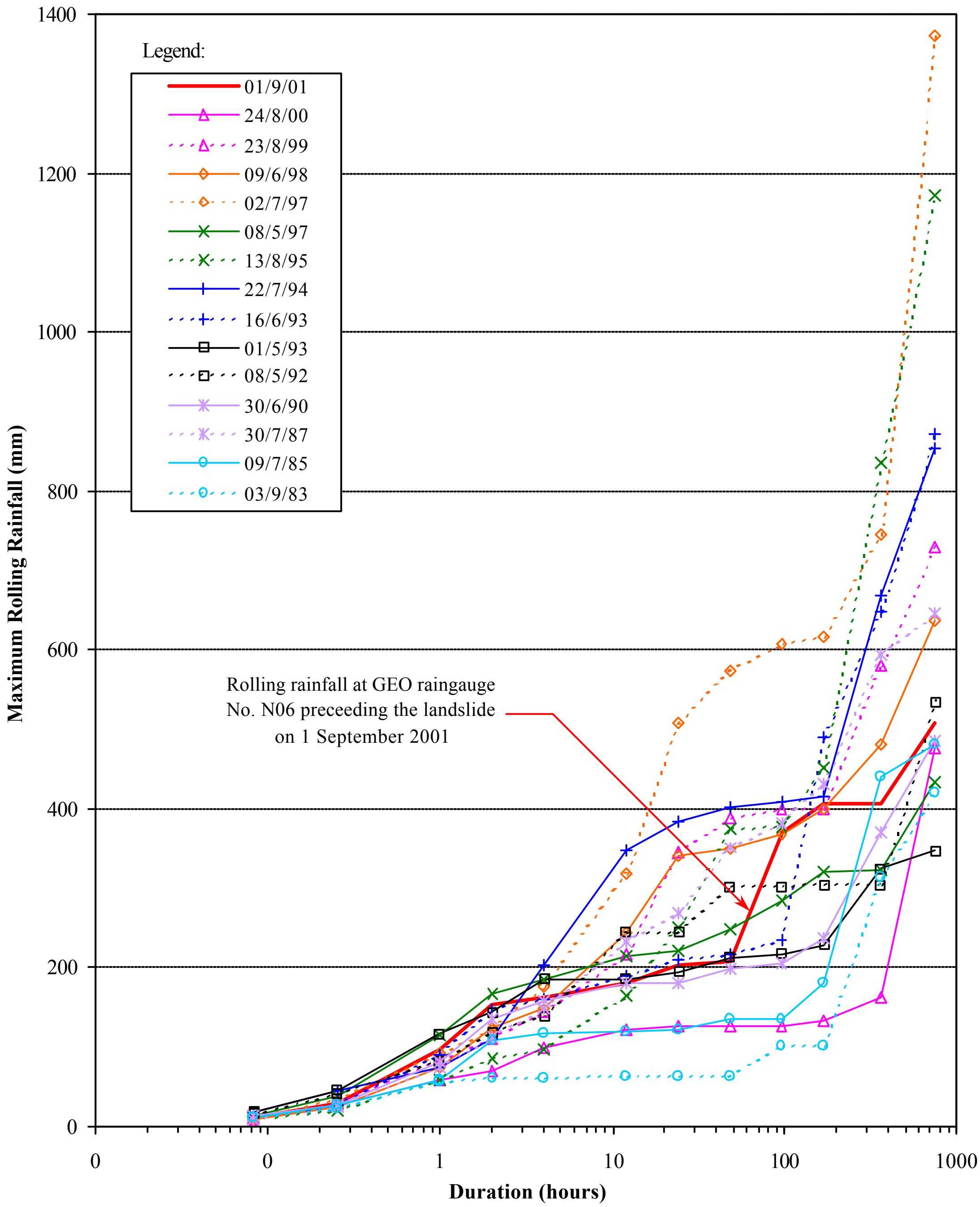

Notes:
(1) Previous rainstorms make reference to GEO Report No. 62 - "Areal Extent of Intense Rainfall in Hong Kong 1975 to 1995" (Malone, 1997) and selected rainstorms from 1996 to 2000.
(2) Rainfall data evaluated from 5-minute readings from GEO raingauge No. N06 (about 0.5 km west of the site).
(3) Rolling rainfall of previous rainstorm calculated at GEO raingauge No. N06 since June 1983 when the raingauge began operation.

Figure 17 - Maximum Rolling Rainfall for Previous Major Rainstorms at GEO Raingauge No. N06

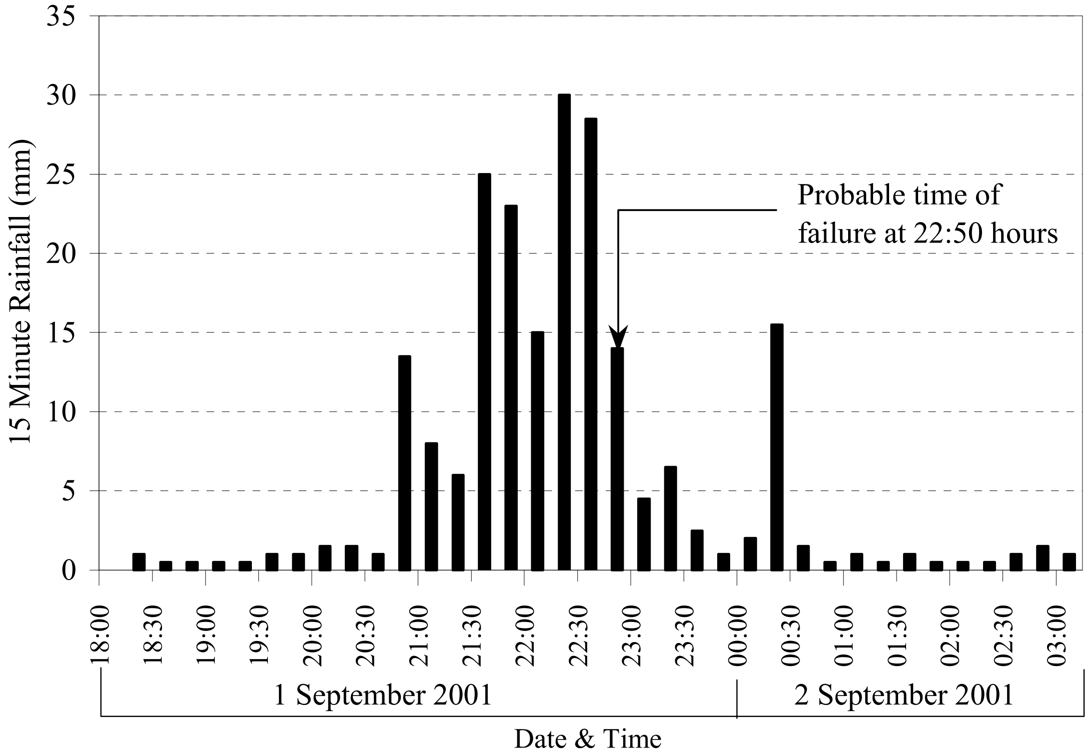

Figure 18 - 15 Minute Rainfall Intensities at GEO Raingauge No. N06

Table of Contents
Table of Contents
Table of Contents
Table of Contents

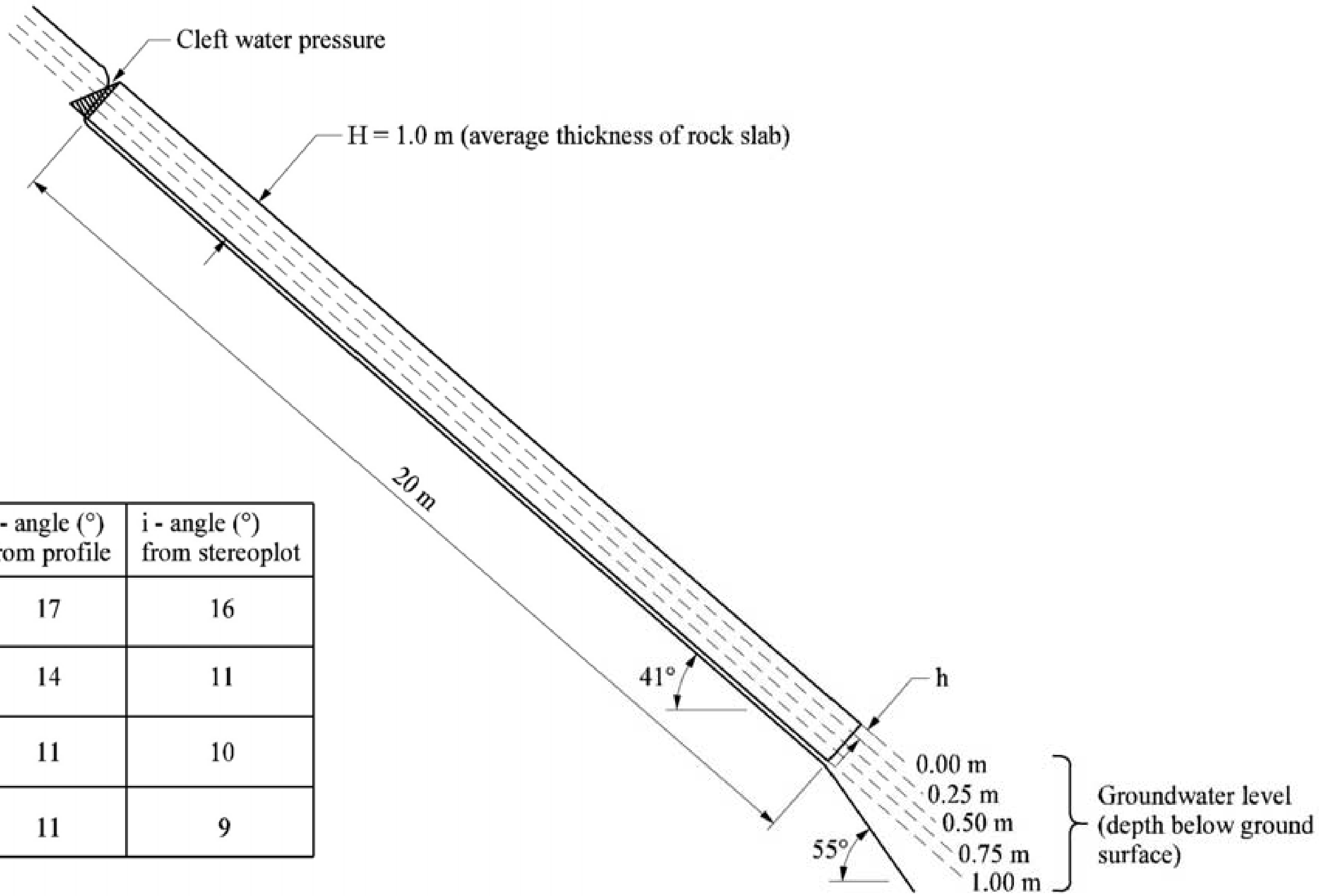

	i - angle (°) from profile	i - angle (°) from stereoplot
Area 1 210 mm plate	17	16
Area 2 210 mm plate	14	11
Area 1 420 mm plate	11	10
Area 2 420 mm plate	11	9

Notes :
(1) $Ø_b$ is the basic friction angle of the rock surface.
(2) i is the roughness angle.
(3) H - thickness of rock slab.
(4) h - depth to ground water table.

Figure 19 - Simplified Section Adopted for Stability Analysis

Table of Contents
Table of Contents
Table of Contents
Table of Contents

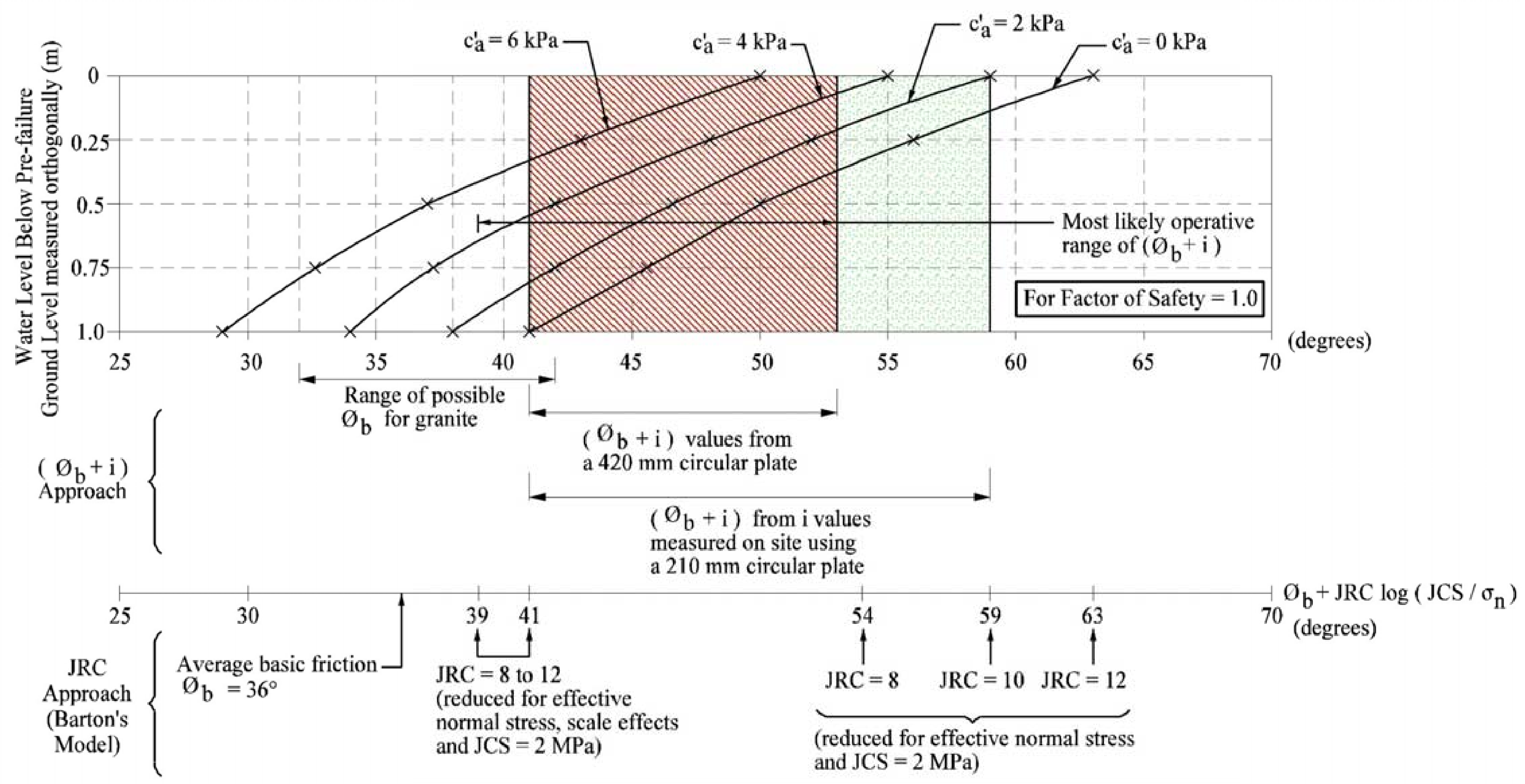

Notes :
(1) Water levels are measured from pre-failure ground level down to failure surface (Figure 19).
(2) JRC is Joint Roughness Coefficient and JCS is Joint Wall Compressive Strength.
(3) $Ø_b$ is the basic friction angle of the surface (derived from site specific laboratory shear box testing). σ_n is the total normal stress, c'_a is the effective apparent cohesion on the failure surface.
(4) JRC approach is based on Barton's equation (ref. Barton, 1990). Detailed calculations refer to Appendix B.
(5) i is the angle of dilation.

Figure 20 - Results of Stability Analysis

Table of Contents
Table of Contents
Table of Contents
Table of Contents

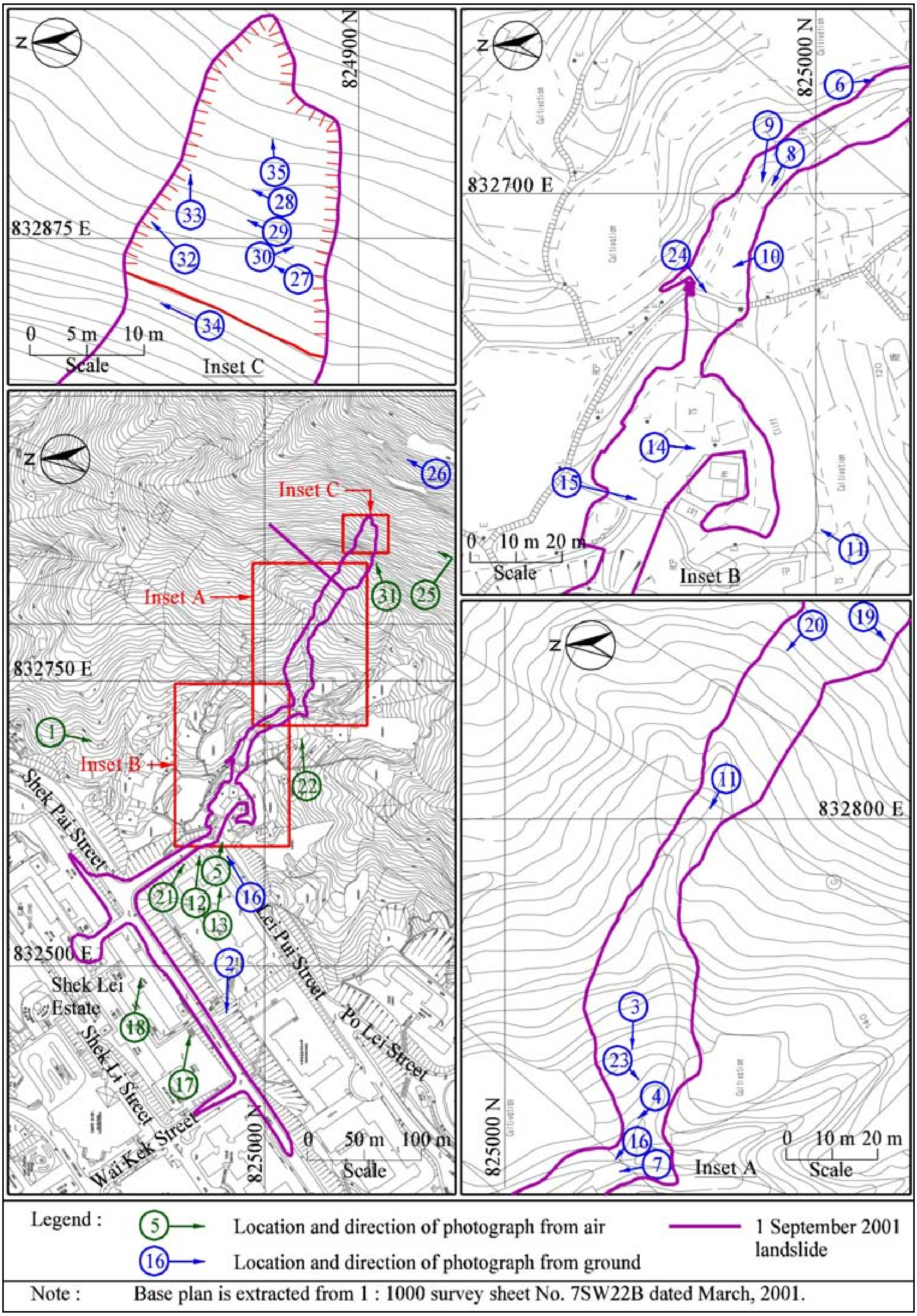

Figure 21 - Locations and Directions of Photographs

Table of Contents
Table of Contents
Table of Contents
Table of Contents

LIST OF PLATES

Table of Contents
Table of Contents
Table of Contents

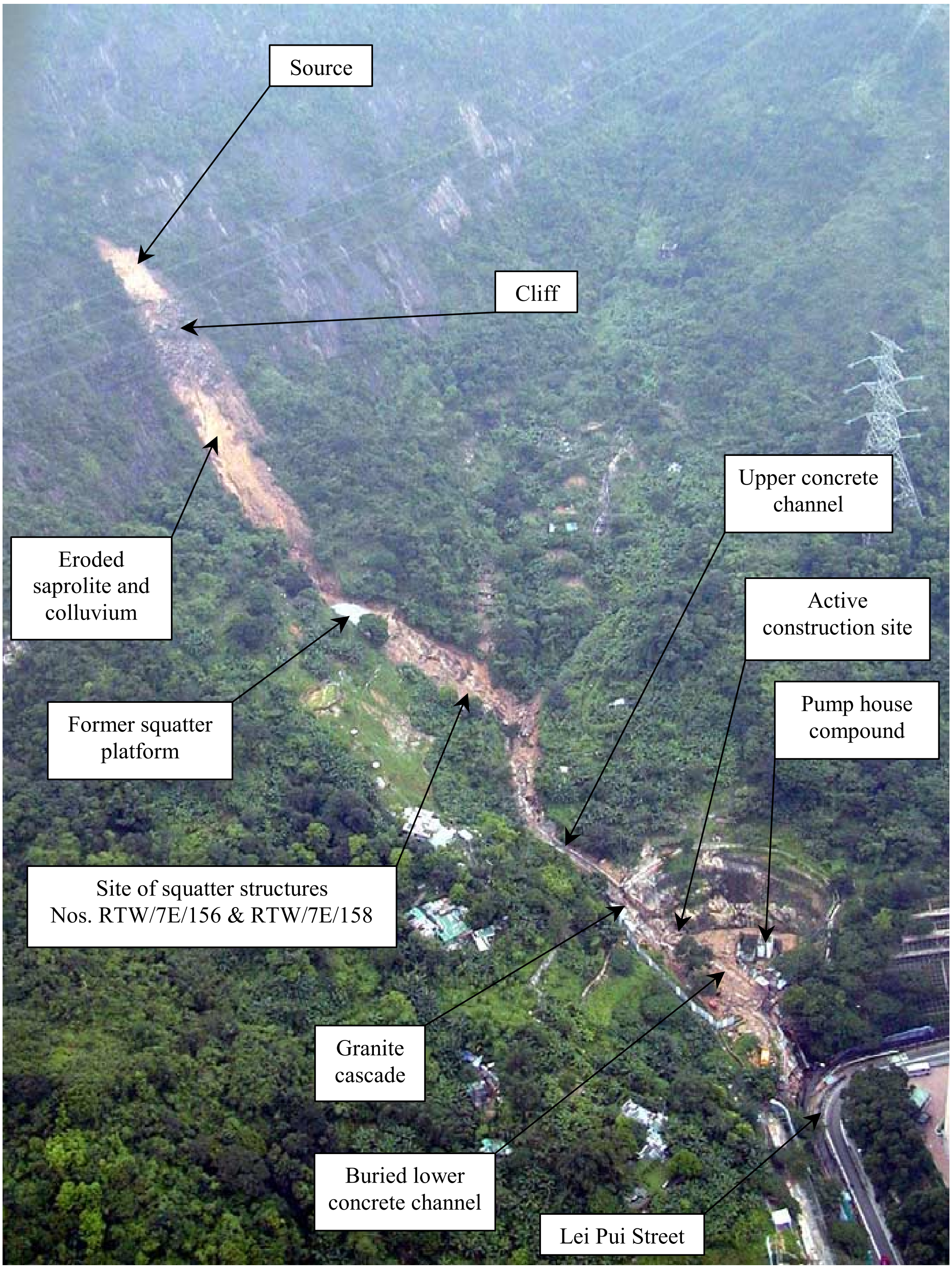

Plate 1 - Oblique Aerial View of the 1 September 2001 Debris Flow (Photograph taken on 10 September 2001)

Note: See Figure 21 for location of photographs.

Table of Contents
Table of Contents
Table of Contents
Table of Contents

Plate 2 - Outwash Material along Shek Pai Street and Wai Kek Street
(Photograph taken on 2 September 2001)

Note: See Figure 21 for location of photographs.

Table of Contents
Table of Contents
Table of Contents
Table of Contents

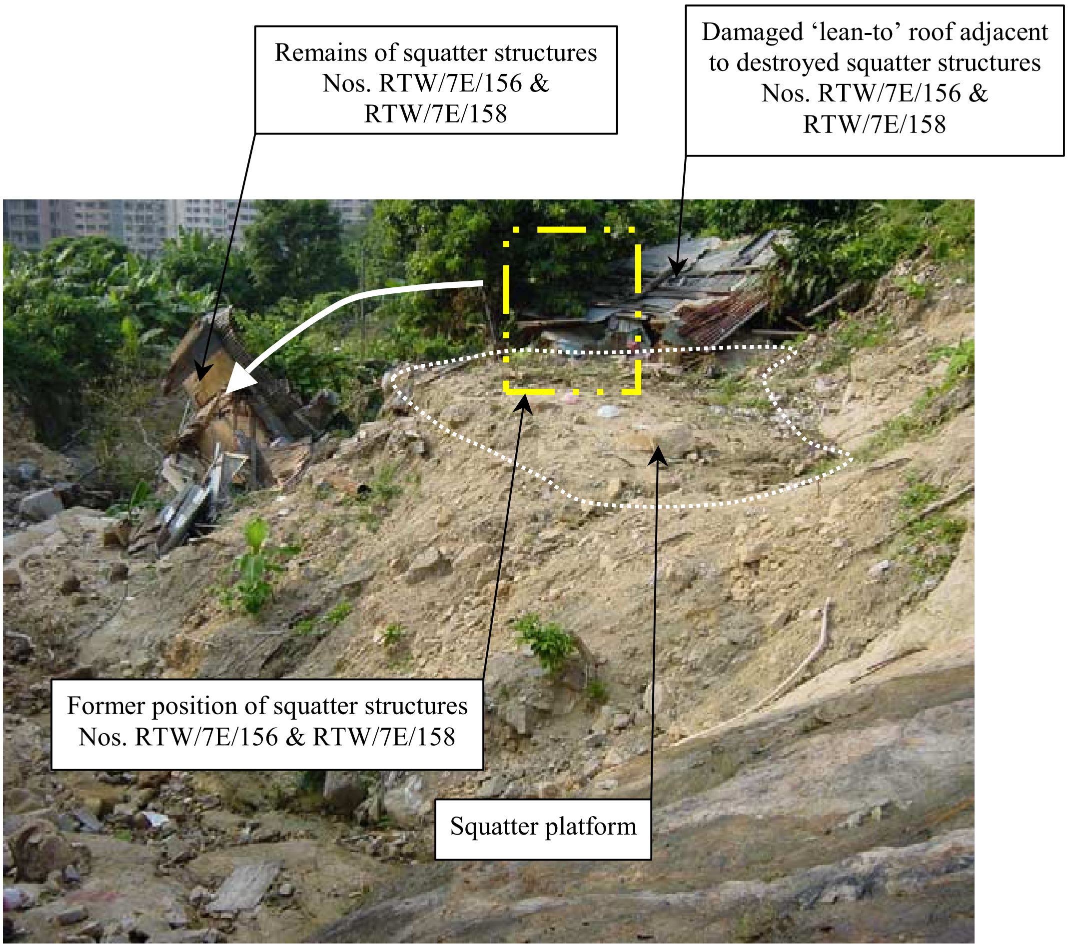

Plate 3 - View Looking West towards Squatter Platform and Destroyed Squatter Structures Nos. RTW/7E/156 and RTW/7E/158 (Photograph taken on 17 October 2001)

Note: See Figure 21 for location of photographs.

Plate 4 - View of Destroyed Squatter Structures Nos. RTW/7E/156 and RTW/7E/158
(Photograph taken on 4 September 2001)

Note: See Figure 21 for location of photographs.

Table of Contents
Table of Contents
Table of Contents
Table of Contents

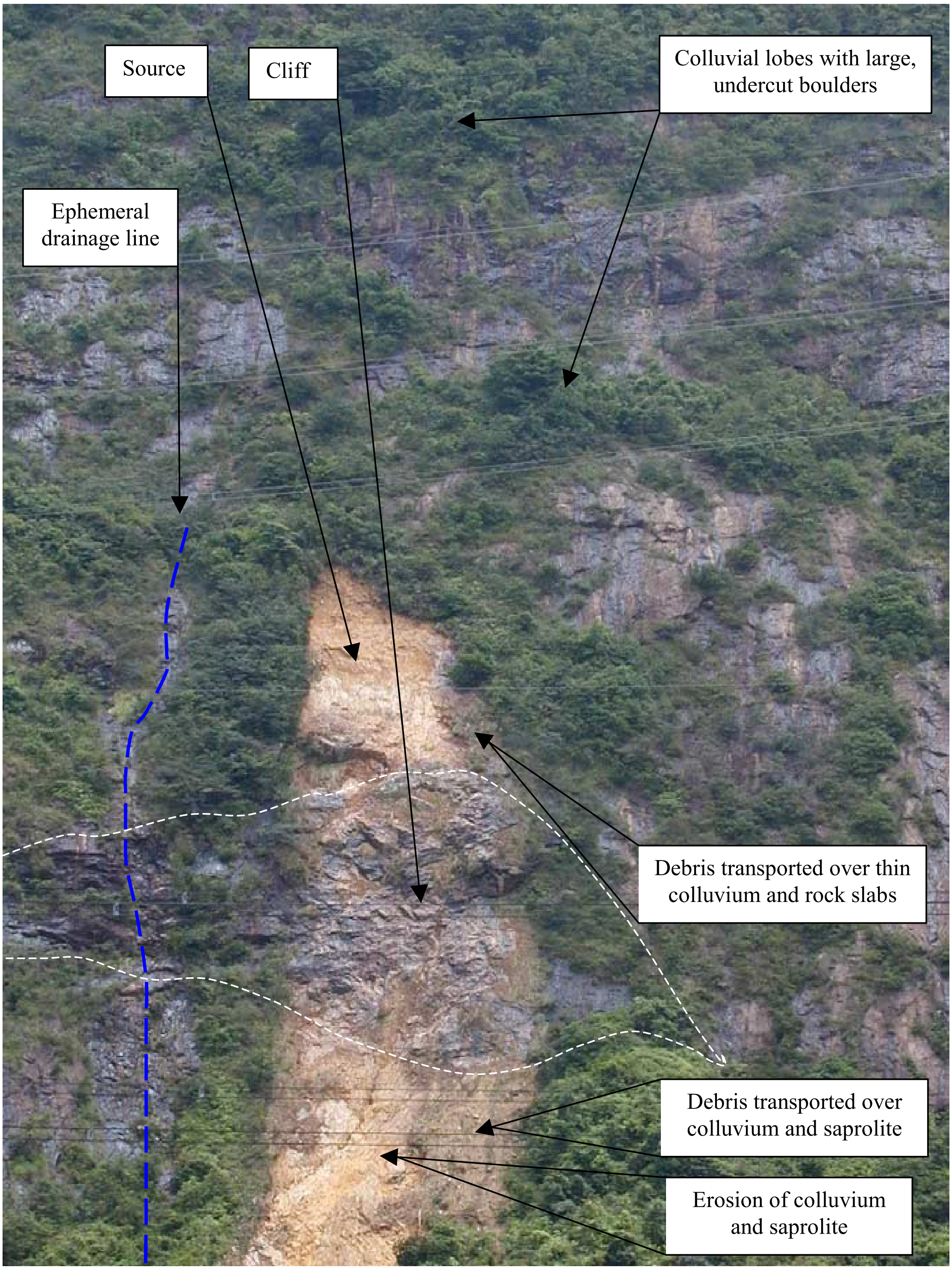

Plate 5 - Oblique Aerial View of the Landslide Source Area
(Photograph taken on 5 September 2001)

Note: See Figure 21 for location of photographs.

Table of Contents Table of Contents Table of Contents Table of Contents

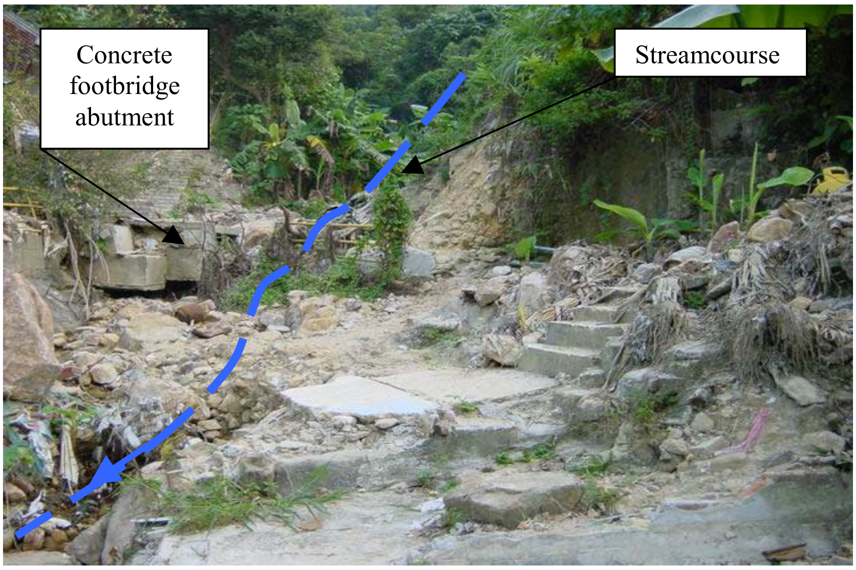

Plate 6 - View of Confluence of Sub-catchment B Streamcourse and Debris Trail
(Photograph taken on 17 October 2001)

Plate 7 - View of Lower Debris Trail Showing Concrete Footbridge Abutments
(Photograph taken on 17 October 2001)

Note: See Figure 21 for location of photographs.

Table of Contents
Table of Contents
Table of Contents
Table of Contents

Plate 8 - View of the Upper Concrete Channel above the Active Construction Site before the 1 September 2001 Landslide (Photograph taken on 1 August 2001)

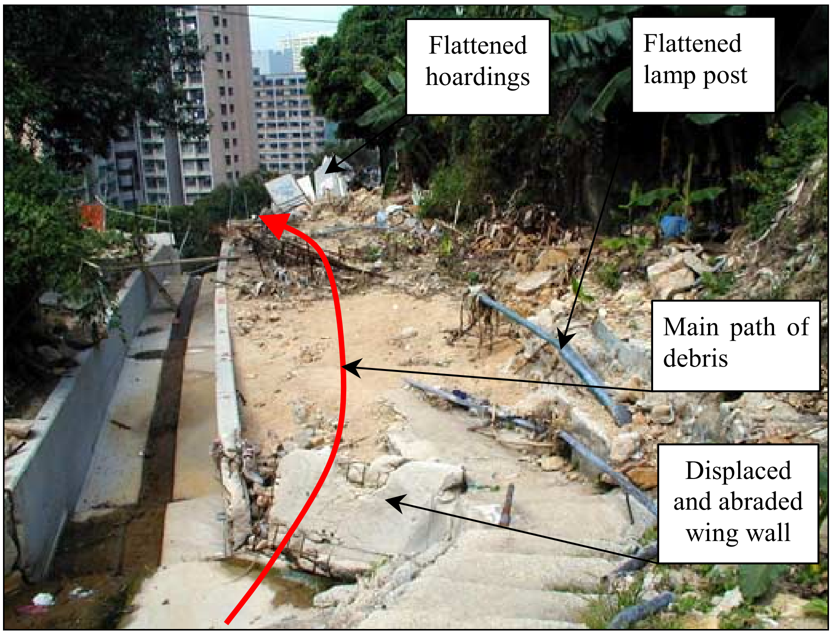

Plate 9 - Upper Concrete Channel above Active Construction Site after the 1 September 2001 Landslide (Photograph taken on 17 October 2001)

Note: See Figure 21 for location of photographs.

Table of Contents
Table of Contents
Table of Contents
Table of Contents

Plate 10 - Bouldery Debris near Downstream End of Upper Concrete Channel
(Photograph taken on 21 October 2001)

Plate 11 - View of the Active Construction Site
(Photograph taken on 1 August 2001)

Note: See Figure 21 for location of photographs.

Table of Contents
Table of Contents
Table of Contents
Table of Contents

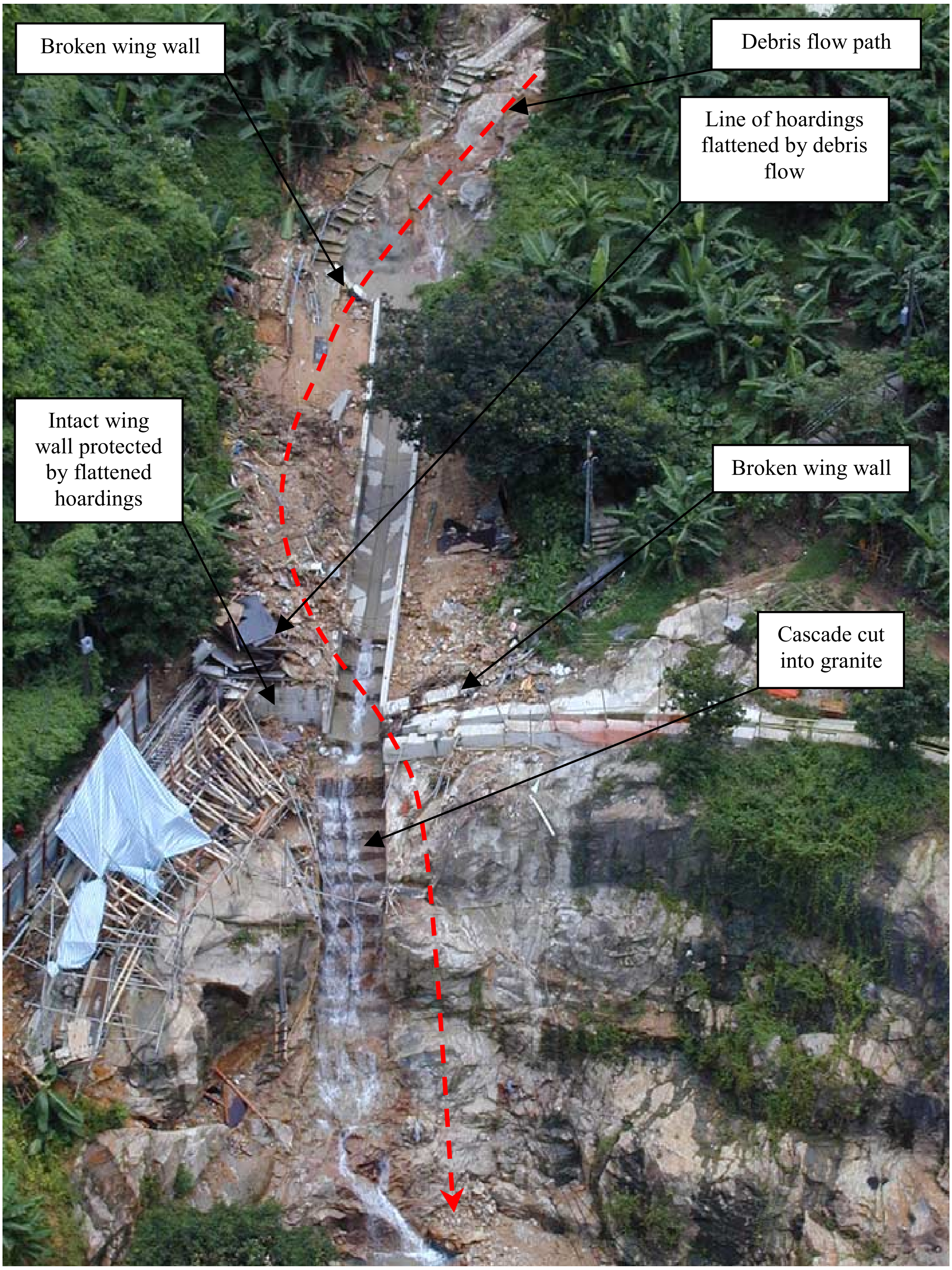

Plate 12 - Oblique Aerial View of Trail from Upper Concrete Channel to Granite Cascade within Active Construction Site (Photograph taken on 5 September 2001)

Note: See Figure 21 for location of photographs.

Table of Contents Table of Contents Table of Contents Table of Contents

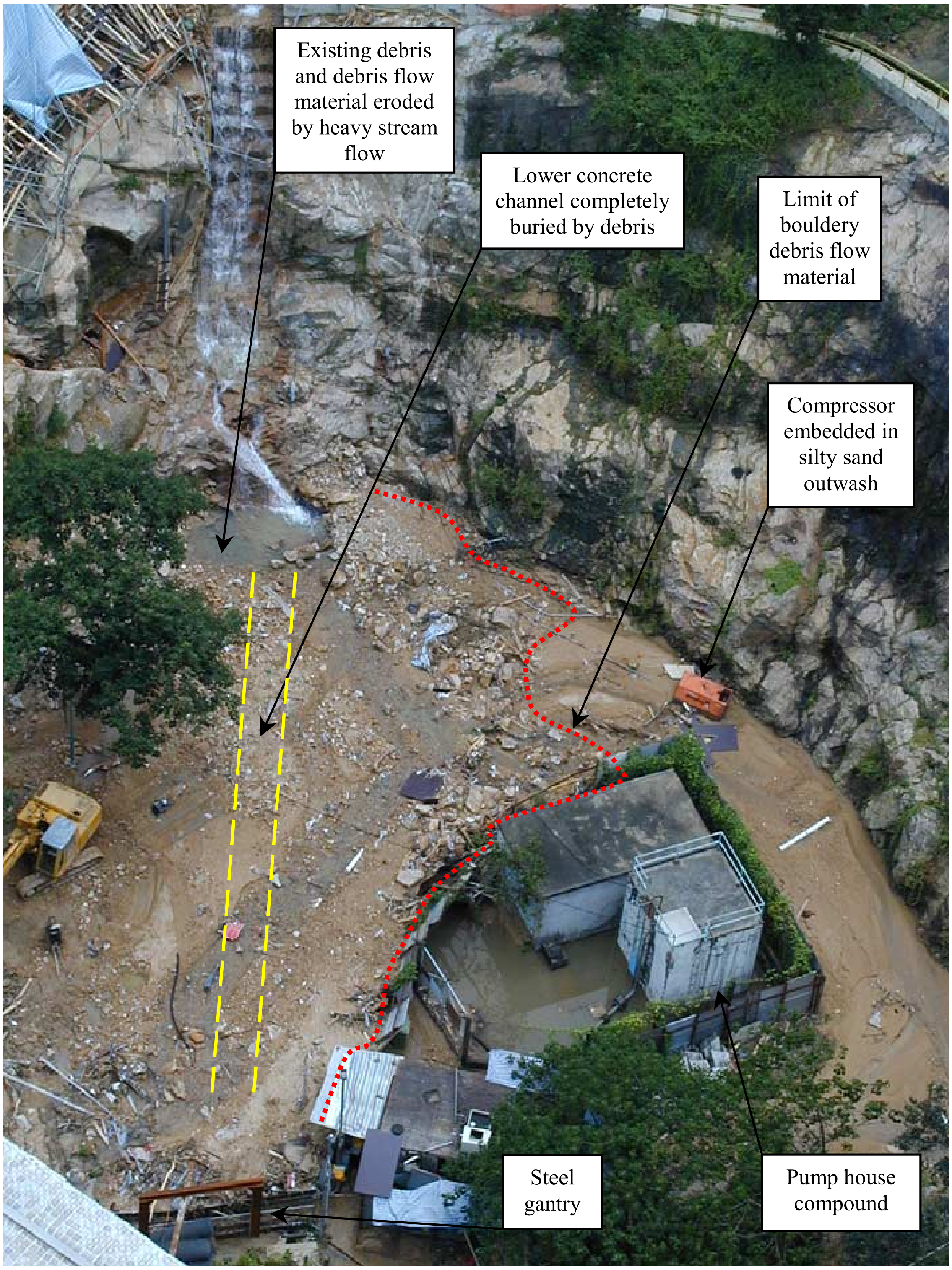

Plate 13 - Oblique Aerial View of Active Construction Site
(Photograph taken on 5 September 2001)

Note: See Figure 21 for location of photographs.

Table of Contents
Table of Contents
Table of Contents
Table of Contents

Plate 14 - Buckled Hoardings Adjacent to Pump House Compound
(Photograph taken on 5 September 2001)

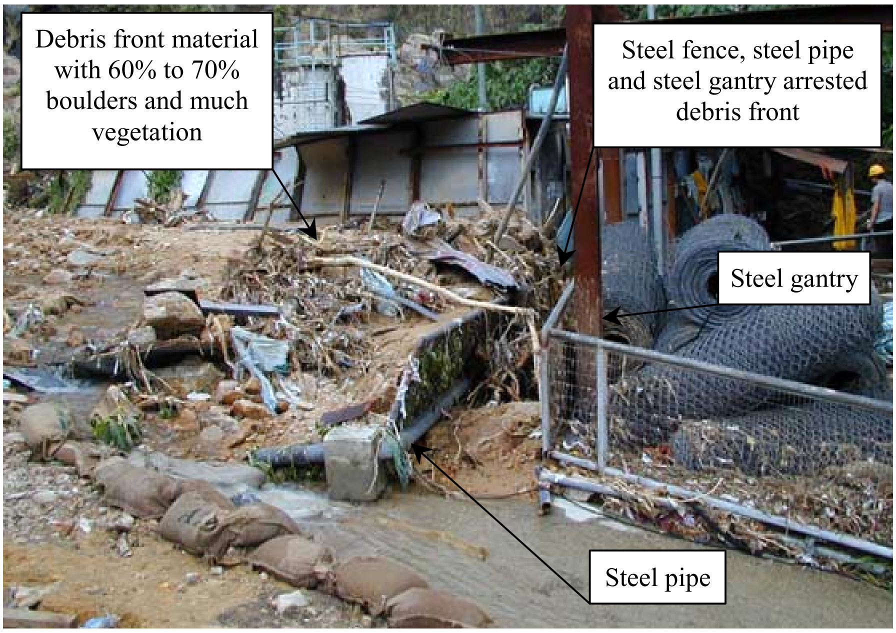

Plate 15 - Debris Front Material near Steel Gantry
(Photograph taken on 5 September 2001)

Note: See Figure 21 for location of photographs.

Table of Contents
Table of Contents
Table of Contents
Table of Contents

Plate 16 - Deformed Temporary Fence on Lei Pui Street below the Active Construction Site
(Photograph taken on 2 September 2001)

Note: See Figure 21 for location of photographs.

Table of Contents
Table of Contents
Table of Contents
Table of Contents

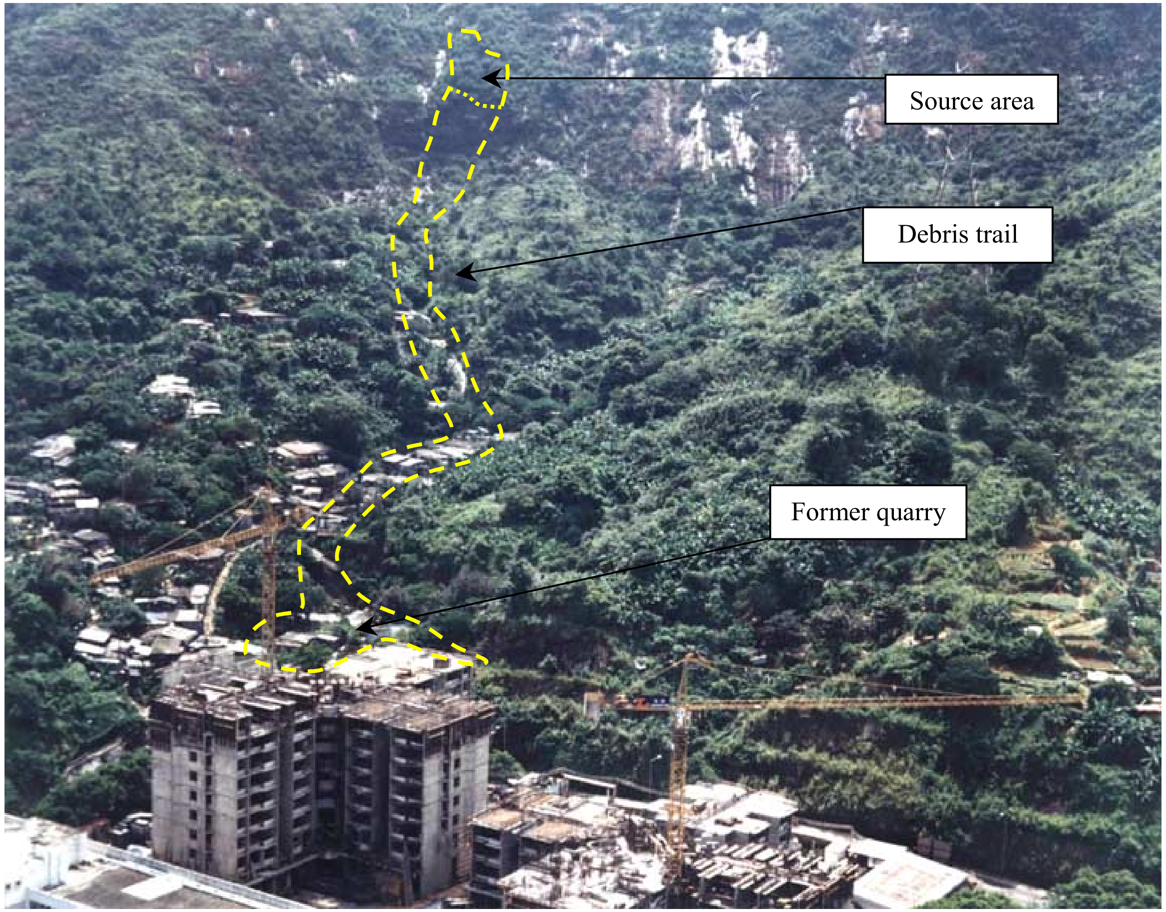

Plate 17 - Oblique Aerial View of the Hillside Prior to the 1 September 2001 Debris Flow Showing Former Squatter Development within the Debris Trail (Photograph taken in early 1993)

Note: See Figure 21 for location of photographs.

Table of Contents
Table of Contents
Table of Contents
Table of Contents

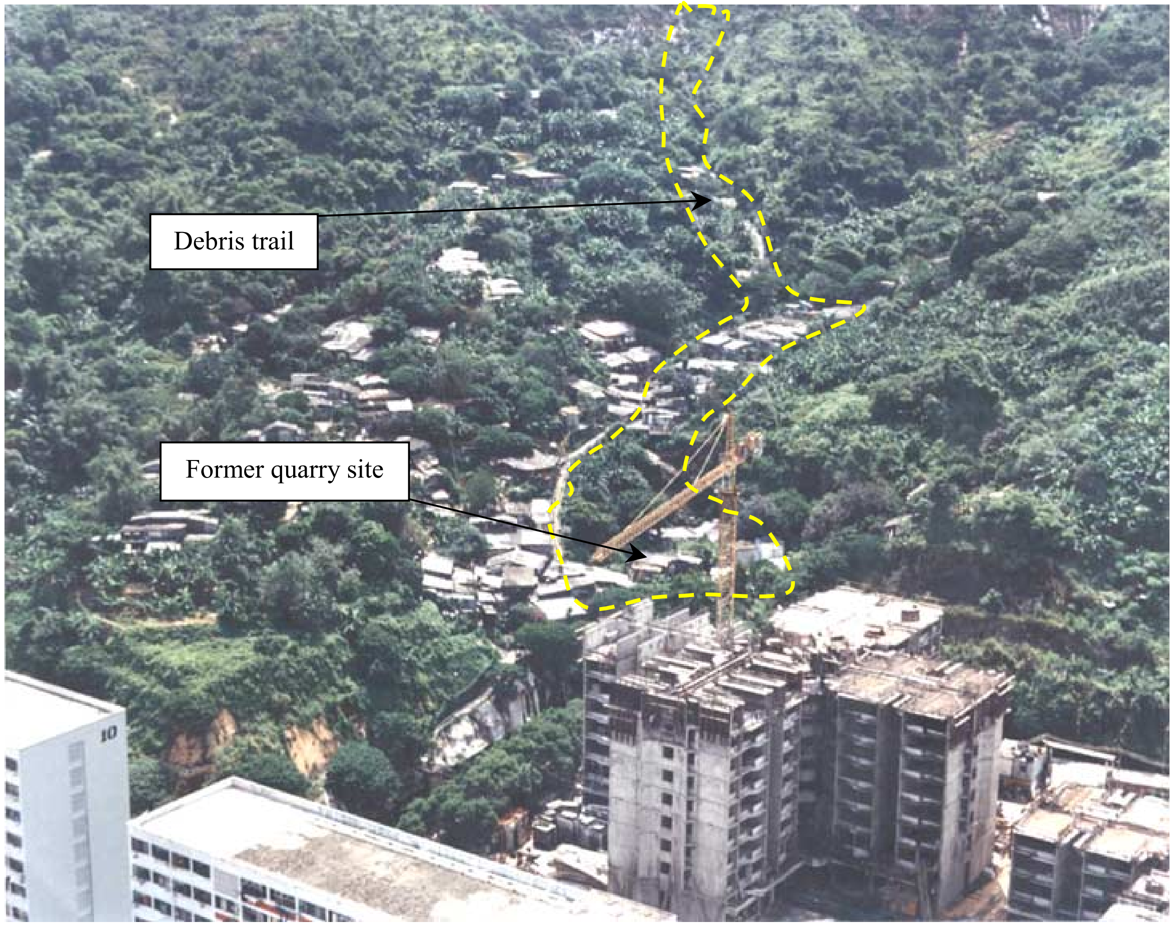

Plate 18 - Oblique Aerial View of Squatter Development in 1993
(Photograph taken in early 1993)

Note: See Figure 21 for location of photographs.

Table of Contents
Table of Contents
Table of Contents
Table of Contents

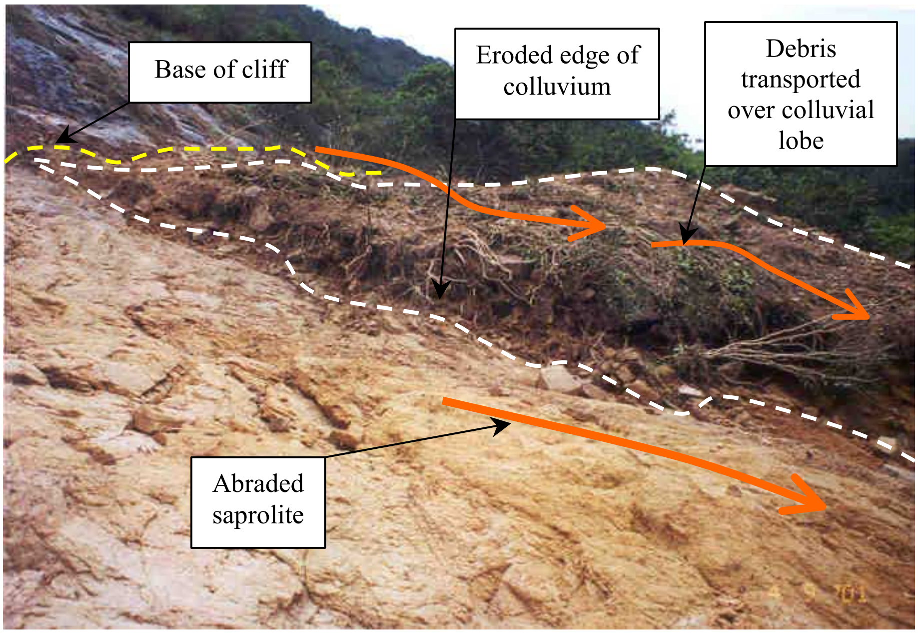

Plate 19 - Erosion of Colluvium and Saprolite at Base of Cliff
(Photograph taken on 4 September 2001)

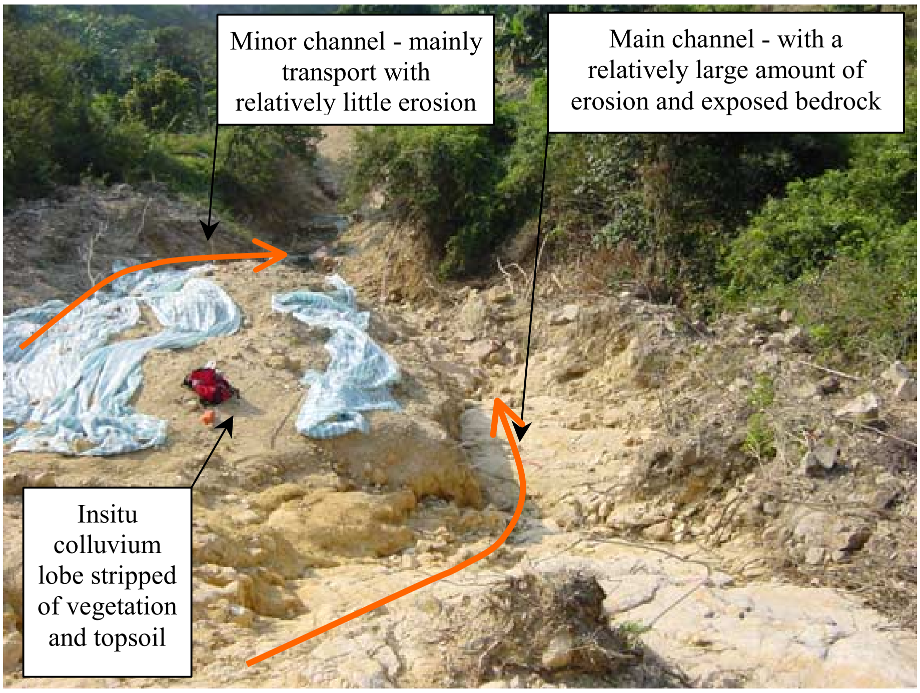

Plate 20 - Bifurcation around Colluvial Lobe
(Photograph taken on 4 September 2001)

Note: See Figure 21 for location of photographs.

Table of Contents
Table of Contents
Table of Contents
Table of Contents

Plate 21 - Oblique Aerial View of Upper Trail Showing Remains of Squatter Structures Nos. RTW/7E/156 and RTW/7E/158 (Photograph taken on 5 September 2001)

Note: See Figure 21 for location of photographs.

Table of Contents
Table of Contents
Table of Contents
Table of Contents

Plate 22 - Oblique Aerial View of Trail between Squatter Structures Nos. RTW/7E/156 and RTW/7E/158 and Upper Concrete Channel (Photograph taken on 5 September 2001)

Note: See Figures 21 for location of photographs.

Table of Contents
Table of Contents
Table of Contents
Table of Contents

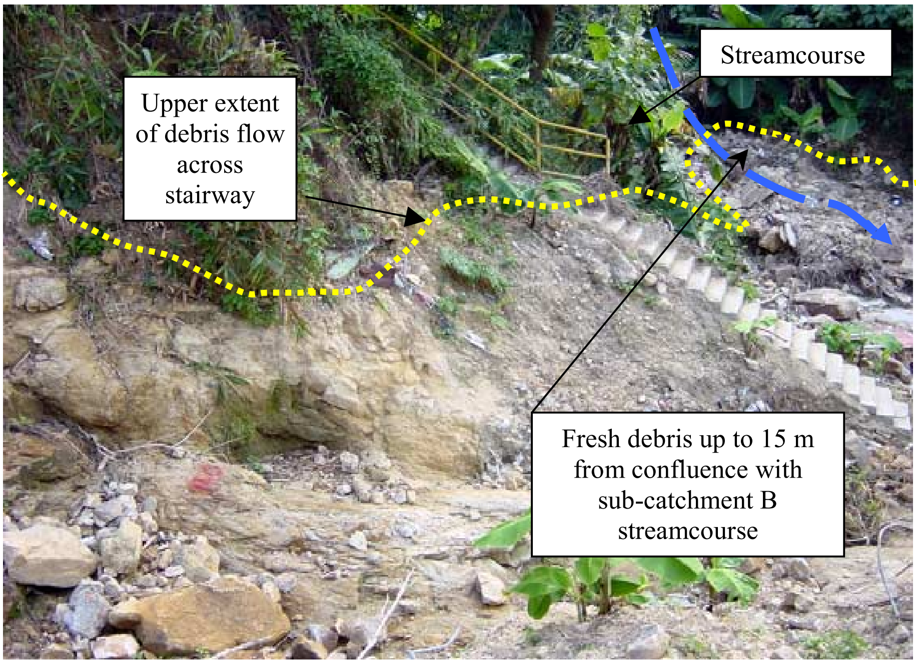

Plate 23 - View of Concrete Stairway near Sharp Bend in Debris Trail at Chainage 185
(Photograph taken on 18 October 2001)

Plate 24 - View of the Concrete Channel above the Active Construction Site Showing Scour Marks on the Wall Face Indicating the Debris Trajectory
(Photograph taken on 18 October 2001)

Note: See Figure 21 for location of photographs.

Table of Contents
Table of Contents
Table of Contents
Table of Contents

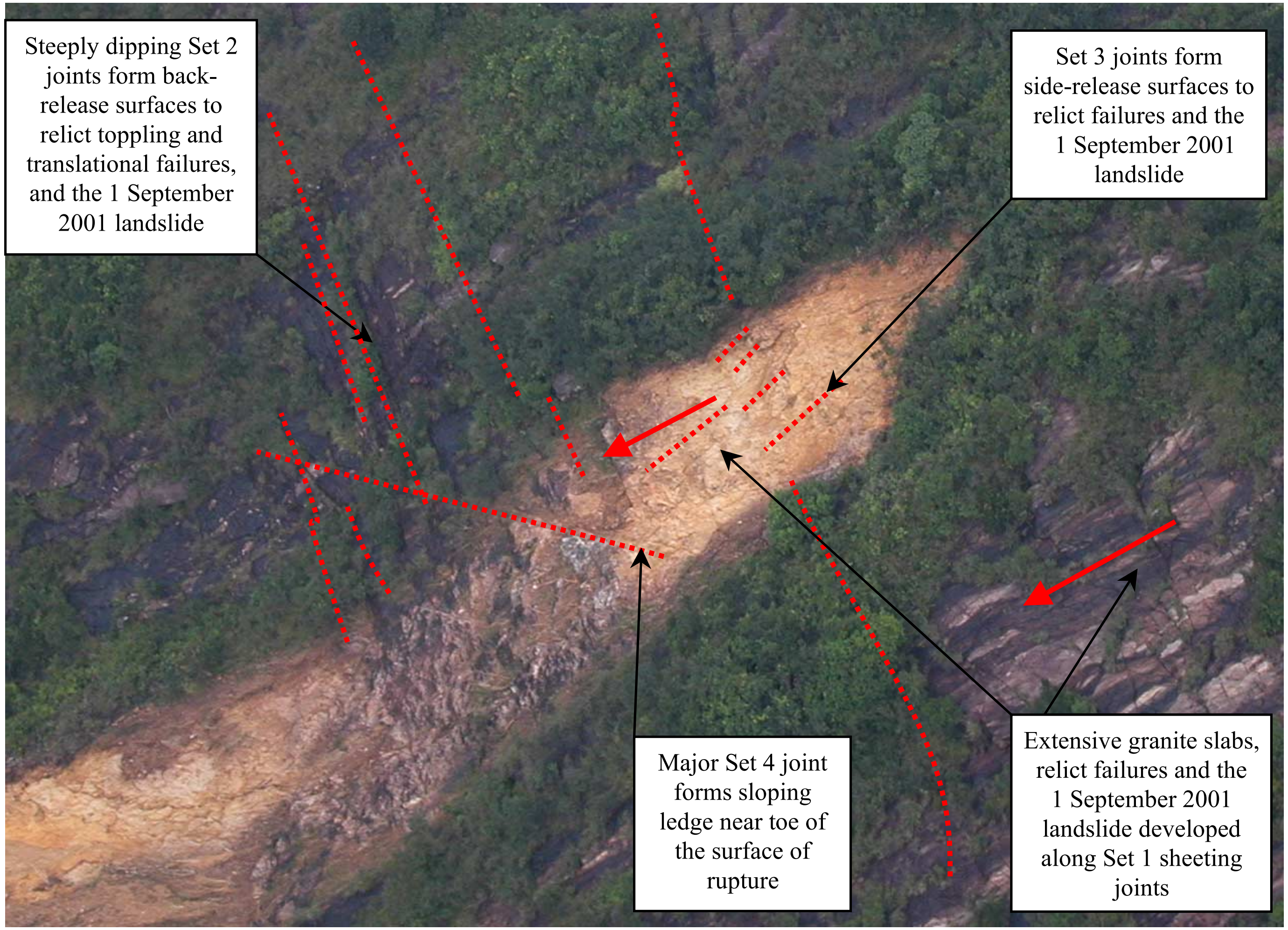

Plate 25 - Main Structural Controls near Source Area
(Photograph taken on 10 September 2001)

Note: See Figure 21 for location of photographs.

Table of Contents Table of Contents Table of Contents Table of Contents

Plate 26 - Dilated Joints in Rock Face above Source Area
(Photograph taken on 4 January 2002)

Note: See Figure 21 for location of photographs.

Table of Contents
Table of Contents
Table of Contents
Table of Contents

Plate 27 - View of the Floor and Lower Right Flank of the Source Area
(Photograph taken on 21 October 2001)

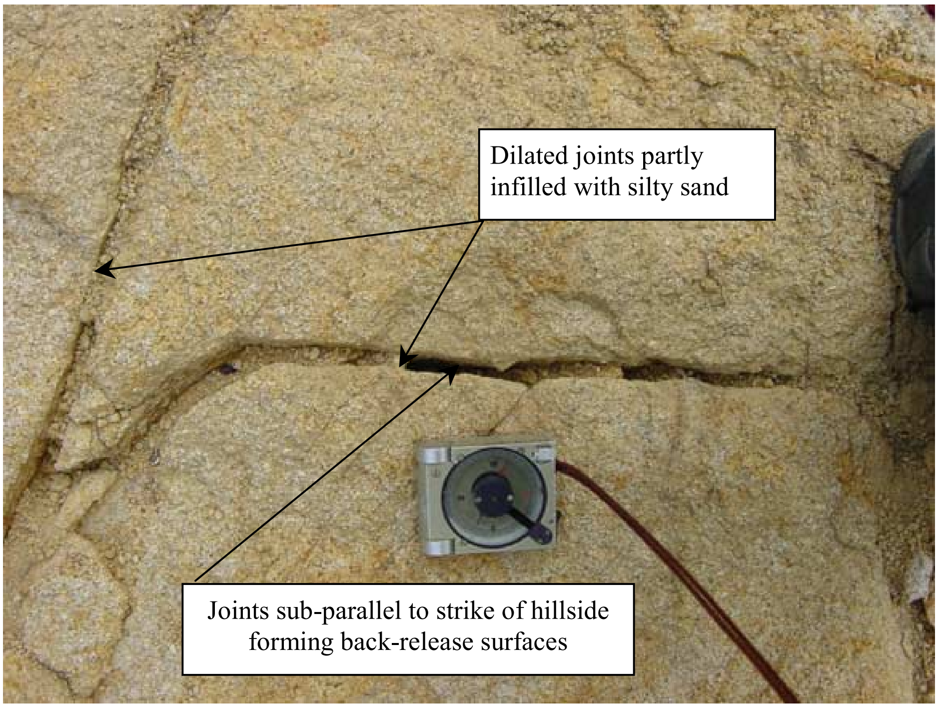

Plate 28 - View of Dilated Joints in the Source Floor
(Photograph taken on 21 October 2001)

Note: See Figure 21 for location of photographs.

Table of Contents
Table of Contents
Table of Contents
Table of Contents

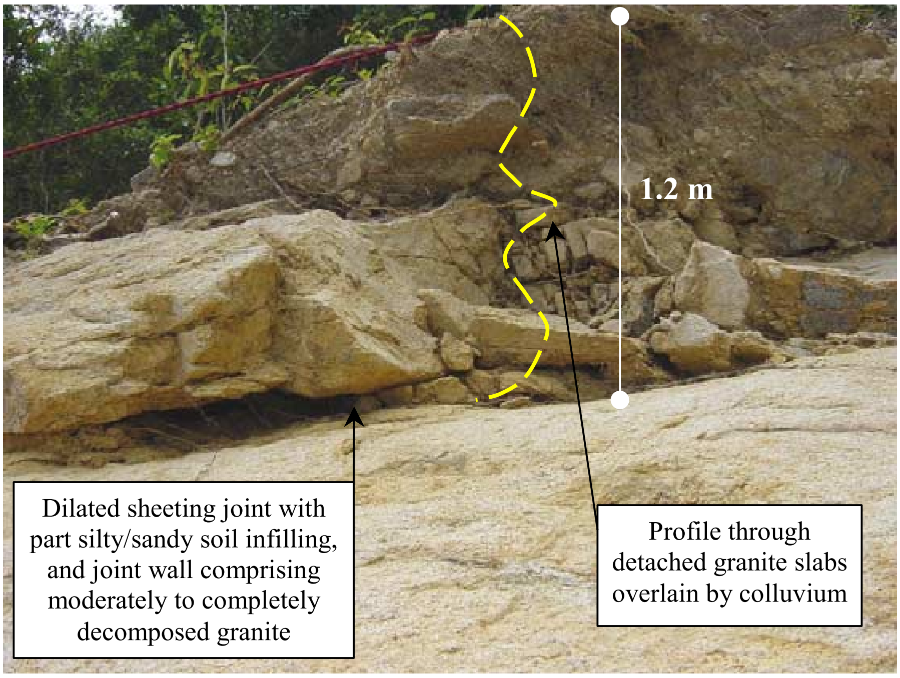

Plate 29 - View of Dilation and Infilling of Sheeting Joints in Right Flank of Source Area
(Photograph taken on 21 October 2001)

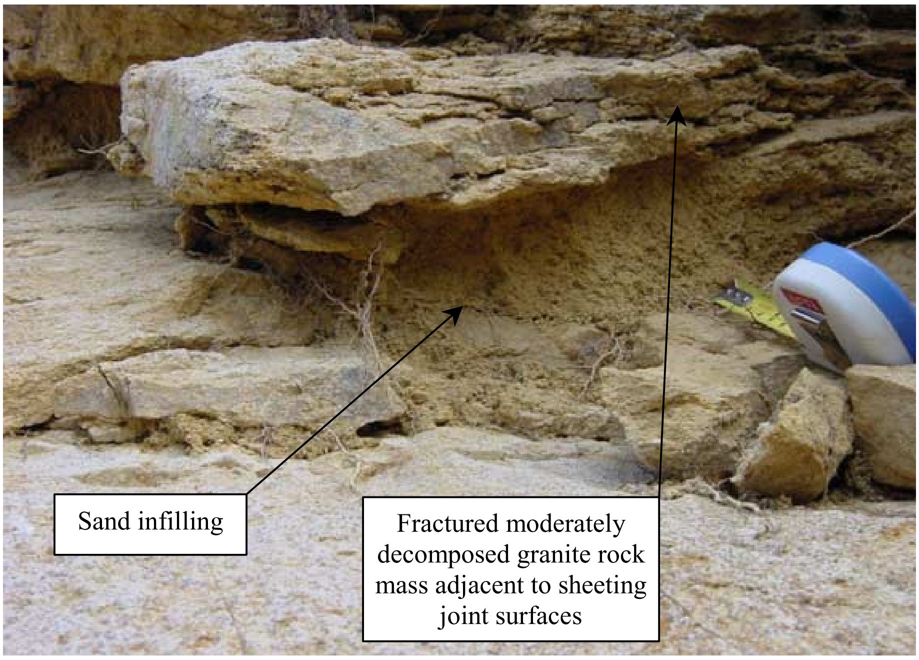

Plate 30 - View of Dilation and Infilling of Sheeting Joints in Left Flank of Source Area
(Photograph taken on 21 October 2001)

Note: See Figure 21 for location of photographs.

Table of Contents
Table of Contents
Table of Contents
Table of Contents

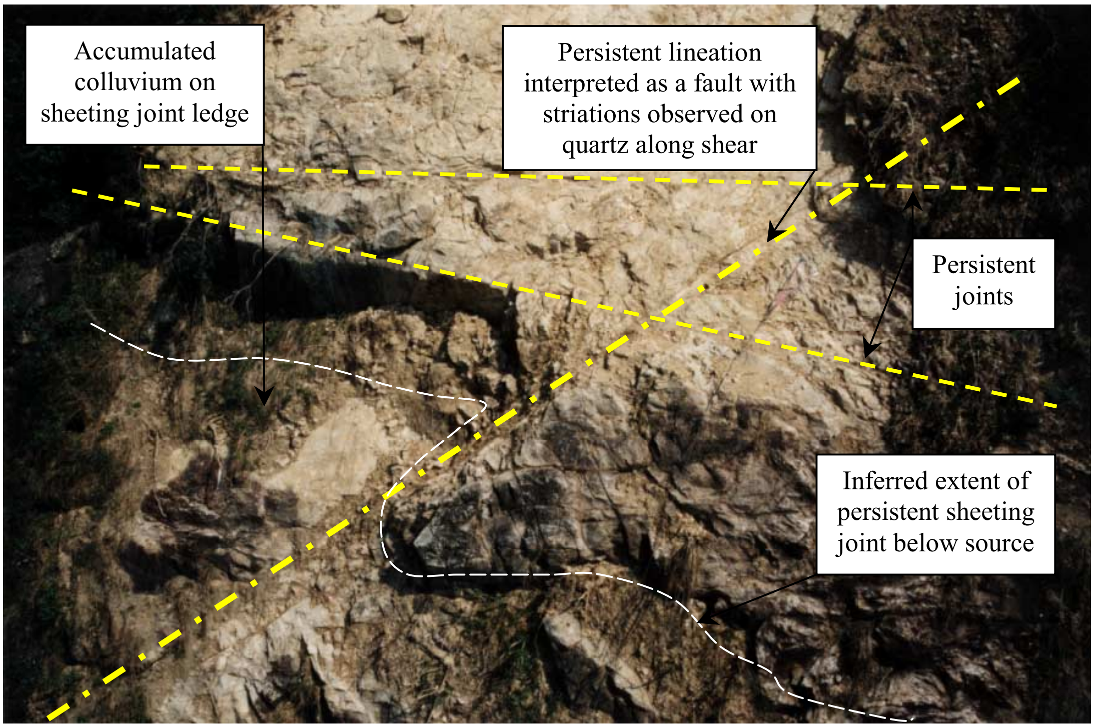

Plate 31 - Oblique Aerial View of the Lower Source Area and Upper Cliff (Photograph taken on 16 October 2001)

Note: See Figure 21 for location of photographs.

Table of Contents Table of Contents Table of Contents Table of Contents

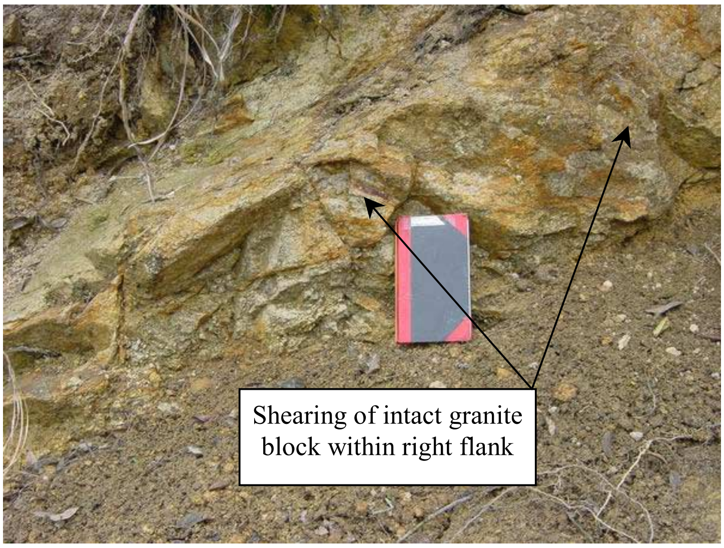

Plate 32 - View of the Lower Right Flank of the Source Area
(Photograph taken on 24 May 2002)

Plate 33 - View of the Right Flank of the Source Area
Showing Stepped Nature of Granite Joints
with Probable Block Interlocking
(Photograph taken on 24 May 2002)

Note: See Figure 21 for location of photographs.

Table of Contents

Table of Contents

Table of Contents

Table of Contents

Plate 34 - View of the Sheeting Joint Ledge below the Source Area
(Photograph taken on 24 May 2002)

Note: See Figure 21 for location of photographs.

Table of Contents Table of Contents Table of Contents Table of Contents

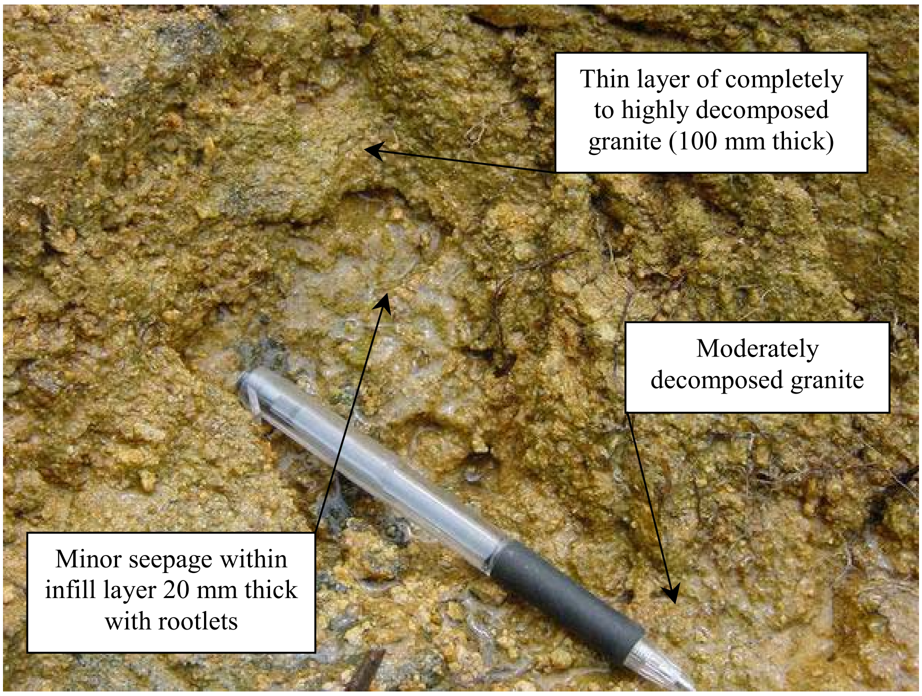

Plate 35 - View of the Surface of Rupture Showing Weathered Surface Materials, Infilling and Seepage (Photograph taken on 24 May 2002)

Note: See Figure 21 for location of photographs.

Table of Contents
Table of Contents
Table of Contents
Table of Contents

Table of Contents

Table of Contents

APPENDIX A

SITE DEVELOPMENT HISTORY

Table of Contents

Table of Contents

CONTENTS

Table of Contents
Table of Contents
Table of Contents

A.1 INTRODUCTION

References

The development history of Shek Lei Hill (Kam Shan) Village has been determined from:

(a) old topographic and ordnance maps,

(b) an interpretation of aerial photographs taken between 1949 and 2000, and

(c) documentary records from GEO's files.

Location of areas and features referred to in the following sections are shown in Figures A1.

A list of aerial photographs examined as part of this study is shown in Table A1.

A.2 SITE DEVELOPMENT

The earliest available documentary record of site development is provided by an ordnance survey map dated 1904, issued by the War Office, which was corrected and re-issued in 1924. This map shows cultivated areas downstream of the site along the south bank of the stream course up to an elevation of about 100 mPD. Above 100 mPD it was an undeveloped natural hillside. Close to the foot of the hillside, at an elevation of about 30 mPD was the macadamised old Castle Peak Road, the only major development on the Shek Lei Hill, which was then referred to as the Golden Hill.

Ordnance Survey 1904. Corrected and printed at the War Office, 1924. Golden Hill Sheet No. 9.

In 1949, agricultural terracing has modified the lower section of the stream course (below 82 mPD).

Aerial Photos Nos. Y02107-8 (5,800 ft)

The 1954 aerial photographs do not show significant change when compared with the 1949 photographs.

Aerial Photos Nos. Y02683-4 (29,200 ft)

By 1963, a grave had been constructed along the minor spurline (SP3A) at location G1, the construction of which has required both localised cutting and filling. A series of minor cultivated terraces had been constructed (AG1 1963). The study area has now become extensively modified by the construction of squatter structures and cultivated areas (Figure A2).

Aerial Photos Nos. Y08803-4 (4 100 ft)

By 1967, a quarry had been formed at the lower end of the study area. The site formation for the Shek Wah House and Shek Kai House immediately opposite to the quarry and for the two colleges is underway (Figure A2).

Aerial Photos Nos. Y13477-8 (3 900 ft)

Table of Contents
Table of Contents
Table of Contents
Table of Contents

By June 1969, Lei Pui Street up to the entrance of CNEC Christian College and Pope Paul VI College and the platform of Shek Wah House have been constructed, as indicated by the topographic maps. Cultivated terraces (currently registered as slope No. 7SW-C/C1255) had also been formed (Figure A3). The cultivated areas previously observed at location AG1 1963 have now been abandoned and a minor squatter structure constructed (SQ1 1973) (Figure A2 and A3). Slope No. 7SW-C/C1056 had been formed due to the construction of a large squatter area. Construction of further cultivation terraces had taken place at location AG1 1973. The transmitter station on the ridge-line above the 2001 landslide has been constructed, with a path bypassing the transmitter station having been constructed across the hillside, just above the main belt of rock slabs (Figure A2).

Topographic Sheet No. C-144-SE-D revised in June 1969 with minor amendments in Jan 1970 produced by Crown Lands and Survey Office, Hong Kong

Aerial Photos Nos. 4481 (2 400 ft)

By 1974, the main ephemeral drainage line and adjacent hillsides had been modified by the construction of agricultural terraces and minor squatter structures. The quarry site now appears no longer in use (Figures A2 and A3).

Aerial Photos Nos. 9576-7 (12 500 ft)

By 1975, the upper end of spurline SP1 had been significantly modified by the construction of cultivation terraces, with few sections of natural terrain remaining. Squatter structures have now been constructed within the abandoned quarry area.

Aerial Photos Nos. 11793-4 (12 500 ft)

Inspection of the aerial photographs of 1977 to 1979 do not indicate any significant development or changes

Aerial Photos Nos. 20051-2 (4 000 ft), 24029-30 (4 000 ft), 28105-6 (10 000 ft)

By 1981, a cut slope (currently registered as slope No. 7SW-C/C1060) had been formed in association with the construction of a small squatter platform. The cultivated area (AG1-1973) appears abandoned. A squatter structure had been constructed at location SQ1 1981 (Figure A2 and A3).

Aerial Photos Nos. 39104-5 (10 000 ft)

By 1982, a fill platform had been constructed below squatter structure SQ1 1981. The fill slope along the edge of the platform extends to the area adjacent to the ephemeral drainage channel AA′. The thickness of the fill is likely to be of a thin veneer only (max. 1.5 m). A minor cut slope (< 1 m) may also have been formed to the rear of the squatter structure but due to its position and dimensions, cannot be clearly observed from the aerial photographs examined.

Aerial Photos Nos. 43076-7 (3 000 ft)

Several squatter structures can be seen within the lower main streamcourse. Additional squatter structures have also been constructed within the recently abandoned quarry area (Figure A3).

The large cultivated area corresponding to slope

Table of Contents
Table of Contents
Table of Contents
Table of Contents

No. 7SW-C/C1255 now appears abandoned. The squatter structures constructed adjacent to slope No. 7SW-C/C1056 have increased and cover a more extensive area.

By 1984, the number of squatter structures present within the former quarry site had increased (Figure A3).

Aerial Photos Nos. 56537-8 (4 000 ft)

By 1986, additional cultivation had taken place at AG1 1986. Several squatter structures within the former quarry site had been demolished. Nevertheless, numerous other structures remained within the former quarry site.

Aerial Photos Nos. A04911-2 (4 000 ft)

By 1987, the vegetation density within the study area had increased. All cultivation areas, including AG1 1986 appear to have been abandoned and vegetated (Figure A2). The pump-house structures and compound in the former quarry site have been constructed.

Aerial Photos Nos. A10514 (4 000 ft)

By 1988, the squatter structure adjacent to slope No. 7SW-C/C1060 had been demolished (Figures A3 and A4). The squatter structures located on the fill platform at SQ1 1981 had been extended. Additionally, a linear retaining structure of less than 1 m in height had been constructed along the southern edge of the fill platform (RW1 1988). The squatter structure at location SQ1 1973 is still visible (Figure A2).

Aerial Photos Nos. A14772-3 (4 000 ft)

By 1989, the platform adjacent to the toe of slope No. 7SW-C/C1060 had become vegetated. A newly formed platform is visible at location SQ1 1989.

Aerial Photos Nos. A19700-1 (10 000 ft)

In 1990, no squatter structures had been constructed on the platform at SQ1 1989 (Figure A2).

Aerial Photos Nos. A24976-7 (4 000 ft)

Discernible changes are not evident in the 1991 to 1992 aerial photographs. The platform at SQ1 1989 appears to have been extended across the ephemeral drainage line and is shown as SQ1 1992 (Figure A2).

Aerial Photos Nos. A28812-3 (10 000 ft), A31227-8 (4 000 ft), A32339-40 (8 000ft)

By 1993, the density of squatter structures along the southern side of the main streamline had decreased due to demolition and removal of several structures (Figure A4). The platform areas formed at locations SQ1 1989 and SQ1 1992 are no longer visible, having now become obscured by vegetation (Figure A2).

Aerial Photos Nos. A36024-5 (4 000 ft)

A highly reflective section (< 2 m wide) of slope No. 7SW-C/C1060 is visible in the 1994 photographs and probably corresponds to a localised landslide or erosion-related incident.

Aerial Photos Nos. A39481-2 (10 000 ft), A39972-3 (4 000 ft)

Table of Contents
Table of Contents
Table of Contents
Table of Contents

Squatter structures along the upper sections of spurline SP2 had all been demolished by September 1995 and only the platforms remain visible (Figure A4). The squatter structure at SQ1 1981 has been demolished, with the platform area now empty. The squatter structure at SQ1 1973 remains visible. The majority of the squatter structures on both flanks of the main streamcourse have been demolished as well as those within the former quarry site.

Aerial Photos Nos. CN11104-5 (3 500 ft),

The platform adjacent to the toe of slope No. 7SW-C/C1060 had been cleared by June 1996. Vegetation is becoming established in the areas where squatter structures have been demolished.

Aerial Photos Nos. CN12468-9 (4 000 ft)

Almost all squatter structures within the study area had been removed by October 1998, except for a few structures within the former quarry site and squatter structures at SQ1 1973 (Figure A4 and A7).

Aerial Photos Nos. A48706-7 (4 000 ft)

By 1999, the study area had become well-vegetated by shrubs and trees. The platform area at SQ1 1981 remains visible (Figure A2). Additional squatter huts have been re-established within the former quarry site.

Aerial Photos Nos. A49716-7 (4 000 ft), CN25461-2 (8 000 ft)

No observable changes can be seen on the year 2000 photographs.

Aerial Photos Nos. CN26066-7 (20 000 ft), CN28025 (5 000 ft), CN20859 (6 000 ft), CN25996-6000 (20 000 ft)

A.3 PREVIOUS ASSESSMENTS

A.3.1 Non-Development Clearance Programme

In accordance with Government's policy of offering re-housing to occupants of squatter structures who are in immediate and obvious danger or those especially vulnerable to landslide risk, studies have been carried out by the GCO (renamed as Geotechnical Engineering Office, GEO in 1991) to identify squatter areas and specific squatter structures that need to be cleared under the Non-Development Clearance (NDC) Programme since the mid-1980's. The studies include terrain classification mapping, aerial photograph interpretation (API) and reference to records of landslide casualties, to identify areas of potential landslide hazard. Squatter structures that warrant clearance are identified following field inspections by GCO working to a Method Statement. Recommendations by GCO for squatter clearance on slope safety grounds and the re-housing of squatter occupants on Government land are implemented by the Lands Department (LD) and the Housing Department (HD).

GCO Instruction No. 2/89 Non-Development Clearance and Restoration Works in Squatter Areas which advocates the use of the Method Statement entitled "Squatter Clearance Studies for Tung Yeung, Tse Mei, Fuk Tak New and Ling Nam New (Upper) Villages"

Table of Contents
Table of Contents
Table of Contents
Table of Contents

In October 1984, HD requested advice from GCO as to whether any squatter structures within the boundary of Shek Lei Hill squatter area should be cleared on geotechnical grounds. In January 1985 GCO responded stating that "The Shek Lei Hill squatter area improvement does not fall within the scope of "Non-development Clearance of Squatters" agreed between the Housing Department (HD) and the GCO". However, following discussions between HD and GCO, it was agreed that "GCO will make recommendations for clearance in accordance with the geotechnical standards/guidelines adopted for Non-development Clearance". Following field inspections and review of site conditions GCO suggested that the site had moderate to extreme geotechnical limitations and subjective engineering judgement played an important role in identifying the areas for clearance along with the guidelines given in the Method Statement for Squatter Clearance titled "Squatter Clearance Studies for Tung Yeung, Tse Mei, Fuk Tak New and Ling Nam New (Upper) Villages". Site visits were carried out by GCO on 28 and 29 November 1984 and again on 18 and 21 December 1984 and squatter structures were identified for clearance (Figure A5).

HD's memo ref. no. HD (SAI) 6/49/2 dated 17/10/84
GCO's memo ref. no. GCMd 4/13/RA3 dated 17/1/85

Squatter Clearance Studies for Tung Yeung, Tse Mei, Fuk Tak New and Ling Nam New (Upper) Villages

Based on GCO's advice, clearance of squatters was carried out, commencing 1985 (Figures A4, A5 and A6). Some of the structures located within the former quarry site were cleared in 1986 and clearing of squatters and demolition of structures continued until 1988. The squatter structures with squatter control survey Nos. RTW/7E/156 and RTW/7E/158, located at SQ1 1973 on Figure A2 were not recommended for clearance (Figure A5). A new platform was constructed in 1989 at SQ1 1989. This platform area was extended in 1992, and is shown as SQ1 1992 in Figure A2.

The number of squatter structures in the Shek Lei Hill (Kam Shan) Village decreased further from 1992 with the implementation of the 1992 NDC Programme. GEO's recommendations for clearance were forwarded to HD and Buildings and Lands Department in November 1992, which included the squatter structures Nos. RTW/7E/156 and RTW/7E/158 that were subsequently destroyed in the 1 September 2001 landslide incident (Figure A6).

GEO's memo ref. no. (26) in GCMd 4/13/RA11 II dated 12/11/92

Following minor landslide incidents (GEO Incidents Nos. MW93/5/3, MW93/5/2 and MW93/5/15) within the former quarry site in May 1993, GEO recommended that several squatter structures located within the former quarry site be permanently and immediately evacuated (Figure A6). Joint inspections by GEO and HD were carried out in May and June 1993 and it was discovered that many squatter structures recommended for clearance under the 1985 NDC Programme were still present. It was recommended that these squatter structures and others adjacent to them, which will become structurally unstable due to the demolition of the adjoining

GEO's memos ref. nos. GCMd 2/E2/93 (W) dated 5/5/93 and GCMd 2/E2/93-1(W) dated 7/5/93
HD's memo ref. No. (20) in TW/C 6/3/93 dated 2/6/93

DLO, Kwai Tsing's memo ref. no. (57) in DLO/KT 7/983/87 dated 11/6/93

Table of Contents Table of Contents Table of Contents Table of Contents

structures, should also be cleared. Following GEO's recommendations, based on GEO guidelines on clearance on geotechnical grounds, all except about 10% of the structures were to be cleared (Figure A6). Given the operational and practical difficulties involved in allowing a small number of squatters to remain, the District Office (DO) Kwai Tsing recommended that the clearance exercise at Shek Lei Village be extended to those remaining squatter structures not covered by the GEO's proposed clearance plan. On 16 July 1993 a pre-clearance survey was conducted which identified that 11 structures were not recommended for clearance on geotechnical grounds. However, due to the difficulties of allowing a small number of squatter structures to remain, the 16th NDC Liaison Meeting held on 24 August 1993 recommended that the remaining squatter structures should also be cleared on "other grounds", subject to following conditions stipulated at the NDC Liaison Meeting being satisfied:

DO (Kwai Tsing) 's memo ref. no. (82) in KC D/2/63 dated 6/8/93 and DLO, Kwai Tsing's memo ref. no. (78) in DLO/KT 7/983/87 dated 17/8/93.
HD's letter ref. no. HD(C) 13/395/93 dated 18/8/93 to Legislative Council
DLO, Kwai Tsing's memo ref. no. (84) in DLO/KT 7/983/87 dated 24/8/93 to GLA/EM

1. "There must be a request from the remaining residents indicating they also wish to be cleared, with reasons".
2. "The request is supported by the D.O. of the District concerned".
3. "The population of the remaining squatters must not be more than 20% within that particular NDC area or must not be more than 30 families, whichever is the less".
4. "Additional resources are available within the concerned Departments (e.g. Lands Department, DLOs, Housing Department)".
5. "If the request is approved by the NDC Liaison Meeting, a separate CAF should be made as a stage II clearance so that the original NDC recommended by GEO on slope safety grounds will not be delayed".

A joint site inspection was conducted by GEO, HD and DLO, Kwai Tsing on 14 July 1993 and structures recommended for clearance under NDC Stage I by February 1994 were confirmed on site. In addition nine structures were to be cleared under the Emergency Relief Scheme (Landslip Cases). A further 25 structures were cleared on "other grounds" (Figure A6).

DLO, Kwai Tsing's memo ref. no. (87) in DLO/KT 7/983/87 dated 2/9/93 to GEO
HD's memos ref. nos. (31) in TW/C 51/3/93 dated 10/11/93 and (53) in TW/C 46/3/93 dated 23/3/94 to Police.

Most of the structures had been cleared on 24 March 1995, the "Day of Clearance" under Clearance No. KT 2/93 (on geotechnical grounds) and KT 6/93 (on other grounds) and the land was handed over to DLO on 24 March 1995 (Figure A7). However, a total of 23 occupants from 19 squatter structures remained on site, immediately after clearance (under clearance Nos. KT 2/93 and KT 6/93), for various reasons including the occupant of the squatter

HD's memos ref. nos. (174) in TW/C 6/3/93 III dated 24/3/95 and (125) in TW/C 94/3/93 dated 24/3/95 to DLO Kwai Tsing

Table of Contents
Table of Contents
Table of Contents
Table of Contents

structures Nos. RTW/7E/156 and RTW/7E/158, the squatter structures, which were demolished during the 1 September 2001 landslide incident. By 1998 most of them had been re-located and re-housed except the occupant of squatter structures Nos. RTW/7E/156 and RTW/7E/158.

At the time of the 1 September 2001 landslide incident, squatter structures Nos. RTW/7E/156 and RTW/7E/158 were occupied by four persons, who were fortunate to have vacated the structures about two hour before the landslide.

Interview with the occupant of squatter structures Nos. RTW/7E/156 and RTW/7E/158 conducted on 7.9.01

A.3.2 <u>Clearance for LPM Works</u>

By 1999 some minor squatter structures had re-established within the former quarry site. Slopes Nos. 7SW-C/C180 and 7SW-C/C182 were identified for upgrading and they were included in the LPM programme in 1999. The site inspections undertaken in November and December 1999 by the consultant, Scott Wilson Hong Kong Ltd., responsible for designing the LPM works, revealed the existence of squatter structures within the abandoned former quarry site and requested "re-clearance" of the site on 1995 NDC grounds. However, DLO informed the consultant that re-clearance does not apply to this site and requested the consultant to apply for clearance using Clearance Application Form (CAF).

DLO, Kwai Tsing's letter ref. no. (8) in L/M 103 in DLO/KT 14/155/76 dated 22/12/99

The consultant in February 2000 submitted a CAF for slope No. 7SW-C/C182. Site inspection by the consultant, HD and DLO was carried out on 23 May 2000 to clarify the clearance limits. Following the inspection, the latrine and the pump house were excluded from clearance. The revised clearance limit was accepted by DLO and Clearance of Land - Clearance No. 3/2000 was issued on 19 June 2000 together with the clearance plan. On 12 July 2000 the clearance was announced by the HD and the pre-clearance survey was carried out (survey No. KT3/2000/1-11), which identified a total of eleven squatter structures (with one occupied squatter structure) and one occupant for clearance. The clearance was carried out on 30 November 2000 (Figure A7) and the site was handed over to the consultant for LPM works on 11 December 2000.

GEO's memo ref. no. GCW 2/A2/227(H) dated 28/2/00

DLO, Kwai Tsing's memo ref. no. (11) in DLO/KT 5/983/2000 dated 19/6/00

HD's memos ref. nos. (15) and (19) in HD(C)NTW 3/8/2000 dated 12 and 18/7/00

HD's memo ref. no. (31) in HD(C)NTW3/8/2000 dated 30/11/00 and DLO, Kwai Tsing's memo ref. no. (37) in DLO/KT 5/983/2000 dated 11/12/00

A.3.3 <u>Aerial Photograph Interpretation</u>

Two aerial photograph interpretation (API) studies discussing the geomorphology and terrain stability of the hillside above Shek Lei Hill (Kam Shan) Village and above slope No. 7SW-C/C182 have been carried out in the past.

Table of Contents
Table of Contents
Table of Contents
Table of Contents

The first API, carried out in July 1986 as part of the Stage 1 study of slope No. 7SW-C/C182. A Stage 1 study of a slope is a preliminary stability assessment comprising a detailed field inspection, a desk study and a geotechnical appraisal based on available information. Stage 1 studies were initiated by GCO as part of their responsibility for the investigation of slopes and retaining structures under the Landslip Prevention Measures Programme. The report noted that the slope (slope No. 7SW-C/C182) was not formed in July 1963; but many terraces had been cut to house squatter structures above the location of the present slope. The July 1967 photograph had shown the start of the quarry as a minor borrow area and the start of the formation of the slope. By 1976 the quarry has been re-vegetated and occupied by squatters. The report noted that by 1982 some of the squatter structures had been removed from the former quarry floor due to squatter clearance.

API report included as part of the Stage 1 Report No. S1R 65/86 dated July 1986 carried out on slope No. 7SW-C/C 182.

The other API, was carried out in December 2000 by Scott Wilson Consultants as part of the LPM Stage 3 study of slope No. 7SW-C/C182. The API notes that “there is a large catchment area to east of the Feature with the drainage lines converging to the main drainage line which is truncated by the Feature. Colluvial deposits are seen to be limited to the valley area above the Feature. Since the formation of the Feature, the area has been occupied by squatters”. The possible relict landslides identified in this report, including the locations of landslide incidents recorded by GEO and inferred locations of landslides from the NTLI and LLS records, are shown in Figure 7 of this report.

API Report as part of the Stage 3 Study Report No. S3R 118/2000 prepared by Scott Wilson Consultants Hong Kong Ltd., on Feature No. 7SW-C/C182 Kam Shan Village, Shek Lei, Kwai Chung dated December 2000.

Table of Contents

Table of Contents

Table of Contents

Table of Contents

LIST OF TABLES

Table A1 - Aerial Photographs Examined

Date	Altitude (ft)	Photograph Number
24 April 1949	5 800	Y02107-8
18 November 1954	29 200	Y02683-4
26 January 1963	4 100	Y08803-4
31 January 1963	3 900	Y08864-5
13 May 1967	3 900	Y13477-8
14 July 1973	2 400	4481
20 November 1974	12 500	9576-7
19 December 1975	12 500	11793-4
12 December 1977	4 000	20051-2
07 December 1978	4 000	24029-30
28 November 1979	10 000	28105-6
26 October 1981	10 000	39104-5
28 July 1982	3 000	43076-7
20 October 1984	4 000	56537-8
28 April 1986	4 000	A04911-2
04 October 1987	4 000	A10514
16 January 1988	10 000	A12070-1
06 October 1988	4 000	A14772-3
29 November 1989	10 000	A19700-1
26 November 1990	4 000	A24976-7
29 October 1991	10 000	A28812-3
13 May 1992	4 000	A31227-8
14 October 1992	8 000	A32339-40
02 November 1993	4 000	A36024-5
21 October 1994	10 000	A39481-2
8 November 1994	4 000	A39972-3
26 September 1995	3 500	CN11104-5
12 June 1996	4 000	CN12468-9
01 November 1997	10 000	CN19028-9
30 October 1998	4 000	A48706-7
30 July 1999	4 000	A49716-7
09 December 1999	8 000	CN25461-2
16 February 2000	20 000	CN26066-7
14 September 2000	5 000	CN28025
	6 000	CN20859
	20 000	CN25996 - 26000

Notes: (1) All aerial photographs are in black and white except those denoted with the CN prefix besides the photograph number.
(2) Additional aerial photographs are likely to exist, but a representative selection has been evaluated.

Table of Contents
Table of Contents
Table of Contents
Table of Contents

LIST OF FIGURES

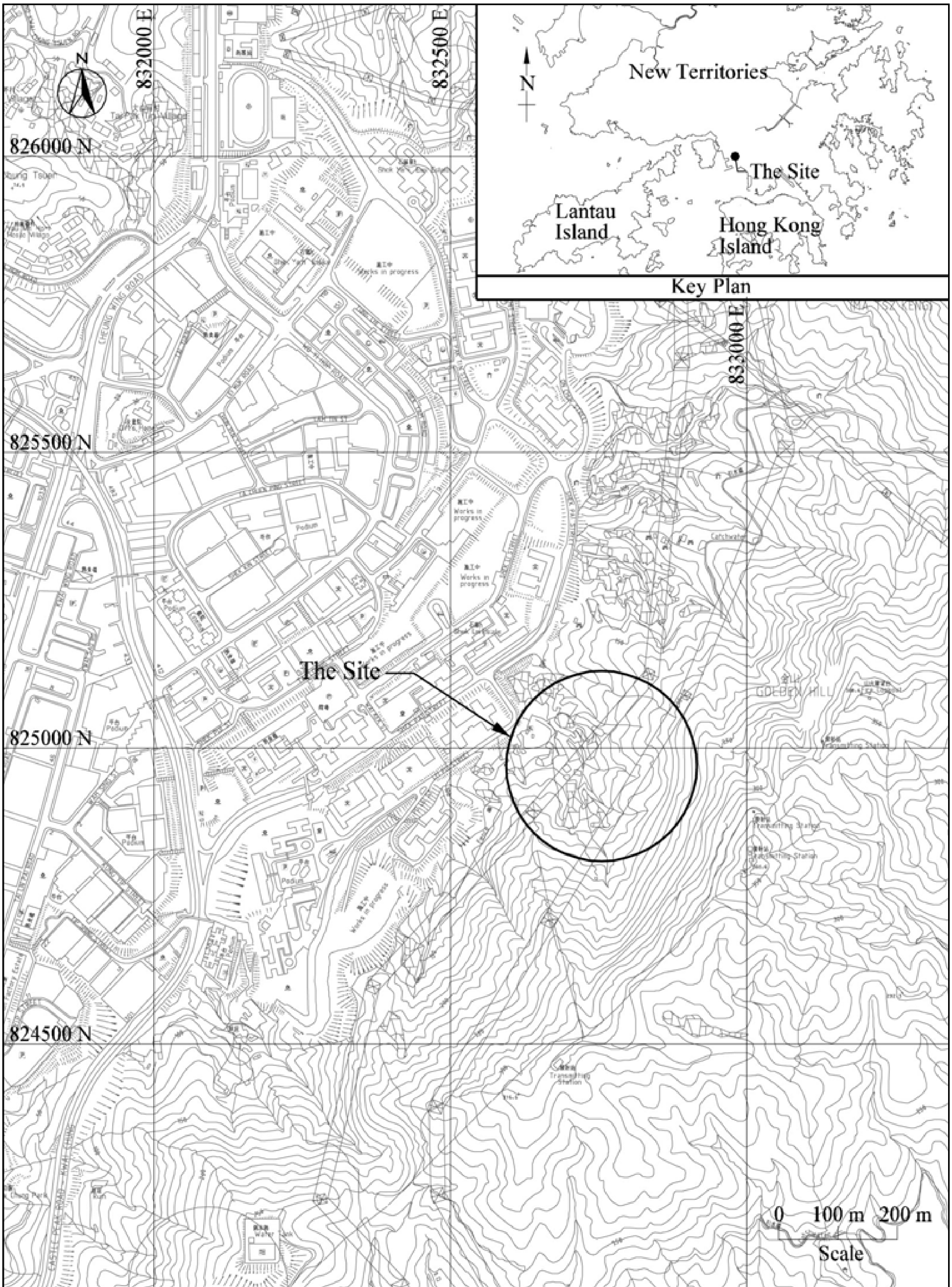

Figure A1 - Site Development Location Plan

Table of Contents Table of Contents Table of Contents Table of Contents

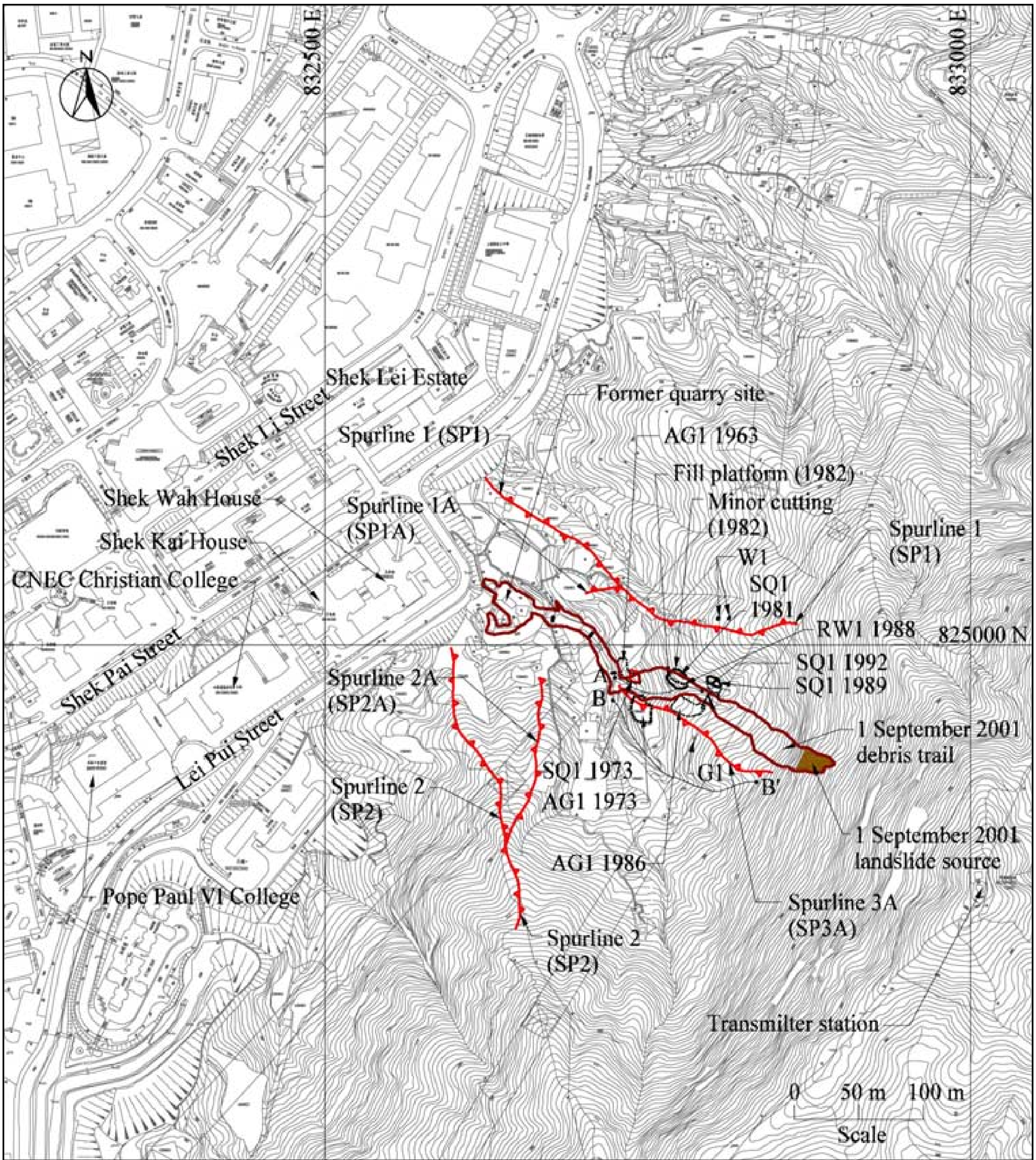

Legend :					
SQ1 1973	Squatter structure SQ1 first visible on 1973 aerial photograph	Fill Platform (1982)	Fill platform first visible on 1982 aerial photograph	(SP2)	Spurline SP2
RW1 1988	Retaining wall RW1 first visible in 1988 aerial photograph	G1	Grave G1	W1	Footbridge or weir W1
AG1 1973	Cultivation terrace AG1 first visible on 1973 aerial photograph	B B'	Streamcourse from B' to B		

Note : Base plan is extracted from 1 : 1000 survey sheets Nos. 7SW22B dated March, 2001.

Figure A2 - Key Features Identified by API

Table of Contents
Table of Contents
Table of Contents
Table of Contents

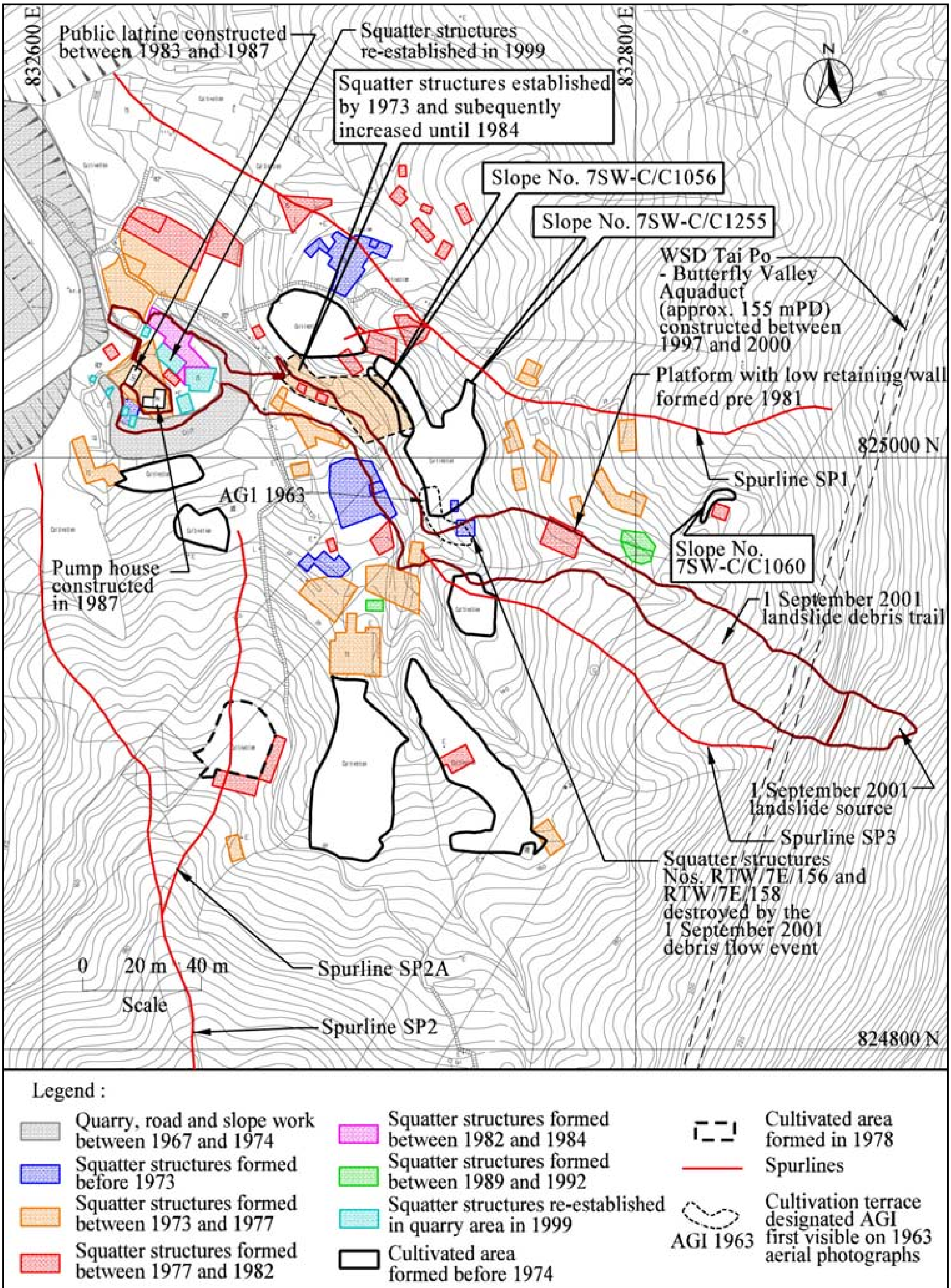

Notes : (1) Base plan is extracted from 1 : 1000 survey sheet No. 7SW22B dated March, 2001.
(2) No significant establishment of squatter structures between 1984 and 1989.

Figure A3 - Site Development History

Table of Contents
Table of Contents
Table of Contents
Table of Contents

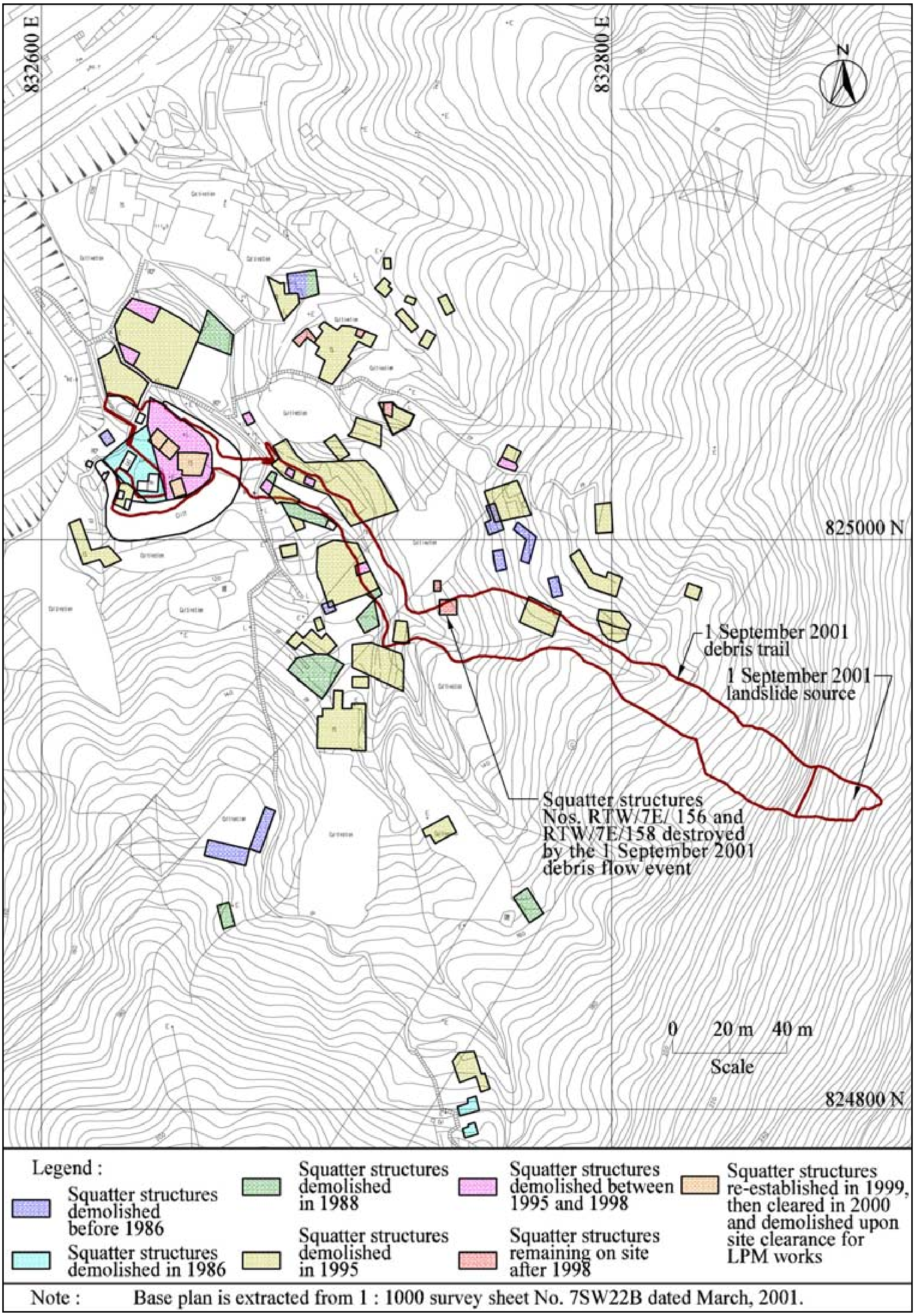

Figure A4 - Demolition History of Squatter Structures

Table of Contents
Table of Contents
Table of Contents
Table of Contents

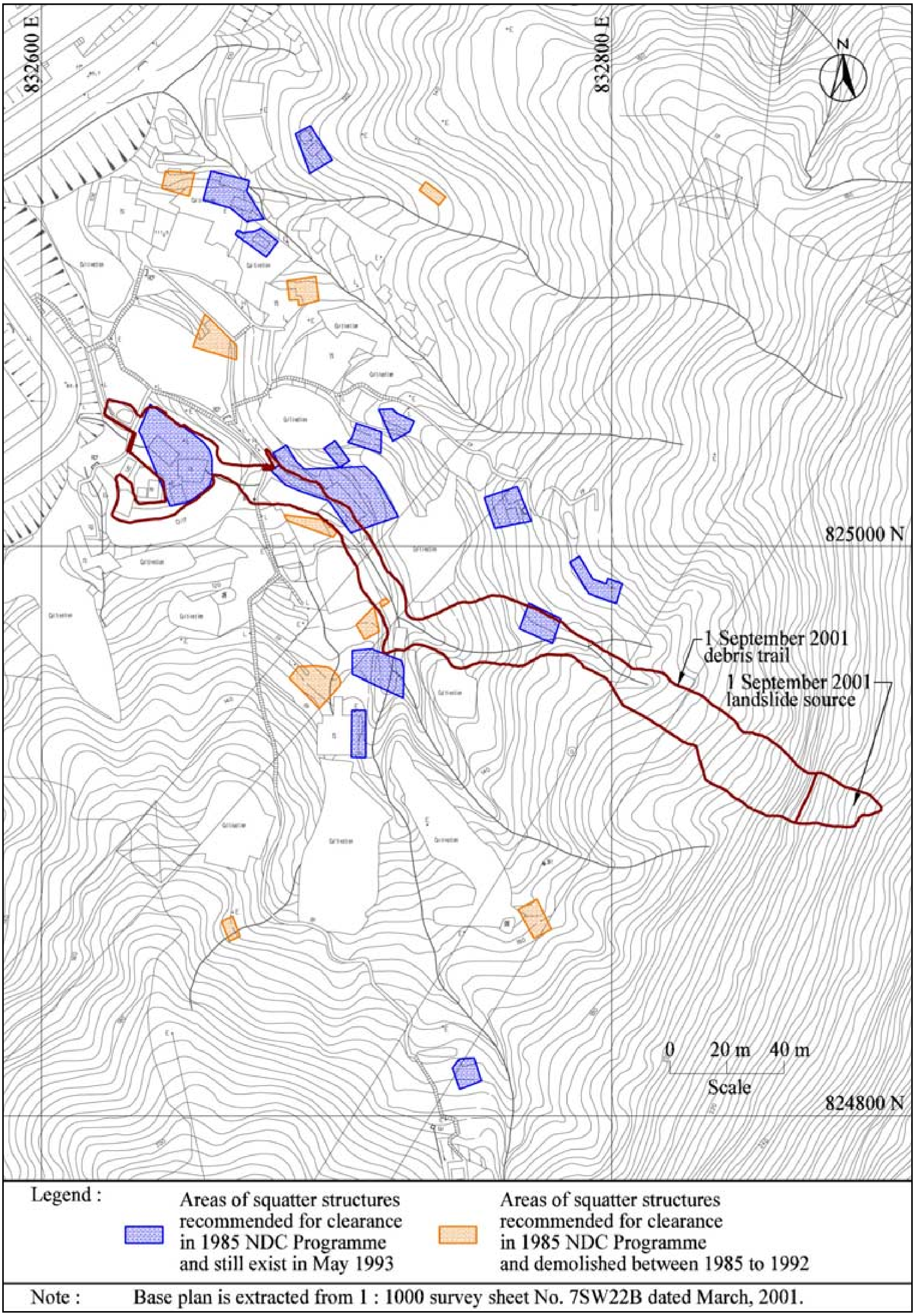

Figure A5 - Squatter Structures Recommended for Clearance under the 1985 NDC Programme

Table of Contents
Table of Contents
Table of Contents
Table of Contents

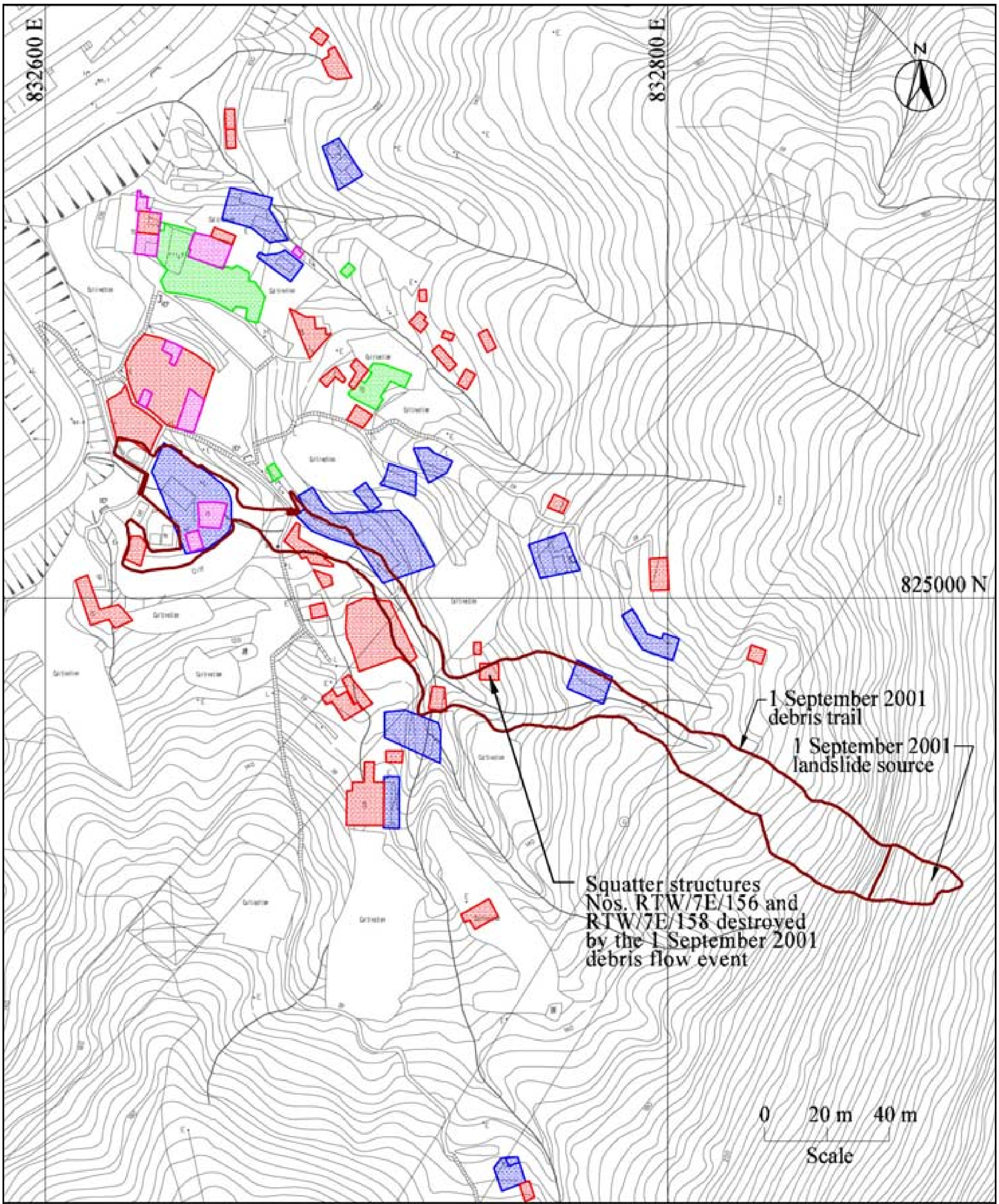

Legend :

- Area of squatter structures recommended for clearance in 1985 NDC programme but still existed in May 1993, and included for clearance in 1992 NDC Re-inspection Programme on "geotechnical grounds"
- Squatter structures recommended for immediately and permanent evacuation due to landslides
- Areas of squatter structures recommended for clearance in 1992 NDC Re-inspection Programme on "geotechnical grounds"
- Additional area of squatter structures recommended for clearance in June 93 under the 1992 NDC Re-inspection Programme on "other grounds"

Note : Base plan is extracted from 1 : 1000 survey sheet No. 7SW22B dated March, 2001.

Figure A6 - Squatter Structures Recommended for Clearance under the 1992 NDC Re-inspection Programme

Table of Contents
Table of Contents
Table of Contents
Table of Contents

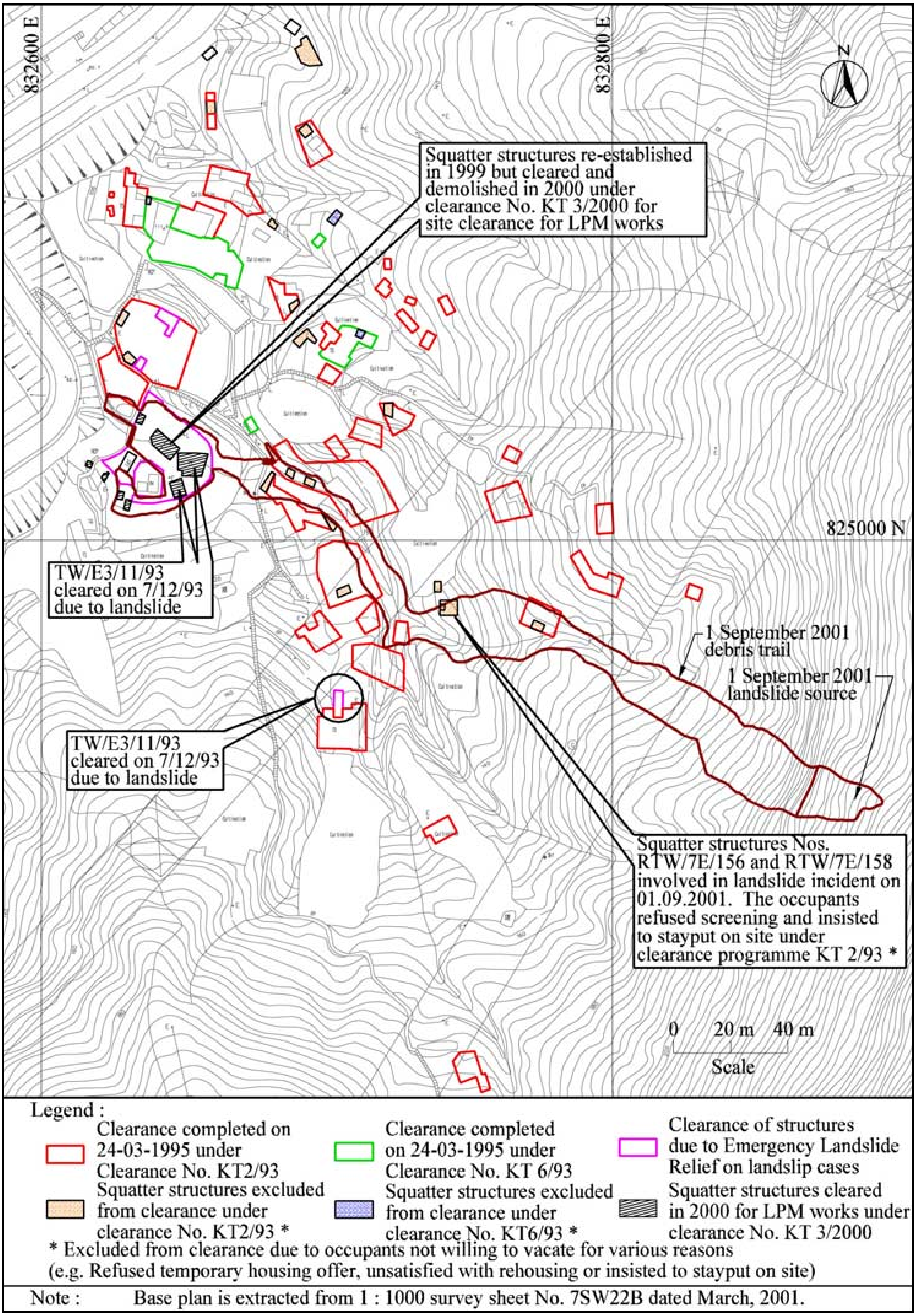

Figure A7 - Squatter Structures Remaining on Shek Lei Hill (Kam Shan) Village after Completion of Clearance on 24 March 1995

Table of Contents
Table of Contents
Table of Contents
Table of Contents

Table of Contents

Table of Contents

APPENDIX B

KINEMATIC STABILITY ANALYSIS AND ESTIMATION OF JOINT ROUGHNESS

Table of Contents

Table of Contents

CONTENTS

B.1 KINEMATIC STABILITY ANALYSIS

Figure B1 shows a stereoplot and a kinematic stability assessment of the joint sets mapped within the site.

B.2 JOINT ROUGHNESS ANGLE (i) BASED ON FIELD MEASURMENTS

The roughness of the rupture surface was surveyed in detail by measuring the local inclination using both a 210 mm and 420 mm diameter plate on a 0.2 m by 0.2 m grid in two areas of the surface of rupture (Figure 8). Area 1 is located on the south side of the source and Area 2 is located on the north side of the source.

The estimate of the local roughness angle (i) was carried out in accordance with Richards and Cowlands (1982). The resulting profiles and stereoplot of the results are shown in Figures B2 and B3 for Areas 1 and 2 respectively.

Profile Estimations

The roughness angle from the profiles in Area 1 varied from 11° to 17° for the 420 mm and 210 mm plates respectively. The roughness angle from the profiles in Area 2 varied from 29° to 14° for the 420 mm and 210 mm plates respectively. The value of 29° for the 420 mm is due to a local ‘lip’ in the profile where an underlying sheeting joint slab has detached. The next highest value of (i) is 11°, on the continuous sheeting joint surface.

Stereoplot Estimations

The roughness angle from the stereoplots was determined from the statistical grouping/contouring of the joint data, ignoring any obvious, local extreme points. The roughness angle (i) from the stereoplots in Area 1 varied from 10° to 16° for the 420 mm and 210 mm plates respectively. The roughness angle (i) from the stereoplots in Area 2 varied from 9° to 11° for the 420 mm and 210 mm plates respectively.

Plate Diameter

Given the scale and decomposed/infilled nature of the exposed sheeting joints in the surface of rupture and flanks of the source area, the results of measurements using the larger scale 420 mm plate are likely to give values that more closely reflect the apparent angle of friction. The roughness angles estimated from the profiles are similar for all of the 420 mm plate readings and give an average angle (i) of approximately 11°.

Large-scale Waviness

Field estimates of the large-scale wavelength and amplitude are approximately 4 to 5 m and 150 - 200 mm respectively. These estimates give extreme (i) values of between 3.5° and 6°.

Representative Range of Roughness Angle (i) for Analysis

The operating range of angle (i) assumed in the sensitivity analysis is 9° to 11° and is based on the 420 mm diameter plate measurements.

Table of Contents
Table of Contents
Table of Contents
Table of Contents

B.3 ESTIMATION OF EFFECTIVE FRICTION ANGLE FROM JOINT ROUGHNESS COEFFICIENT VALUES

Estimates of the Joint Roughness Coefficient (JRC) obtained by comparing the profiles of the exposed sheeting joints with published profiles (Barton, 1990), gave values of JRC that ranged from 8 to 12.

Barton (1990) and Barton & Bandis (1990) suggest that three factors control the strength of natural discontinuities: the basic friction angle ϕ_b, a geometrical joint roughness component (JRC), and an asperity failure component JCS/σn. Also, as the scale increases, the effective roughness of the surface JRC decreases, and thus the shear strength of the surface decreases. It is also possible that the joint wall compressive strength (JCS) may decrease with increasing scale due to the higher probability of zones of weak materials occurring over larger areas. Weathering and infill along a joint surface can significantly reduce the shear strength of the joint. A JCS value of 2 MPa has been used in the shear strength calculations, as the basal rupture surface contains significant areas of highly to completely decomposed granite along the sheeting joints. The shear strength is also likely to be reduced significantly when large parts of the rock joint surfaces are not in rock-to-rock contact.

The average basic friction angle is assumed to be 36° (derived from shear tests on saw-cut test samples). Calculations of joint shear strength are shown in Sheets B1 and B2. Two sets of calculations are presented. The first set does not consider scale effects and results in high values of effective friction angle (52° to 63°). The second set considers scale effects that reduce the effect of the small-scale asperities and allows for the presence of infill or much softer wall-rock which may occur within a very extensive sheeting joint. The second set of calculations results in a much lower range of effective friction angles of 39° to 41°.

Table of Contents
Table of Contents
Table of Contents
Table of Contents

LIST OF FIGURES

Table of Contents
Table of Contents
Table of Contents

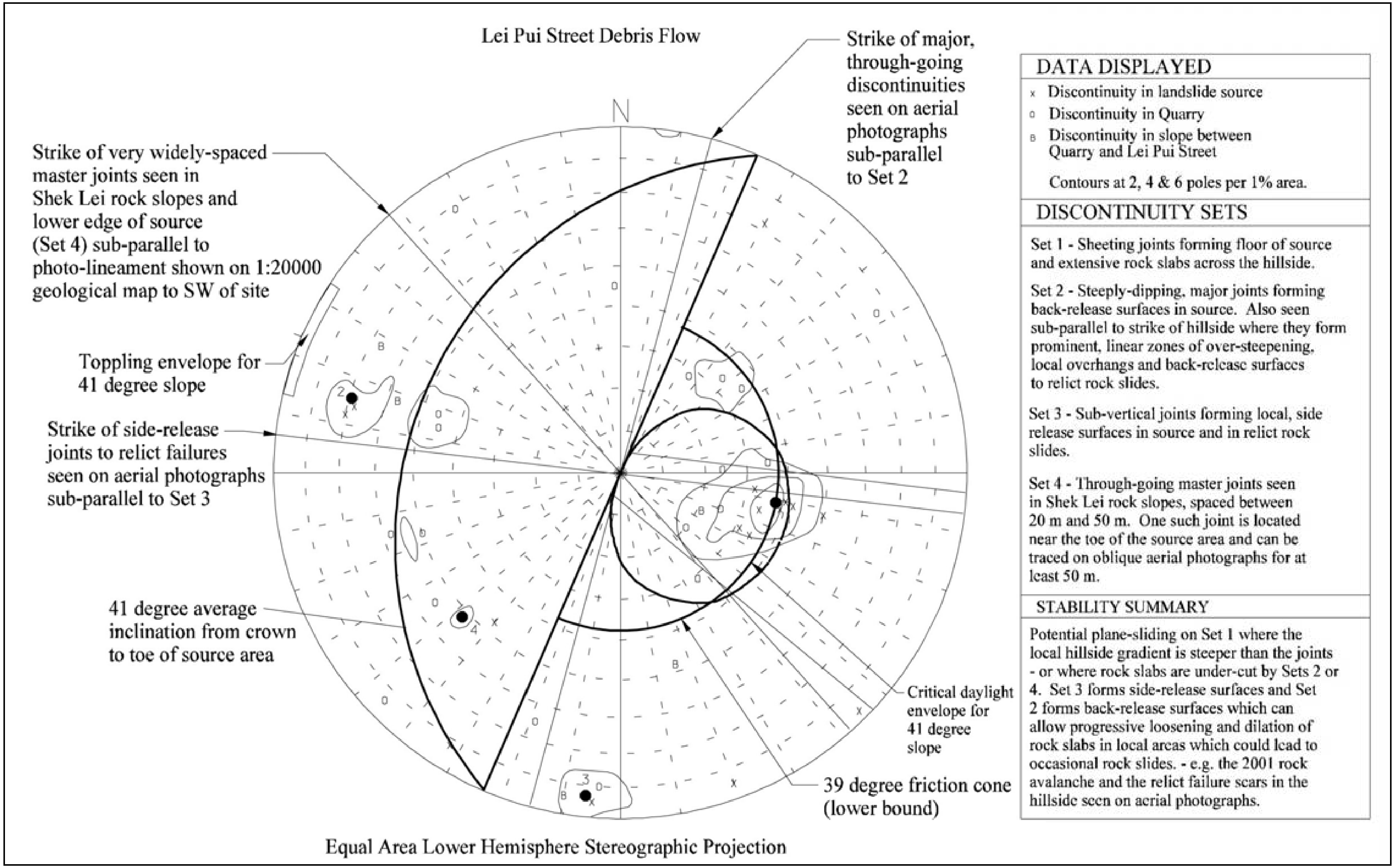

Figure B1 - Stereoplot of Joint Sets and Kinematic Stability Assessment of the Landslide Source Area

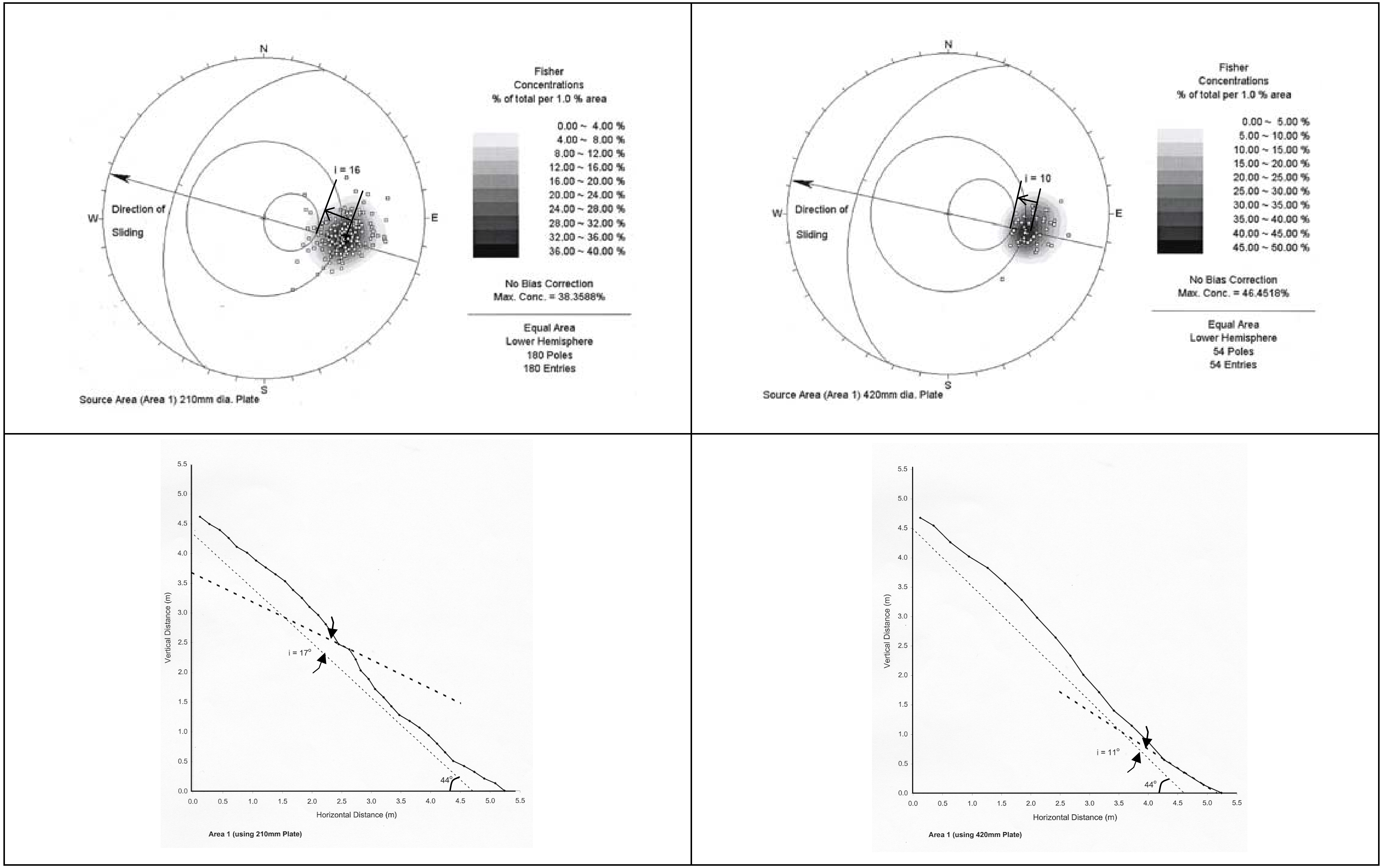

Figure B2 - Joint Roughness Characteristics of the Surface of Rupture (Area 1)

Table of Contents
Table of Contents
Table of Contents
Table of Contents

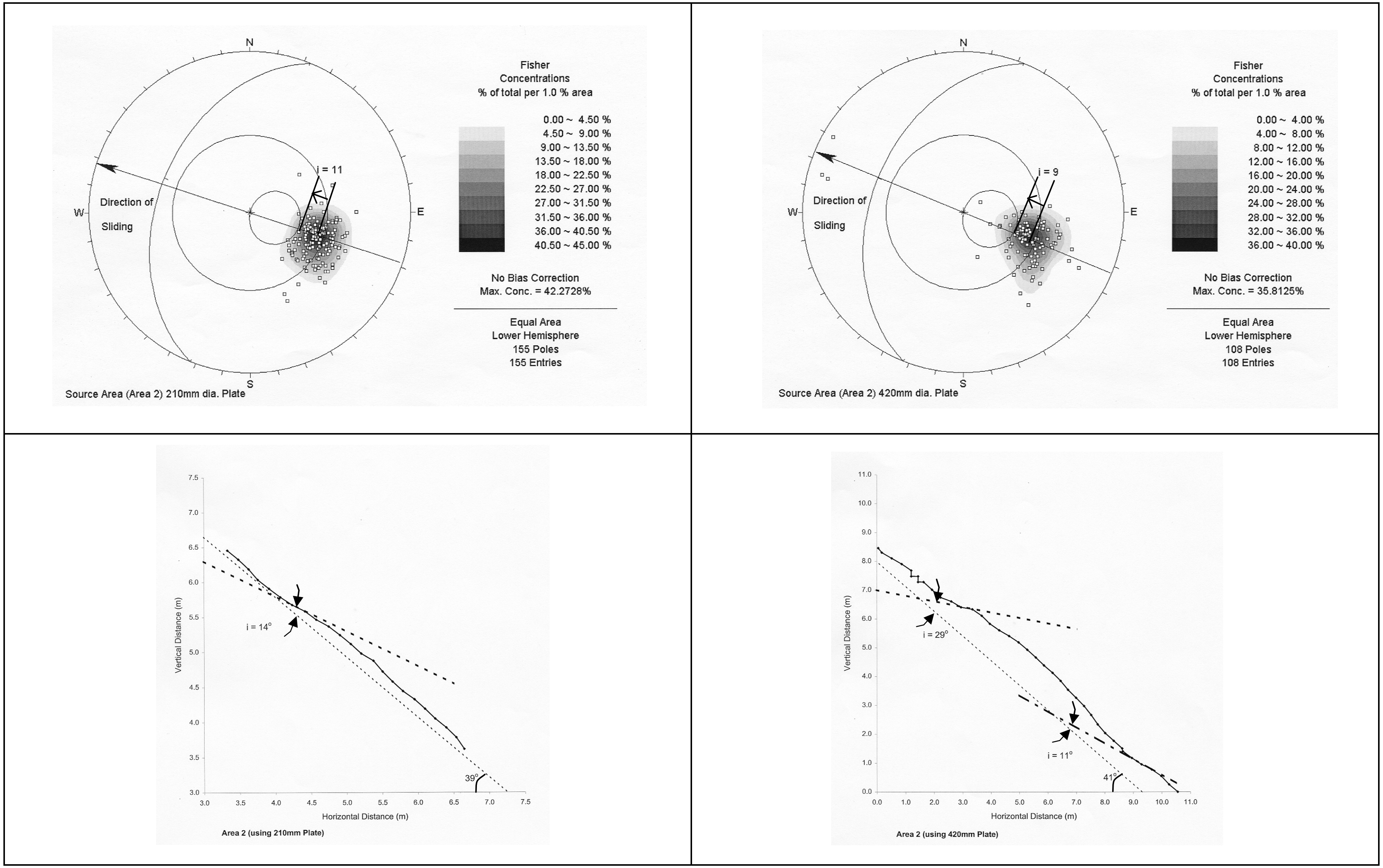

Figure B3 - Joint Roughness Characteristics of the Surface of Rupture (Area 2)

Table of Contents
Table of Contents
Table of Contents
Table of Contents

Project :	Detailed Study of Landslide at Hillside above Lei Pui Street, Shek Lei	**Calculation Sheet 1/2**
Subject :	Stability analysis-joint surface roughness using JRC approach	

1. Shear strength of rough surfaces

Based on Patton's saw-tooth specimens, the shear strength can be represented as below:

$$\tau = \sigma_n \tan(\phi_b + i) \quad \text{-----} \quad (1)$$

where where ϕ_b is the basic friction angle of the surface and
i is the angle of the saw-tooth face

2. Barton's model

Barton and his co-workers (1973, 1976, 1977, 1990) re-written the above equation (1) as below:

$$\tau = \sigma_n \tan((\phi_b + JRC * \log(JCS / \sigma_n)) \quad \text{-----} \quad (2)$$

From above equation (1) and (2), i can be derived as below:

$$i = JRC \log(JCS / \sigma_n) \quad \text{-----} \quad (3)$$

where JRC is the joint roughness coefficient,
JCS is the joint wall compressive strength and
σ_n is the total normal stress

3. Scale effects on shear strength estimation

Based on Barton's paper " Scale effects or sampling bias? " (1990),
the approximate equations for estimating JRCn and JCSn at larger scale are as below:

$$JRC_n = JRC_o (L_n/L_o)^{-0.02*JRCo} \quad \text{-----} \quad (4)$$

$$JCS_n = JCS_o (L_n/L_o)^{-0.03*JRCo} \quad \text{-----} \quad (5)$$

where L_o is the laboratory joint samples (nominal 100 mm)
L_n is the natural block size

4. Using the JRC approach to calculate roughness angle for Source Area of the Landslide at Lei Pui Street, Shek Lei (Not corrected for scale)

Use the cross section A-A of Source Area in Figure 8.

Assume γ' = 24 kN/m3 JCS_o = 2 Mpa ϕ_b = 36 degrees (ref. Barton, 1993)
JRC_o = 8 to 12 Z = 1 m (assumed average depth measured from pre-failure ground level)
Average slope angle = 41 degrees
L_o = 0.01 m (laboratory size joint samples)
L_n = 6 m (natural block size)
σ_n' = 11 kPa (assumed water table at pre-failure ground level)
σ_n = 18 kPa (assumed water table below slip surface (i.e. dry condition))

Table of Contents
Table of Contents
Table of Contents
Table of Contents

Project :	Detailed Study of Landslide at Hillside above Lei Pui Street, Shek Lei	**Calculation Sheet 2/2**
Subject :	Stability analysis-joint surface roughness using JRC approach	

1) Assumed water table at pre-failure ground level, then the effective normal stress (σ_n')

a) If JRC_o = 8 , then $i = JRC_o \log (JCS_o/\sigma_n')$ = 18.2 degrees $\phi_b + i$ = 54 degrees

b) If JRC_o = 10 , then $i = JRC_o \log (JCS_o/\sigma_n')$ = 22.7 degrees $\phi_b + i$ = 59 degrees

c) If JRC_o = 12 , then $i = JRC_o \log (JCS_o/\sigma_n')$ = 27.3 degrees $\phi_b + i$ = 63 degrees

2) Assumed water table below slip surface (i.e. dry condition)

a) If JRC_o = 8 , then $i = JRC_o \log (JCS_o/\sigma_n)$ = 16.3 degrees $\phi_b + i$ = 52 degrees

b) If JRC_o = 10 , then $i = JRC_o \log (JCS_o/\sigma_n)$ = 20.4 degrees $\phi_b + i$ = 56 degrees

c) If JRC_o = 12 , then $i = JRC_o \log (JCS_o/\sigma_n)$ = 24.5 degrees $\phi_b + i$ = 61 degrees

5. Using the JRC approach to calculate roughness angle for Source Area of the Landslide at Lei Pui Street, Shek Lei (Corrected for scale)

1) Assumed water table at pre-failure ground level, then the effective normal stress (σ_n')

a) If JRC_o = 8 , then
$JRC_n = JRC_o (L_n/L_o)^{-0.02*JRCo}$ = 2.9
$JCS_n = JCS_o (L_n/L_o)^{-0.03*JRCo}$ = 0.4 MPa
$i = JRC_n * \log(JCS_n/\sigma_n')$ = 5 degrees
$\phi_b + i$ = 41 degrees

b) If JRC_o = 10 , then
$JRC_n = JRC_o (L_n/L_o)^{-0.02*JRCo}$ = 2.8
$JCS_n = JCS_o (L_n/L_o)^{-0.03*JRCo}$ = 0.3 MPa
$i = JRC_n * \log(JCS_n/\sigma_n')$ = 4 degrees
$\phi_b + i$ = 40 degrees

c) If JRC_o = 12 , then
$JRC_n = JRC_o (L_n/L_o)^{-0.02*JRCo}$ = 2.6
$JCS_n = JCS_o (L_n/L_o)^{-0.03*JRCo}$ = 0.2 MPa
$i = JRC_n * \log(JCS_n/\sigma_n')$ = 3 degrees
$\phi_b + i$ = 39 degrees

2) Assumed water table below slip surface (i.e. dry condition)

a) If JRC_o = 8 , then
$JRC_n = JRC_o (L_n/L_o)^{-0.02*JRCo}$ = 2.9
$JCS_n = JCS_o (L_n/L_o)^{-0.03*JRCo}$ = 0.4 MPa
$i = JRC_n * \log(JCS_n/\sigma_n)$ = 4 degrees
$\phi_b + i$ = 40 degrees

b) If JRC_o = 10 , then
$JRC_n = JRC_o (L_n/L_o)^{-0.02*JRCo}$ = 2.8
$JCS_n = JCS_o (L_n/L_o)^{-0.03*JRCo}$ = 0.3 MPa
$i = JRC_n * \log(JCS_n/\sigma_n)$ = 3 degrees
$\phi_b + i$ = 39 degrees

c) If JRC_o = 12 , then
$JRC_n = JRC_o (L_n/L_o)^{-0.02*JRCo}$ = 2.6
$JCS_n = JCS_o (L_n/L_o)^{-0.03*JRCo}$ = 0.2 MPa
$i = JRC_n * \log(JCS_n/\sigma_n)$ = 3 degrees
$\phi_b + i$ = 39 degrees

Table of Contents
Table of Contents
Table of Contents
Table of Contents

Table of Contents

Table of Contents

APPENDIX C

THEORETICAL DEBRIS MOBILITY ANALYSIS

Table of Contents

Table of Contents

CONTENTS

Table of Contents
Table of Contents
Table of Contents

C.1 GENERAL

A series of calculations using MGSL's 'debriflo2000' spreadsheet program has been carried out to gain more insight into the likely sequence of events and mobility of the debris flow. The spreadsheet program has previously been used to successfully model past debris flow events in Hong Kong including the 1990 Tsing Shan debris flow (King, 1996) and the 1999 Sham Tseng debris flow (Maunsell Geotechnical Services Ltd., 2000). It should, however, be noted that the results from any debris flow modelling program can only be expected to give a fairly coarse approximation of the actual behaviour of a debris flow, owing to the highly complex and chaotic nature of this type of event.

The program models the debris front as a single pulse. The governing equations are based on Takahashi and Yoshida's 'Leading Edge' model (1979), which is based on the principles of conservation of momentum and continuity of flow for a fluid medium. The influence of turbulence has also been considered by incorporating the Voellmy turbulence coefficient (Hungr, 1995) into the equations. The 'debriflo2000' program has been checked by the GEO and is pending approval. A full discussion of the spreadsheet program and derivation of the governing equations is outside the scope of this appendix, and only a brief description of the main, relevant assumptions is given below.

The program simulates the passage of a debris front by considering the effects of frictional and turbulence resistance, slope angle and thrust immediately behind the debris front. The effects of entrainment and changes in cross-section and bends in the debris trail are also simulated. The thrust behind the debris front is proportional to square of the height of the debris which is varied in the spreadsheet in response to the initial conditions, upstream discharge rate, changes in flow resistance, entrainment, channel cross-section and variations in slope angle. The coefficient of effective lateral pressure within the debris front is assumed to be 1.0 for the purpose of calculating the lateral thrust.

Any positive entrainment is assumed to immediately affect the discharge rate and thrust directly behind the debris front. The erosion and entrainment of debris in the 'tail' portion of a debris flow (and the successive pulses of material) will not immediately affect the initial debris front and such debris is therefore not modelled in the program. The two-dimensional nature of the calculations means that, unless the negative entrainment (deposition) input in the spreadsheet exceeds the assumed initial volume plus all the entrained material (positive entrainment), the supply behind the front is effectively taken to be infinite in this programme.

Negative entrainment (deposition) occurs behind a debris front where: (a) the bulk friction angle (ϕ_{bulk} = equivalent total stress friction angle) is greater than the slope of the trail in poorly-channelised areas; (b) where material is deposited as levees on either side of the trail; and (c) where material is flung by centrifugal forces beyond the outside edge of a bend in the channel. This latter case can result in appreciable deposition, particularly where a large opening such as another stream channel joins the debris trail on the outside of a bend (e.g. confluence of Sub-catchments A and B). As deposition primarily takes place behind the debris front, the effect of negative entrainment is modelled by reducing the upstream discharge rate (and therefore thrust) in proportion to the ratio between the active volumes calculated in the two segments immediately preceding the front. As the spreadsheet divides the active part of the trail (in this case about 340 m in horizontal distance) into 300 segments,

Table of Contents
Table of Contents
Table of Contents
Table of Contents

the passage of the debris front is modelled in very small increments, which means that the effect of any deposition is modelled very gradually.

C.2 THE MODEL

The initial mass after commencement of failure was modelled as a 0.75 m thick by 15 m wide sheet of saturated solids inclined at 41° with a saturated bulk density of 2400 kg/m³. Assuming an intergranular friction angle of 30°, 100% non-suspended solids by volume and full saturation, the total stress bulk friction angle (ϕ_{bulk}) was calculated to be 18.6° according to the principles originally developed by Bagnold (1954) and as reported by Hungr et al (1984). A very high turbulence coefficient of 500 m/s² was assumed at the onset of failure, effectively modelling zero turbulence. The initial velocity was assumed to be 0.01 m/s.

The parameters of the debris are gradually changed in the model to simulate the breaking up and mixing of the mass as it cascades down the cliff face. After Chainage 50, it is assumed that the mass is a mixture of failed colluvium, boulders and entrained material. About 64% of boulders by volume were assumed to be contained in a matrix of saturated slurry with a density of 1300 kg/m³. The resulting debris front parameters are: a saturated unit weight of 19.7 kN/m³ and a ϕ_{bulk} of 11.3°. A turbulence coefficient of 500 m/s² was also assumed. These parameters are similar to those derived from back analyses of previous debris flows in Hong Kong carried out by MGSL, Ayotte et al (1999) and Hungr et al (1999). The percentage of boulders was based on field assessments of the deposited material.

The debris trail geometry is characterised in the model by a longitudinal profile and a series of 35 cross-sections that are based on the results of the field survey, site measurements and observations. The cross-sections are representations of the actual wetted profile of the debris trail and correspond to the fullest extent of the debris given by the highest debris marks observed along the trail at the referenced chainages. All locations along the debris trail are referenced to the horizontal chainage-line shown in Drawing No. 1 in the main body of the report. The plan geometry of the trail is defined in the model by a series of horizontal radii at specified chainages.

Several analyses were carried out, with the debris parameters, volume of entrainment and deposition immediately affecting the thrust on the debris front adjusted to obtain best-fit calculated average debris height profiles and velocity with the field measurements of debris height and influence of velocity based on field measurement.

The active volume, longitudinal profile, calculated velocity, average measured height and average calculated height vs. chainage are shown on the graphical plots in Figure C1. The sharp peaks in the velocity profile indicate abrupt steepenings in the channel profile where the debris front becomes airborne with no frictional or turbulent reaction from the ground. Also shown in the figure are the field estimates of velocity derived from: the superelevation measurements at Chainage 137; the calculation of impact velocity necessary to deform the reinforced concrete wing-wall at Chainage 243; and, the calculation of velocity from the curvature of gouge-marks on the walls of the reinforced concrete channel caused by boulders at Chainage 270.

Table of Contents
Table of Contents
Table of Contents
Table of Contents

The velocity profile indicates an impact velocity of about 14 m/s at the base of the cliff, and velocities of between 8 m/s and 11 m/s along the upper trail to Chainage 125. The velocity then sharply reduces to about 5 m/s on the flat-lying abandoned squatter platform between Chainage 125 and 145, before accelerating to about 14 m/s over the steep, rocky slope between Chainages 145 and 173. The demolished squatter structures Nos. RTW/7E/156 and RTW/7E/158 were located at Chainage 168 where the calculated velocity is about 10 m/s.

A volume of about 50 m^3 of immediate entrainment of colluvium and saprolite at the base of the cliff gives a good match between the calculated and measured average height profiles up to Chainage 190 at the junction with Sub-catchment B. At this point, the debris trail changes direction by about 85°, and about 12 m^3 of fresh debris consisting of boulders up to 1 m in length was found to be scattered up the drainage line of Sub-catchment B for about 15 m. It is considered that a much larger amount of bouldery debris front material would have been initially deposited in the open mouth of the drainage line in the form of a levee (which was subsequently removed by a dam-break, probably within a matter of minutes after the initial debris front had passed this point).

In the model, about 80 m^3 of debris is lost from the debris front at the mouth of Sub-catchment B. The removal of bouldery material and the mixing with flood-water from Sub-catchment B (calculated discharge between 2 m^3/s and 3 m^3/s) is considered likely to have increased the mobility of the initial debris front. In the model, the ϕ_{bulk} value was reduced to about 8° below Chainage 190.

Beyond the confluence with Sub-catchment B, the velocity gradually reduces to about 4 m/s by the lower end of the upper concrete channel at Chainage 270. After falling over the former quarry face at Chainage 280, the debris began to spread out and deposit on the former quarry floor to the extent that by Chainage 320, the debris front had very little active thrust and was rapidly decelerating to a halt. The calculated velocity at Chainage 305 (corner of the pump-house) is approximately 4 m/s. The total length of time between failure at the source and deposition of the debris front at Chainage 320 was calculated in the model to be 47 seconds.

Owing to the good match with the field data shown in Figure C1, the model is considered to represent a reasonable approximation of the mobility of the initial debris front. The remaining debris deposited in the former quarry probably travelled behind the initial front as a long, stretched-out ‘tail’, possibly with minor pulses, and as water-borne debris eroded by subsequent overland flow.

Table of Contents
Table of Contents
Table of Contents
Table of Contents

LIST OF FIGURES

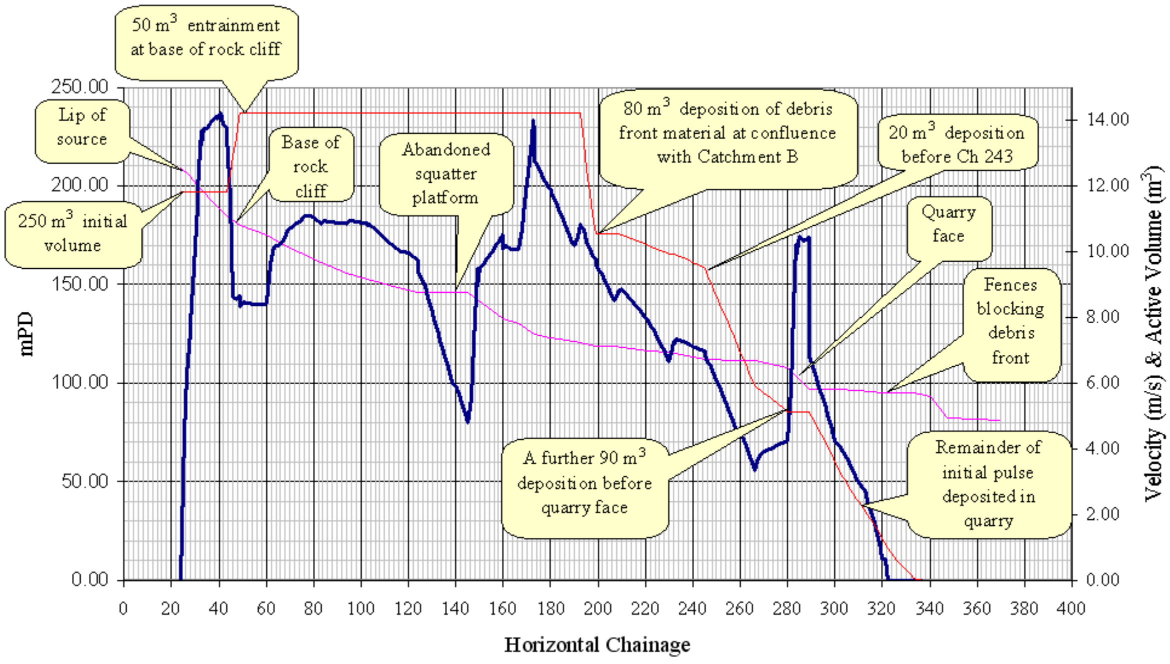

(a) Active Debris Volume and Debris Velocity versus Horizontal Chainage Plot

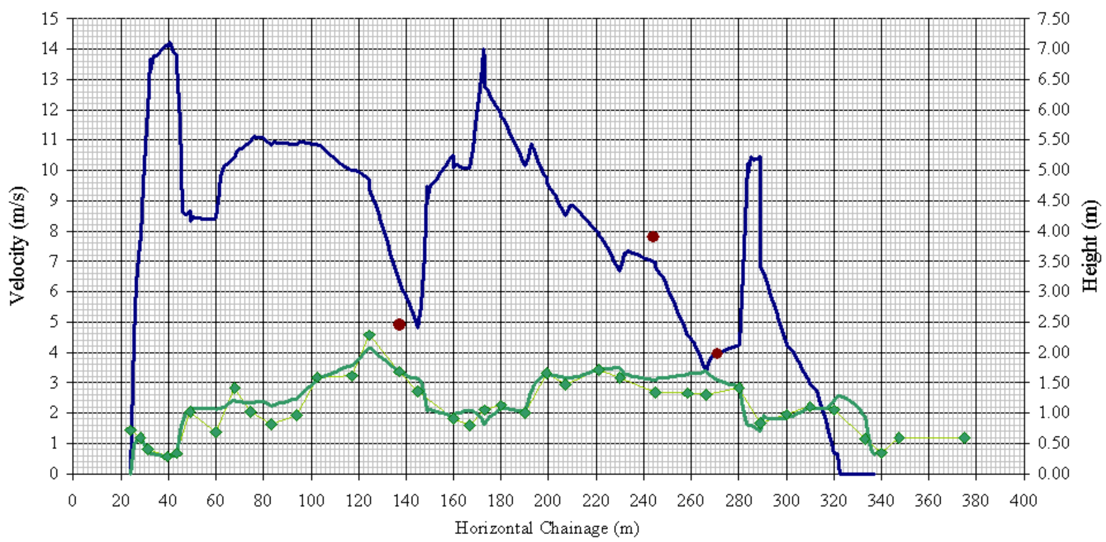

(b) Debris Velocity and Debris Height versus Horizontal Chainage Plot

Legend:

●	Velocity (field estimations)	▬	Calculated velocity
◆	Average measured height	▬	Calculated average height
▬	Slope profile	▬	Active volume

Note: Active Volume of debris (in cubic metres) can be obtained by multiplying the value shown on the velocity scale in the plot (a) above by the non-dimensional factor 21.12.

Figure C1 - Dynamic Analysis of Mobility of the Initial Debris Front

Table of Contents
Table of Contents
Table of Contents
Table of Contents

LIST OF DRAWINGS

Landslide Mass Balance Summary

Source and Debris Trail

Chainage (m)	Slope angle (°)	Deposition (m^3)	Material Deposited	Material Eroded (m^3)	MT Eroded
Source (0 - 24)	42	1	MT 6	250	MT 1, 3 & 4
Cliff (24 - 40)	58	0	-	5	-
Main Zone of Erosion (40 - 128)	33	37	MT 5 & 6	455	-
Squatter Platform (128 - 148)	8	15	MT 5 & 6	20	MT 1
Rock Slope (148 - 168)	35	1	MT 5 & 6	5	MT 1 + Fill
Squatter Platform (168 - 185)	12	35	MT 5 & 6	10	MT 1 & 3
Zone of Accumulation (185 - 270)	6	105	MT 5 & 6	1	MT 1
Quarry (270 - 325)	2	530	MT 5, 6 & 7	0	-
Lei Pui Street	-	50	MT 7	0	-
Total Volume		774		746	

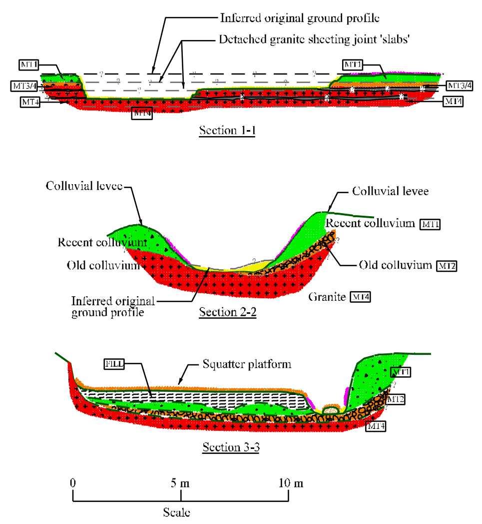

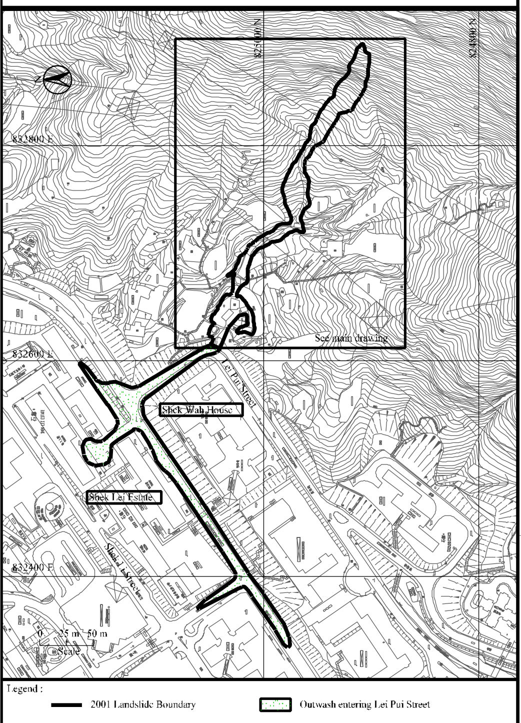

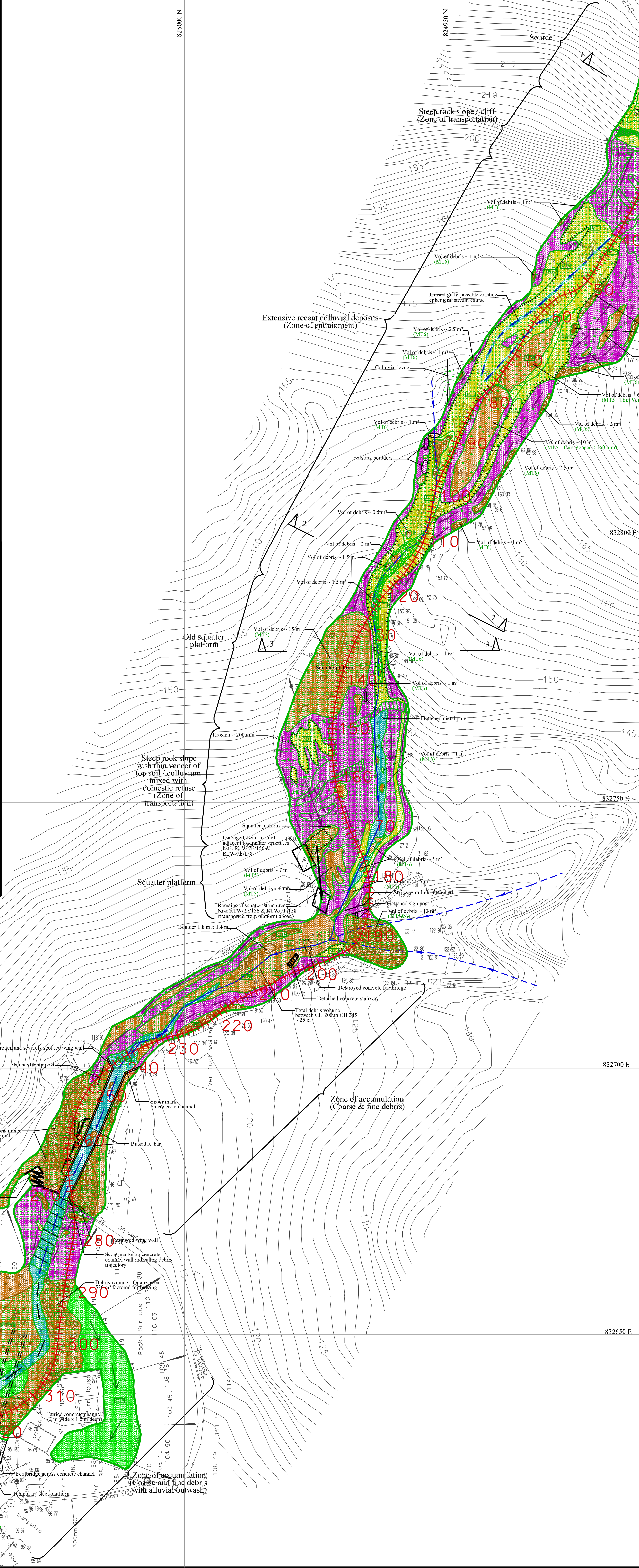

LEGEND :

- Boundary of landslide scar / debris trail
- Boundary of outwash material on Lei Pui Street
- Erosion scarp
- Stream course

Substrate Mapping

- Boundary of substrate type
- Granite-fresh to partially weathered - PW 90/100 (Intact material grade SDG & MDG)
- Granite-partially weathered - PW 0/30 & PW 30/50 (Intact material grade HDG & CDG)
- Recent sub-angular bouldery granite colluvium
- Old sub-rounded bouldery colluvium
- Superficial fill

Interpreted debris flow processes

- Erosion/depletion: Freshly exposed substrate, interpreted > 0.1 m eroded
- Transportation: Abraded original ground surface with removal of vegetation, minor erosion (< 0.1 m) and traces of debris (< 0.1 m)
- Water flow: Traces of washed sand and gravel with flow structures
- Deposition: Landslide debris of boulders, cobbles and gravel with silt and sand
- Outwash material (sand and silt)

Material Types (MT)

MATERIAL ERODED

MT1 'RECENT' COLLUVIUM
Yellowish brown and brown, sub rounded to angular, moderately to slightly decomposed, COBBLE and BOULDER sized granite fragments, with some to much loose, gravelly, silty sand matrix, and some soil pipes observed generally less than 20 mm dia.

MT2 'OLD' COLLUVIUM
Medium Dense to dense, dark yellowish and orangish brown, slightly gravelly, silty SAND, with many highly to completely decomposed, rounded to sub angular cobble and occasional boulder fragments. Generally no soil pipes and is observed at the base of some eroded channels.

MT3 GRANITE SAPROLITE
Extremely weak to weak, dark yellowish brown and brown, completely to highly decomposed, fine grained granite. (Generally corresponding to partially weathered rock mass grade PW 0-30).

MT4 GRANITE BEDROCK
Moderately strong to strong, light pinkish grey, and yellowish brown, moderately to slightly decomposed, fine grained granite. (Generally corresponding to partially weathered rock mass grade PW 90-100).

(FILL) Local covering of fill was exposed although this was generally mixed with refuse on slopes or formed squatter platforms.

MATERIAL DEPOSITED

MT5 REMOULDED (Matrix supported) DEBRIS
Loose, yellowish brown, gravelly, very silty SAND matrix, containing between 10% and 65% sub rounded to angular, moderately to slightly decomposed, cobble and boulder sized granite fragments.

MT6 CLASTIC (clast supported) DEBRIS
Yellowish and greyish brown, gravelly, silty, sandy, sub rounded to angular, moderately to slightly decomposed, COBBLE and BOULDER sized granite fragments, with some gravelly, silty sand.

MT7 ALLUVIAL OUTWASH
Loose, yellow and yellowish brown, gravelly SILT and SAND, with occasional sub rounded to angular, moderately to slightly decomposed, cobble sized granite fragments.

- 128 - Horizontal chainage measured from crown of landslide along debris flow path

2 Section line

no.	date	description	chk.	appr.

REVISION

	name	date
surveyed		
designed	SJW	5/2002
drawn	ATCL	5/2002
traced		
checked		

examined

contract no.

file no.

job no.

project

Detailed Study of the 1 September 2001 Debris Flow on the Natural Hillside Above Lei Pui Street

drawing title

The Debris Flow Scar Materials and Mass Balance

drawing no.

DRAWING NO. 1

scale

1 : 250

office

LANDSLIP INVESTIGATION DIVISION
GEOTECHNICAL ENGINEERING OFFICE

CIVIL ENGINEERING DEPARTMENT
HONG KONG

GEO PUBLICATIONS AND ORDERING INFORMATION
土力工程處刊物及訂購資料

A selected list of major GEO publications is given in the next page. An up-to-date full list of GEO publications can be found at the CEDD Website http://www.cedd.gov.hk on the Internet under "Publications". Abstracts for the documents can also be found at the same website. Technical Guidance Notes are published on the CEDD Website from time to time to provide updates to GEO publications prior to their next revision.

部份土力工程處的主要刊物目錄刊載於下頁。而詳盡及最新的土力工程處刊物目錄，則登載於土木工程拓展署的互聯網網頁 http://www.cedd.gov.hk 的"刊物"版面之內。刊物的摘要及更新刊物內容的工程技術指引，亦可在這個網址找到。

Copies of GEO publications (except maps and other publications which are free of charge) can be purchased either by:

writing to
Publications Sales Section,
Information Services Department,
Room 402, 4th Floor, Murray Building,
Garden Road, Central, Hong Kong.
Fax: (852) 2598 7482

or

- Calling the Publications Sales Section of Information Services Department (ISD) at (852) 2537 1910
- Visiting the online Government Bookstore at http://bookstore.esdlife.com
- Downloading the order form from the ISD website at http://www.isd.gov.hk and submit the order online or by fax to (852) 2523 7195
- Placing order with ISD by e-mail at puborder@isd.gov.hk

讀者可採用以下方法購買土力工程處刊物(地質圖及免費刊物除外):

書面訂購
香港中環花園道
美利大廈4樓402室
政府新聞處
刊物銷售組
傳真: (852) 2598 7482

或

- 致電政府新聞處刊物銷售小組訂購 (電話：(852) 2537 1910)
- 進入網上「政府書店」選購，網址爲 http://bookstore.esdlife.com
- 透過政府新聞處的網站 (http://www.isd.gov.hk) 於網上遞交訂購表格，或將表格傳真至刊物銷售小組 (傳真：(852) 2523 7195)
- 以電郵方式訂購 (電郵地址：puborder@isd.gov.hk)

1:100 000, 1:20 000 and 1:5 000 maps can be purchased from:

Map Publications Centre/HK,
Survey & Mapping Office, Lands Department,
23th Floor, North Point Government Offices,
333 Java Road, North Point, Hong Kong.
Tel: 2231 3187
Fax: (852) 2116 0774

讀者可於下列地點購買1:100 000，1:20 000及1:5 000地質圖：

香港北角渣華道333號
北角政府合署23樓
地政總署測繪處
電話: 2231 3187
傳真: (852) 2116 0774

Requests for copies of Geological Survey Sheet Reports, publications and maps which are free of charge should be sent to:

For Geological Survey Sheet Reports and maps which are free of charge:
Chief Geotechnical Engineer/Planning,
(Attn: Hong Kong Geological Survey Section)
Geotechnical Engineering Office,
Civil Engineering and Development Department,
Civil Engineering and Development Building,
101 Princess Margaret Road,
Homantin, Kowloon, Hong Kong.
Tel: (852) 2762 5380
Fax: (852) 2714 0247
E-mail: sdcampbell@cedd.gov.hk

For other publications which are free of charge:
Chief Geotechnical Engineer/Standards and Testing,
Geotechnical Engineering Office,
Civil Engineering and Development Department,
Civil Engineering and Development Building,
101 Princess Margaret Road,
Homantin, Kowloon, Hong Kong.
Tel: (852) 2762 5345
Fax: (852) 2714 0275
E-mail: ykhui@cedd.gov.hk

如欲索取地質調查報告、其他免費刊物及地質圖，請致函：

地質調查報告及地質圖:
香港九龍何文田公主道101號
土木工程拓展署大樓
土木工程拓展署
土力工程處
規劃部總土力工程師
(請交:香港地質調查組)
電話: (852) 2762 5380
傳真: (852) 2714 0247
電子郵件: sdcampbell@cedd.gov.hk

其他免費刊物:
香港九龍何文田公主道101號
土木工程拓展署大樓
土木工程拓展署
土力工程處
標準及測試部總土力工程師
電話: (852) 2762 5345
傳真: (852) 2714 0275
電子郵件: ykhui@cedd.gov.hk

Table of Contents
Table of Contents
Table of Contents
Table of Contents

MAJOR GEOTECHNICAL ENGINEERING OFFICE PUBLICATIONS
土力工程處之主要刊物

GEOTECHNICAL MANUALS

Geotechnical Manual for Slopes, 2nd Edition (1984), 300 p. (English Version), (Reprinted, 2000).

斜坡岩土工程手冊(1998)，308頁(1984年英文版的中文譯本)。

Highway Slope Manual (2000), 114 p.

GEOGUIDES

Geoguide 1	Guide to Retaining Wall Design, 2nd Edition (1993), 258 p. (Reprinted, 2000).
Geoguide 2	Guide to Site Investigation (1987), 359 p. (Reprinted, 2000).
Geoguide 3	Guide to Rock and Soil Descriptions (1988), 186 p. (Reprinted, 2000).
Geoguide 4	Guide to Cavern Engineering (1992), 148 p. (Reprinted, 1998).
Geoguide 5	Guide to Slope Maintenance, 3rd Edition (2003), 132 p. (English Version).
岩土指南第五冊	斜坡維修指南，第三版(2003)，120頁(中文版)。
Geoguide 6	Guide to Reinforced Fill Structure and Slope Design (2002), 236 p.

GEOSPECS

Geospec 1	Model Specification for Prestressed Ground Anchors, 2nd Edition (1989), 164 p. (Reprinted, 1997).
Geospec 2	Model Specification for Reinforced Fill Structures (1989), 135 p. (Reprinted, 1997).
Geospec 3	Model Specification for Soil Testing (2001), 340 p.

GEO PUBLICATIONS

GCO Publication No. 1/90	Review of Design Methods for Excavations (1990), 187 p. (Reprinted, 2002).
GEO Publication No. 1/93	Review of Granular and Geotextile Filters (1993), 141 p.
GEO Publication No. 1/96	Pile Design and Construction (1996), 348 p. (Reprinted, 2003).
GEO Publication No. 1/2000	Technical Guidelines on Landscape Treatment and Bio-engineering for Man-made Slopes and Retaining Walls (2000), 146 p.

GEOLOGICAL PUBLICATIONS

The Quaternary Geology of Hong Kong, by J.A. Fyfe, R. Shaw, S.D.G. Campbell, K.W. Lai & P.A. Kirk (2000), 210 p. plus 6 maps.

The Pre-Quaternary Geology of Hong Kong, by R.J. Sewell, S.D.G. Campbell, C.J.N. Fletcher, K.W. Lai & P.A. Kirk (2000), 181 p. plus 4 maps.

TECHNICAL GUIDANCE NOTES

TGN 1	Technical Guidance Documents

Table of Contents
Table of Contents
Table of Contents
Table of Contents